

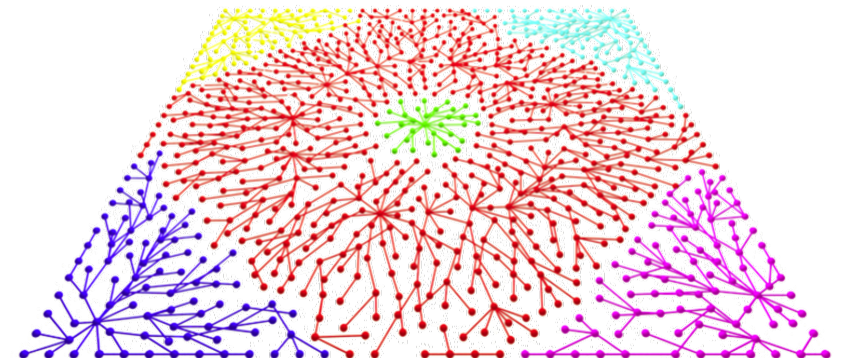
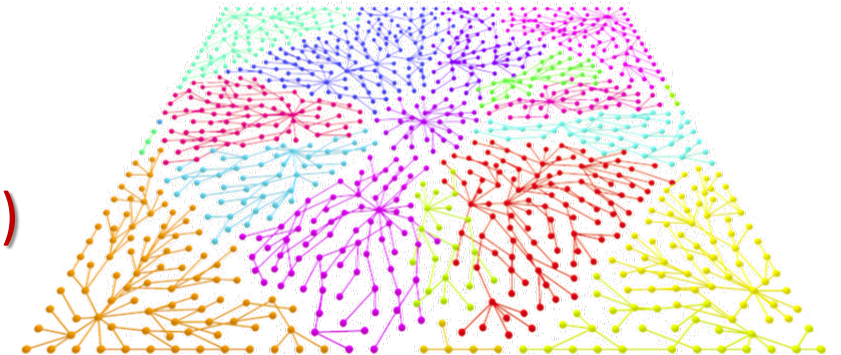
# CS233, CME251: Geometric and Topological Data Analysis

Leonidas Guibas  
Computer Science Department  
Stanford University

Guest lecture: Samir Chowdhury (Stanford)



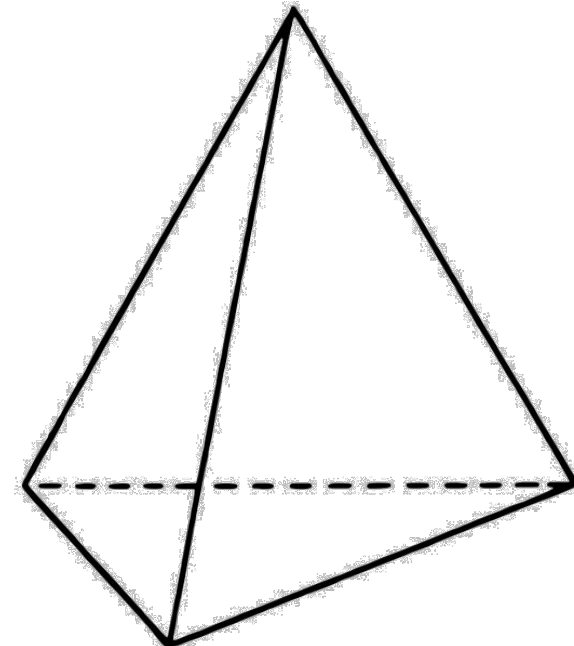
Lecture 9  
04 May 2020



**Last Time: Persistent homology**

# Betti Numbers $\beta_i$

- Ranks of the free part of homology groups  $H_i$
- $\beta_0$  counts the number of connected components
- $\beta_1$  counts the number of independent loops
- $\beta_2$  counts the number of independent voids
- ...



Topology is fundamentally a tool for classification

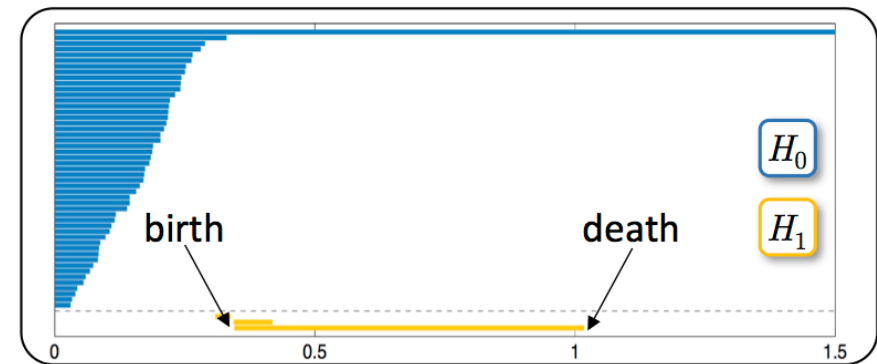
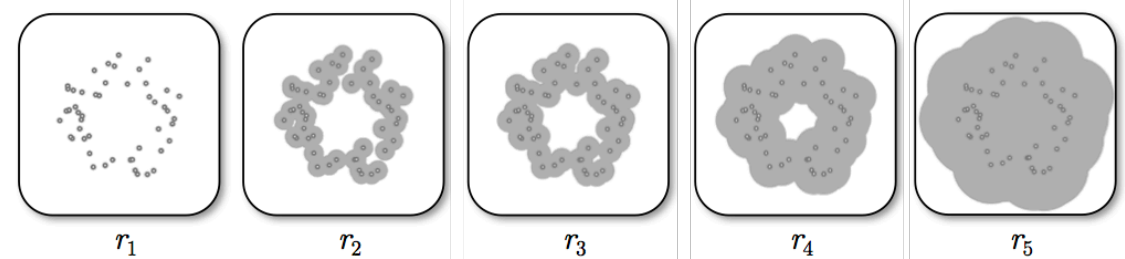
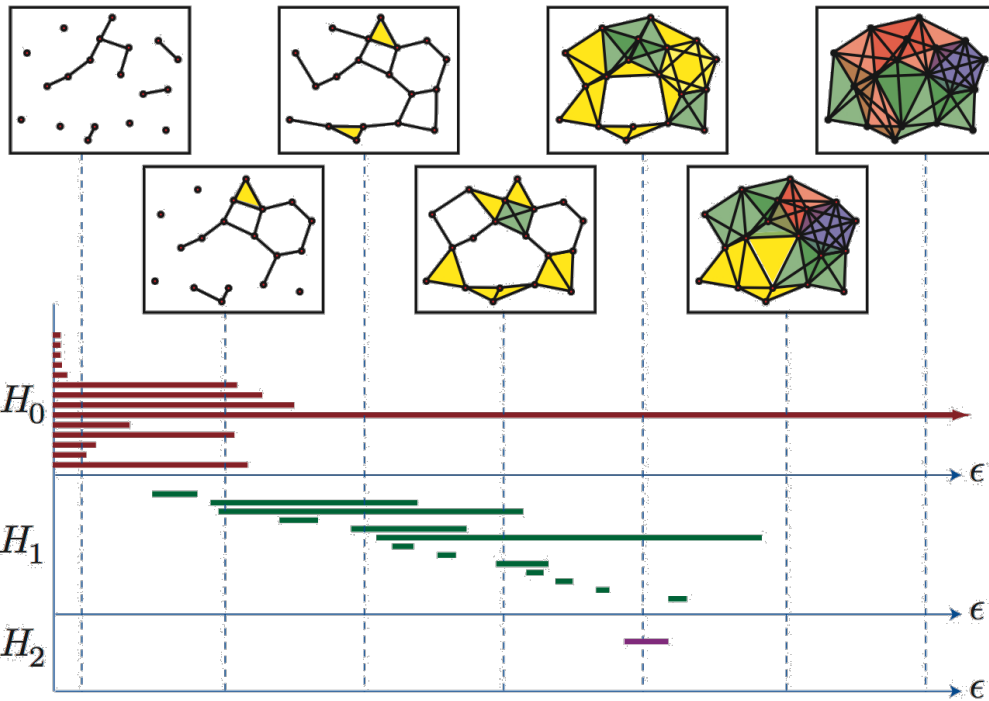
# Pipeline

Dataset:  
- Euclidean point cloud data  
- Metric spaces  
- Triangulated shape  
- Graphs, matrices...

Filtered simplicial complex  
• Possible to have both inclusions and deletions (dynamic data)

Vector spaces with linear maps: a **persistent vector space**

Visual summary: a **persistence diagram** or **persistence barcode**  
• Persistence landscapes for ML-friendly output





# Stability of persistent homology

- ◆ Persistent homology outputs are robust to small perturbations of data

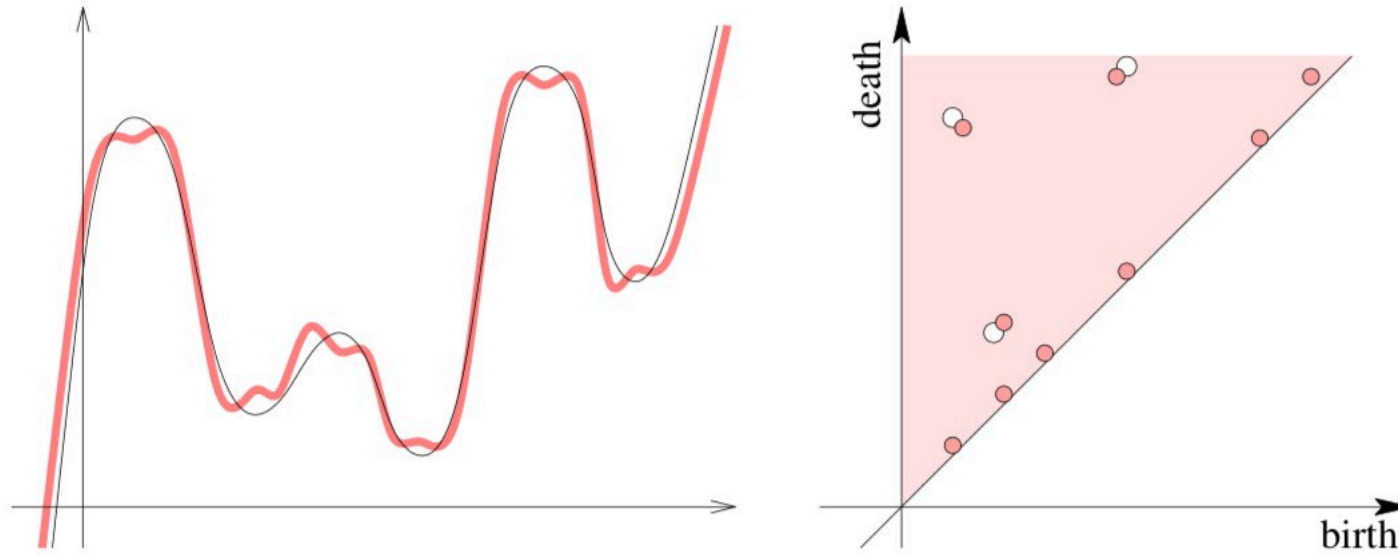


Figure from Edelsbrunner, Harer,  
*Computational Topology*

- ◆ Theorem (Cohen-Steiner, Edelsbrunner, Harer):  $\mathcal{M}$  a triangulable space,  $f, g: \mathcal{M} \rightarrow \mathbb{R}$  “nice”. Then,  
$$d_B(D_k(f), D_k(g)) \leq \|f - g\|_\infty.$$

Here  $D_k$  is the persistence diagram in dimension  $k$ ,  $\|\cdot\|_\infty$  is the max-norm, and  $d_B$  is the bottleneck distance (TBD)

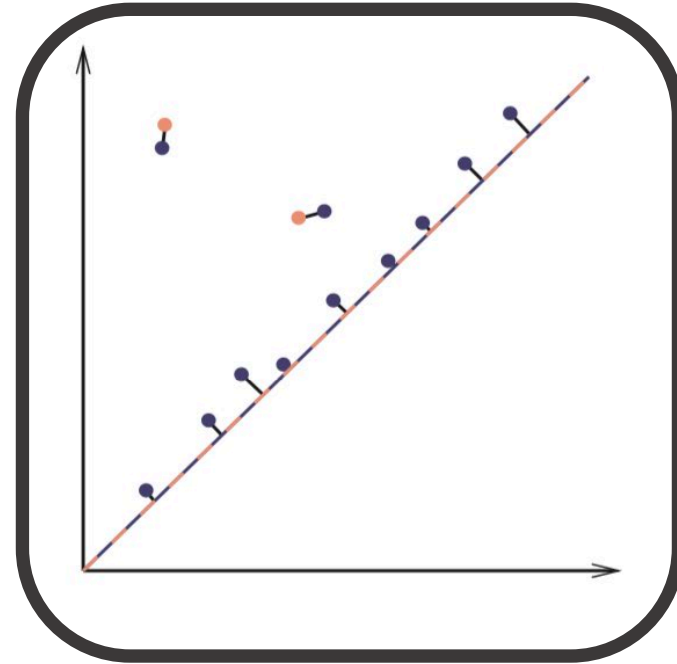
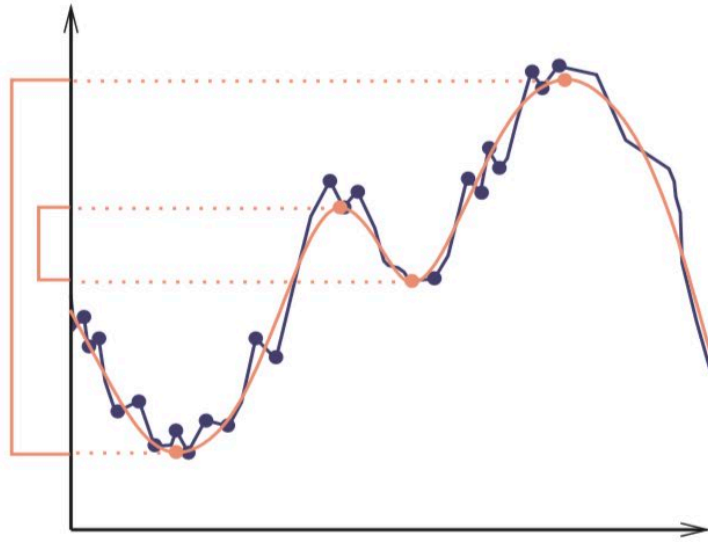
# Simplices are creators or destroyers

- ◆ A  $k$ -simplex either creates a  $k$ -dimensional feature or destroys a  $(k - 1)$ -dimensional feature
- ◆ Persistence pairs a creator simplex  $\sigma$  with a destroyer simplex  $\tau$ , and records the birth-death times  $(b, d)$  as the appearance times of  $(\sigma, \tau)$ .

Proof: Suppose we add a  $p$ -simplex  $\sigma$ . Assume simplices are added incrementally, so we have not yet added a  $(p + 1)$ -simplex with  $\sigma$  as a face.

- Case 1:  $\partial_p(\sigma) \in \text{im}(\partial_p)$ , i.e.  $\partial_p(\sigma) = \partial_p(\tau)$  for some  $\tau$ . Then  $\partial_p(\sigma - \tau) = 0$ , so  $\ker(\partial_p)$  grows by one dimension. Because we don't yet have a  $(p + 1)$ -simplex with  $\sigma$  as a face,  $\text{im}(\partial_{p+1})$  is unchanged. Therefore  $H_p$  grows by one dimension, i.e. we created a  $p$ -dimensional feature.
- Case 2:  $\partial_p(\sigma) \notin \text{im}(\partial_p)$ , i.e.  $\text{im}(\partial_p)$  grows by one dimension. But  $\partial_{p-1}\partial_p(\sigma) = 0$ , and the elements in  $\partial_p(\sigma)$  had already been added by the incremental addition assumption, so  $\ker(\partial_{p-1})$  remains unchanged. Thus  $H_{p-1}$  loses one dimension, i.e. we destroyed a  $(p - 1)$ -dimensional feature.

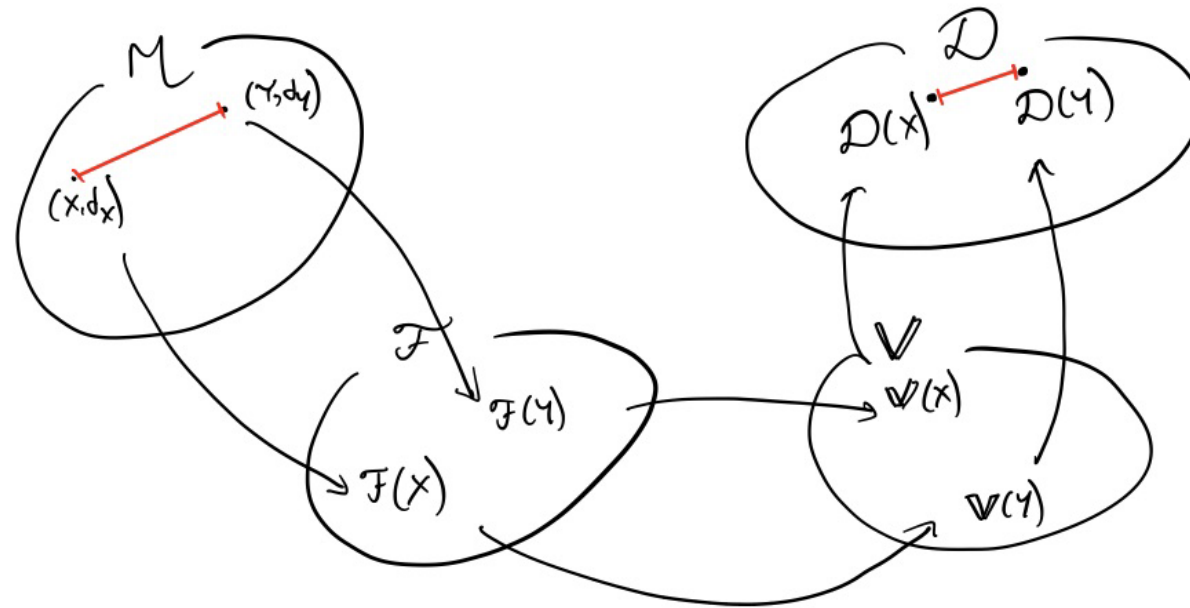
# The bottleneck distance



$A, B$  two persistence diagrams.

$$d_B(A, B) := \inf \left\{ \sup_{x \in A \cup \Delta} \|x - \phi(x)\|_\infty : \phi : A \cup \Delta \rightarrow B \cup \Delta \text{ a bijection} \right\}$$

# Gromov-Hausdorff stability



$\mathcal{M}$  = finite metric spaces  
 $\mathcal{F}$  = filtered simplicial complexes  
 $\mathbb{V}$  = persistent vector spaces  
 $\mathbb{D}$  = persistence diagrams

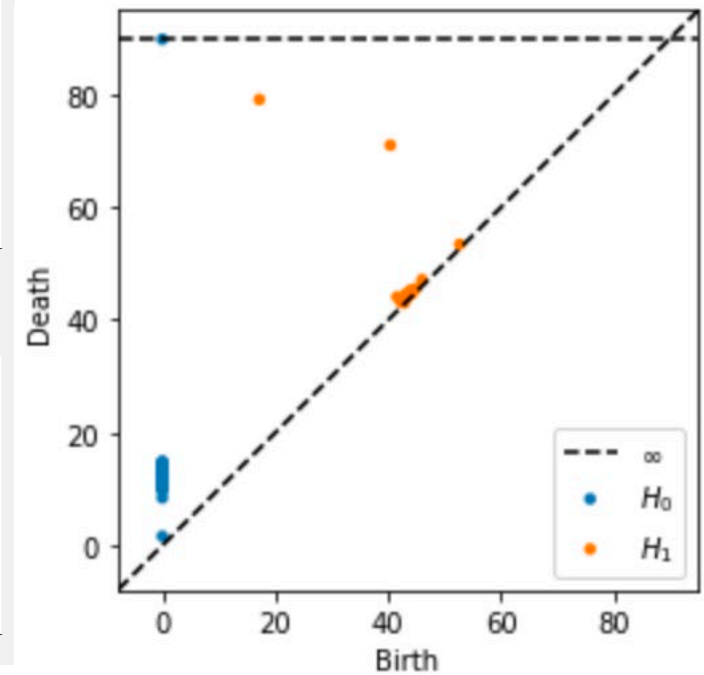
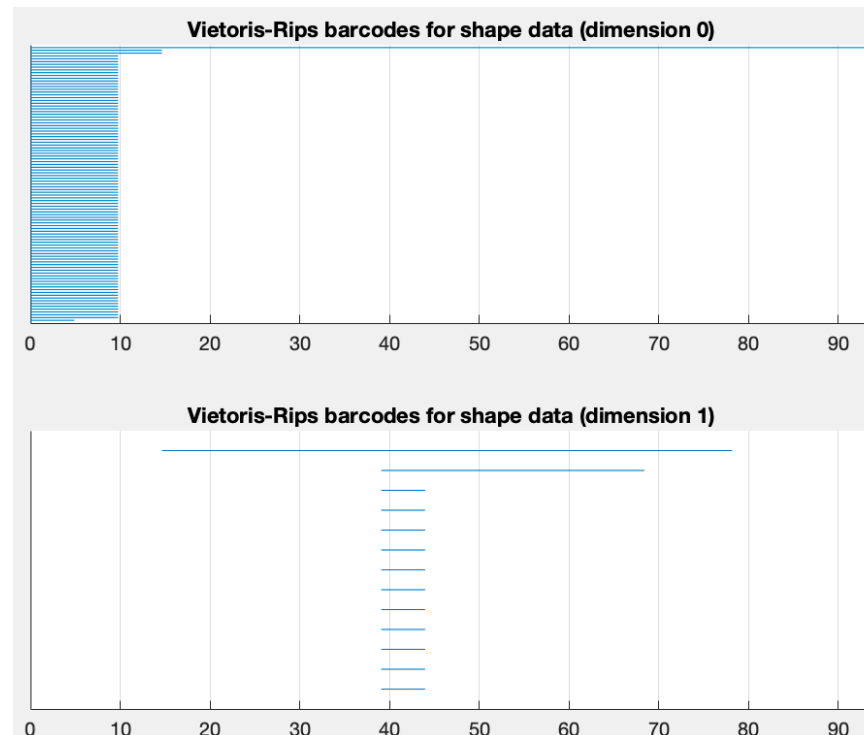
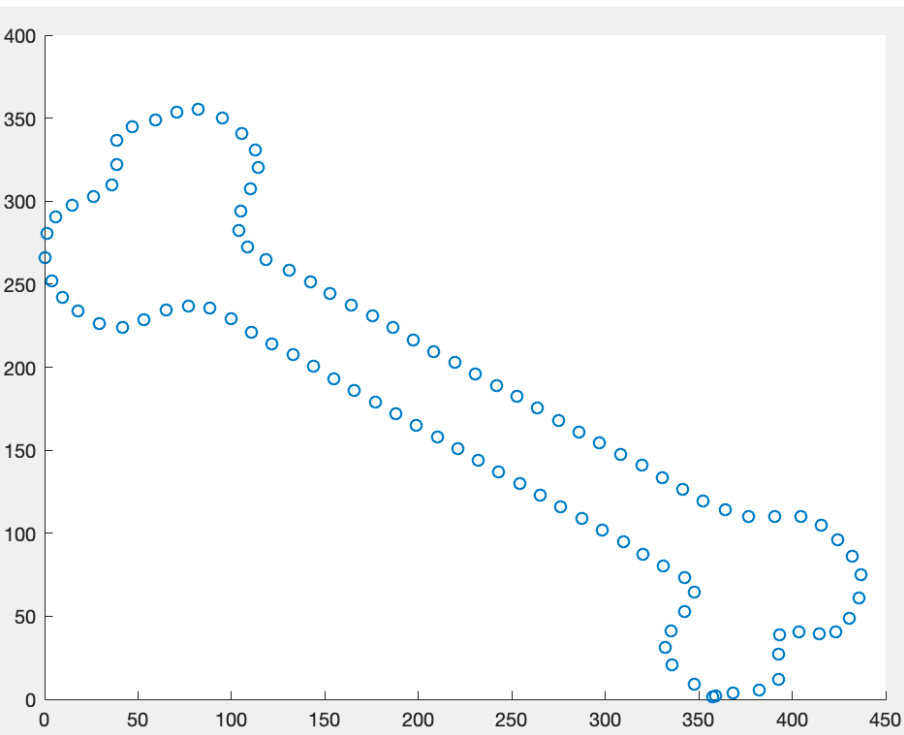
- Theorem (Chazal, Cohen-Steiner, Guibas, Mémoli, Oudot):  $(X, d_X), (Y, d_Y)$  finite metric spaces. Then,

$$d_B(D_k(VR(X)), D_k(VR(Y))) \leq 2d_{GH}(X, Y).$$

$O(n^3)$  with Hungarian algorithm,  
 $O(n^{3/2})$  state-of-the-art (Kerber, Morozov,  
 Nigmatov 2017)

NP-hard

# Demo – Javaplex and Ripser



# Today: Applications

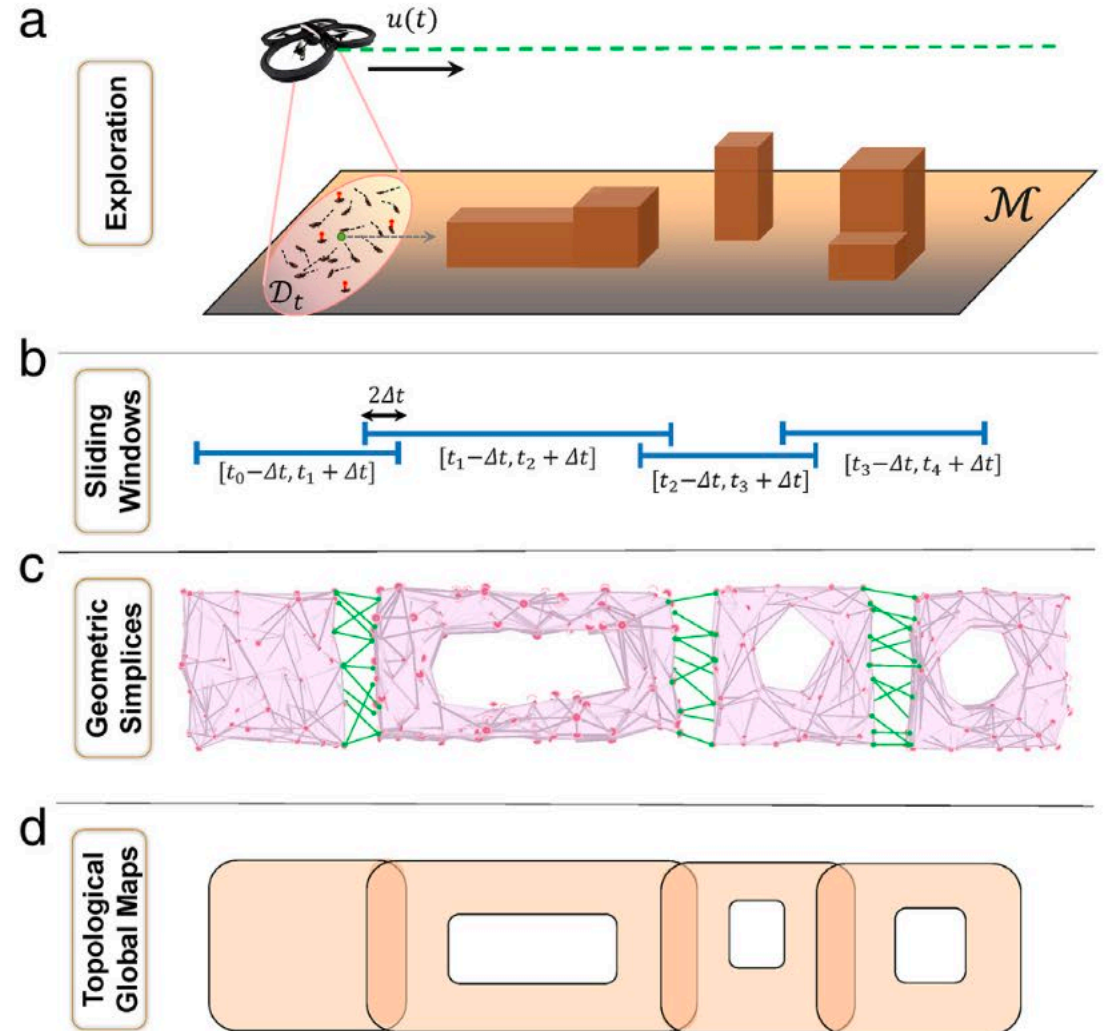
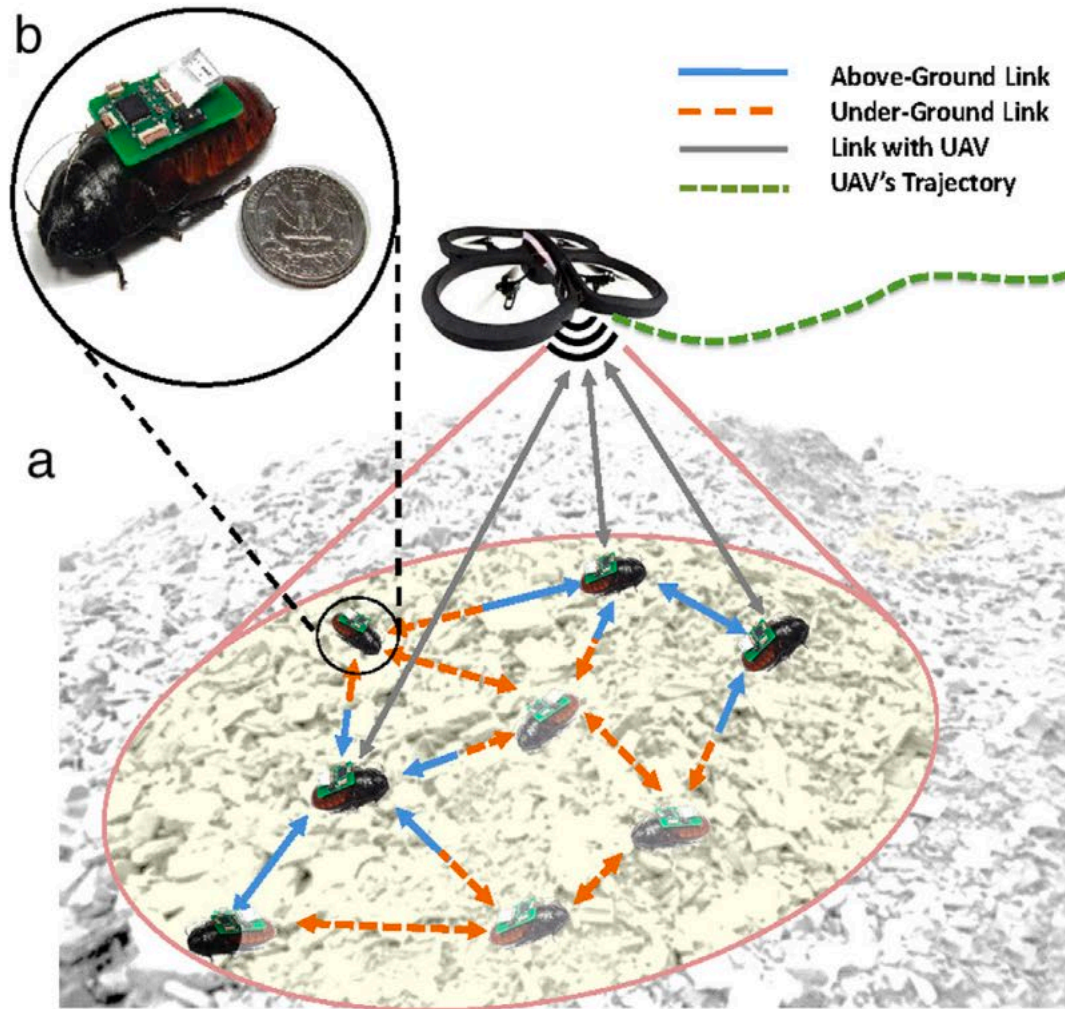
# Plan

- ◆ Improved image segmentation and scalar field analysis via persistence
- ◆ Topological time series analysis
- ◆ Natural image statistics via TDA
- ◆ Geometry-aware filtrations for persistent homology
- ◆ Mapper and some of its applications

# Scalar field analysis and persistence- based clustering

# Mapping spaces with cyborg insects

Dirafzoon, Bozkurt, Lobaton, *A framework for mapping with biobotic insect networks*



# Underlying problem: Characterizing a landscape from limited data

Chazal, Guibas, Oudot, Skraba, *Scalar Field Analysis over Point Cloud Data*. DCG 2011

## Problem setup

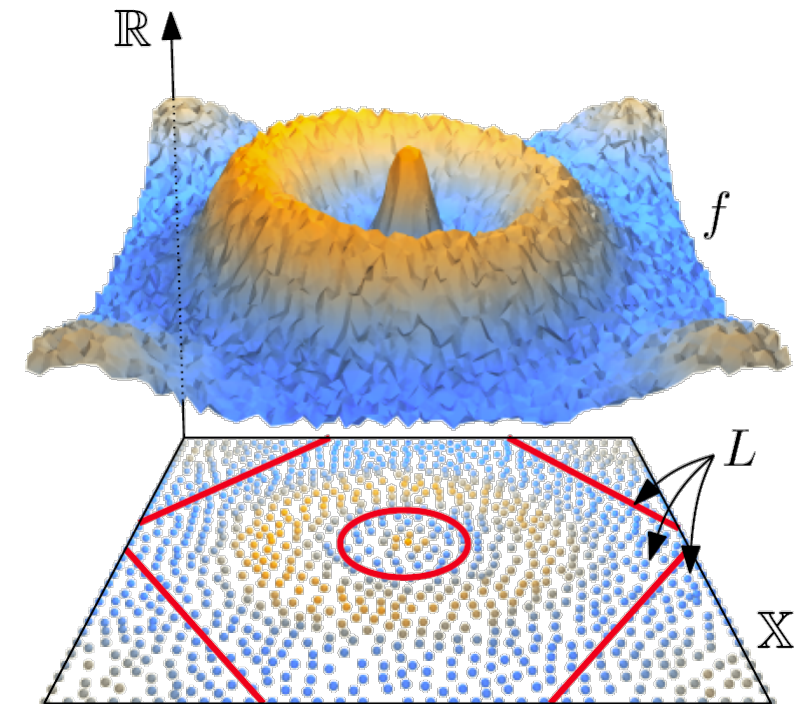
$(X, d)$  a metric space,  $f: X \rightarrow \mathbb{R}$  some function (say Lipschitz)

**Given:**  $L \subseteq X$  a finite subsample,  $f|_L$  restriction of  $f$  to  $L$ ,  $d|_{L \times L}$  restriction of metric to  $L$

(not given: relative locations/coordinates of  $L$  to  $X$ , values of  $f$  outside  $L$ )

**Goal:** Recover salient properties of the graph of  $f$ , namely:

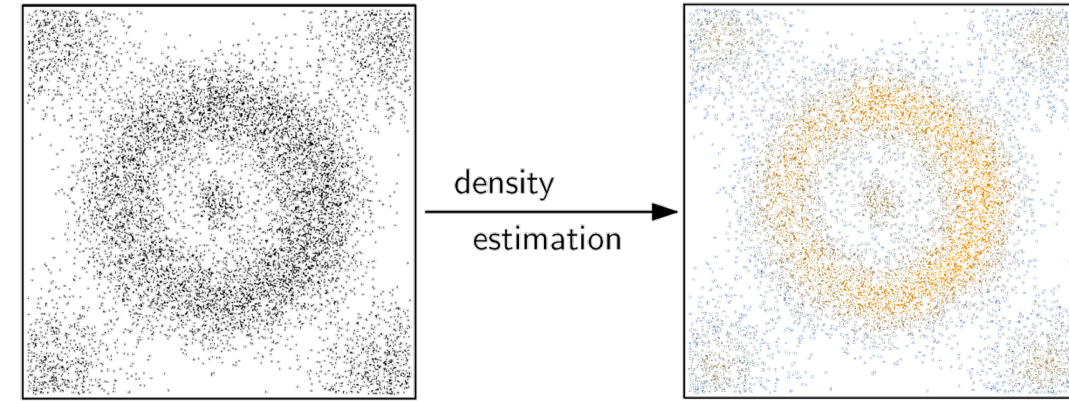
- peaks, valleys
- basins of attraction



# Motivating applications

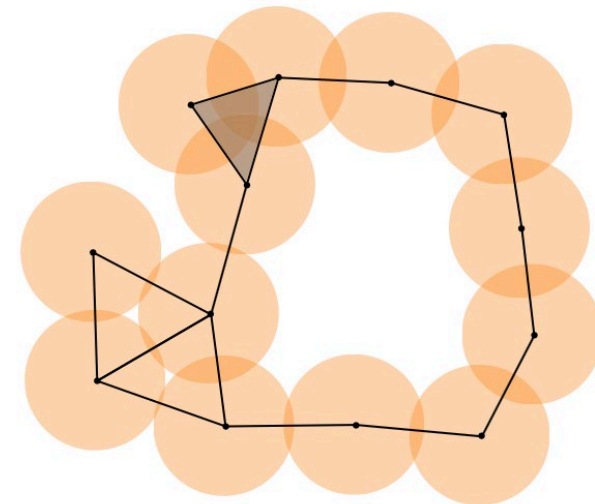
## Unsupervised learning

- Data (and function values) sampled from some unknown underlying distribution  $f$
- Obtain approximation through density estimator  $\hat{f}$
- Characterize peaks, valleys, basins of attraction



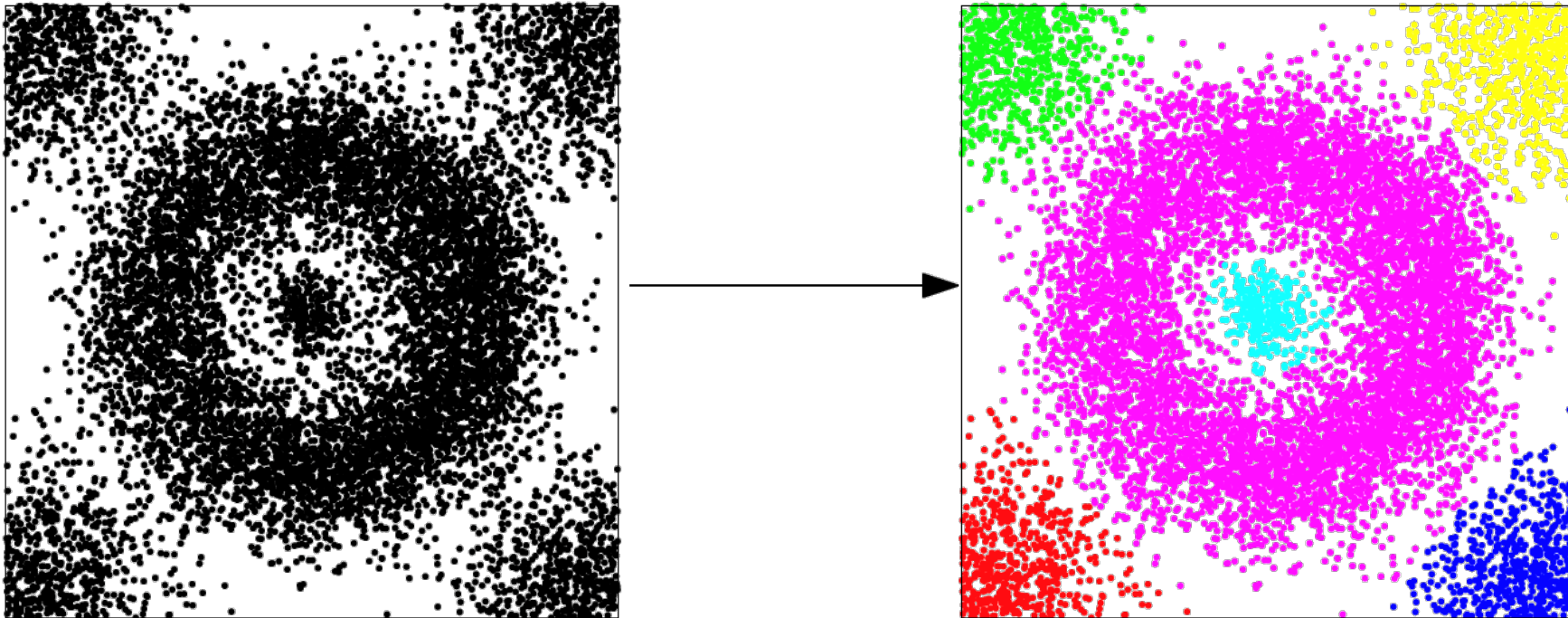
## Sensor networks

- Sensors distributed in some unknown area
- Measure some quantity  $f$
- Communicate with nearby sensors
- **Want:** to understand landscape of  $f$



# Cluster analysis

**Input:** a finite set of observations: - point cloud with coordinates  
- distance / (dis-)similarity matrix



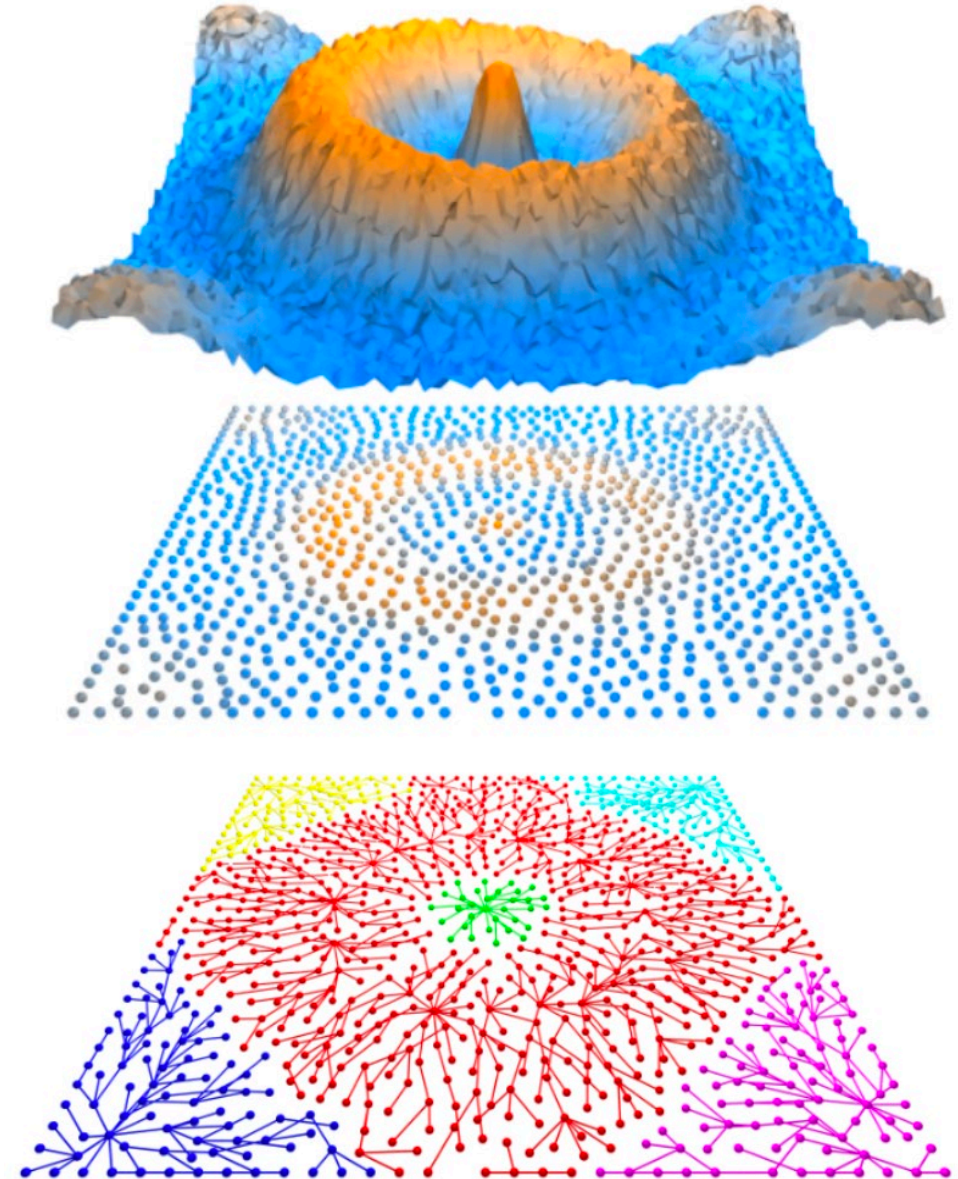
**Task:**

partition the data points into a collection of *relevant* subsets called clusters

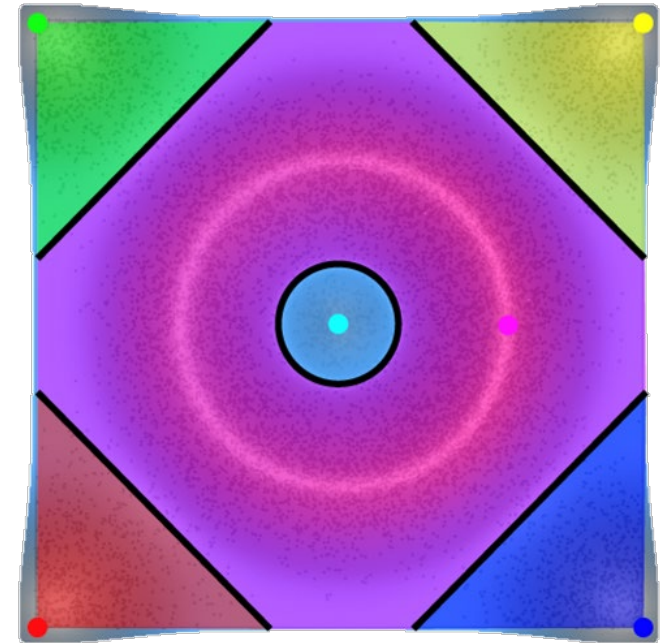
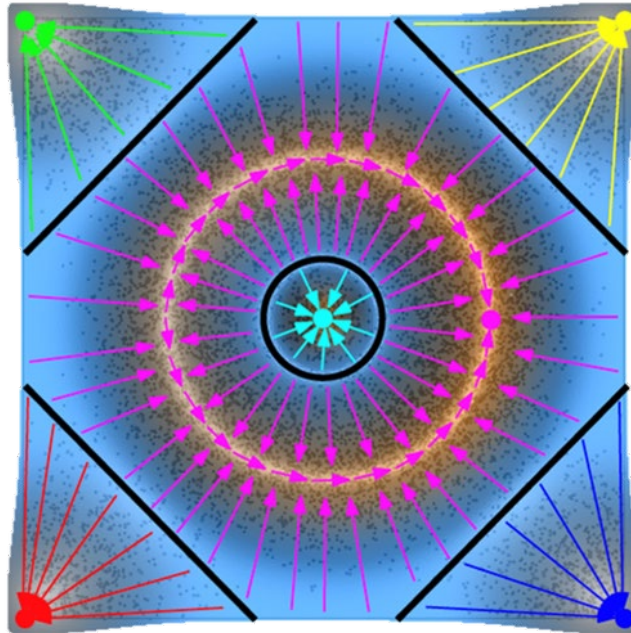
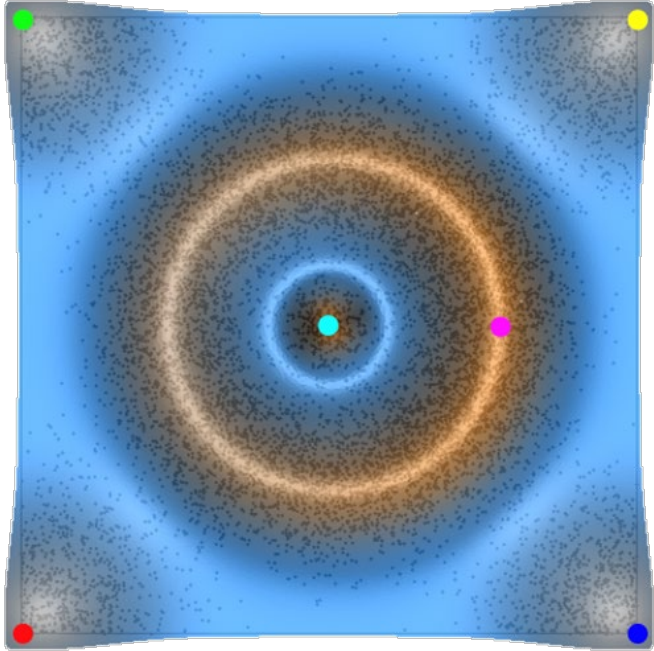
# Overview

## Mode-seeking paradigm (Mean-Shift and variants)

- Set local peaks of  $\hat{f}$  to be cluster centers
- Partition data according to basins of attraction, i.e. subsets of data that reach a cluster center by some greedy hill-climbing procedure
- Problem: can be highly unstable/unpredictable
- Proactive solution: apply smoothing before hill-climbing (but unclear how this affects output, e.g. number of clusters)
- *Reactive* solution: Use **topological persistence** to detect and merge clusters *after* computation

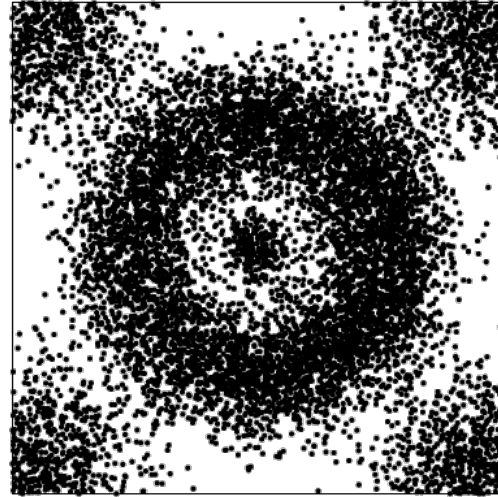


# Mode-seeking paradigm

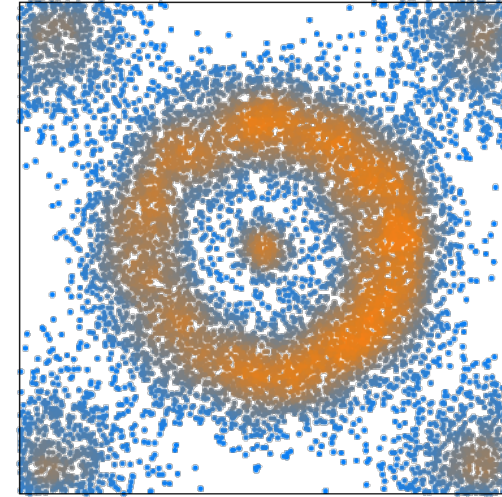


# Mean-Shift and variants

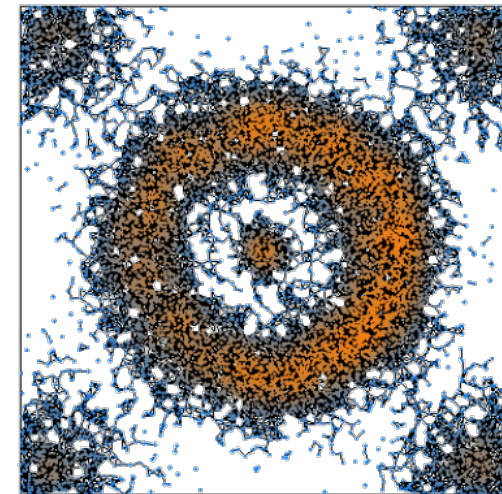
- Estimate density  $f$
- Build neighborhood graph (e.g. via Vietoris-Rips at scale  $\delta$ )
- Approximate gradient: at each vertex  $v$ , either connect  $v$  to neighbor with highest  $f$  value or declare  $v$  to be a peak
- Resulting collection of edges forms a spanning forest of the neighborhood graph



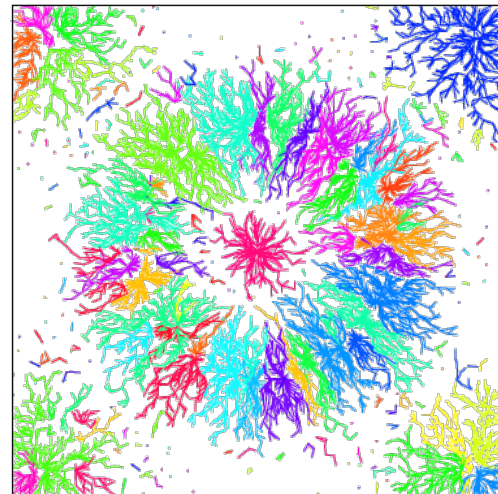
estimate density  
at the data points



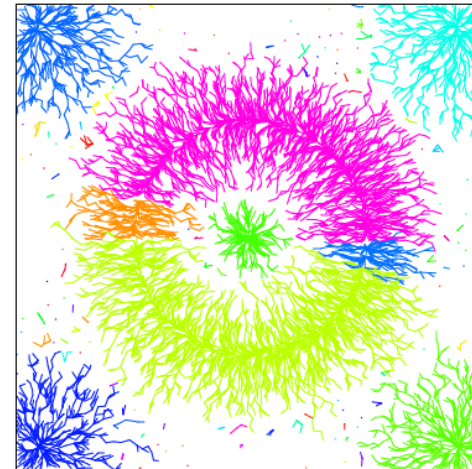
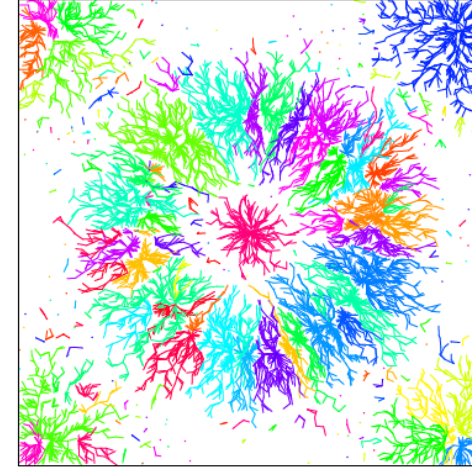
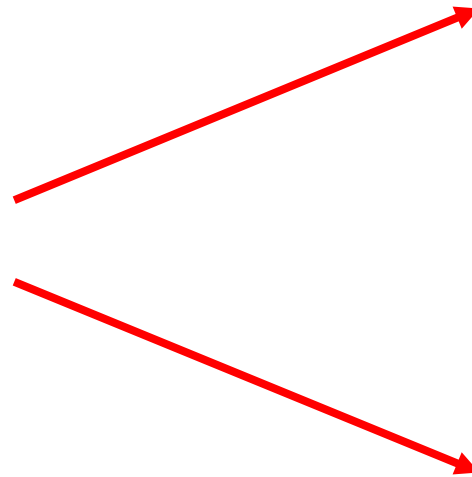
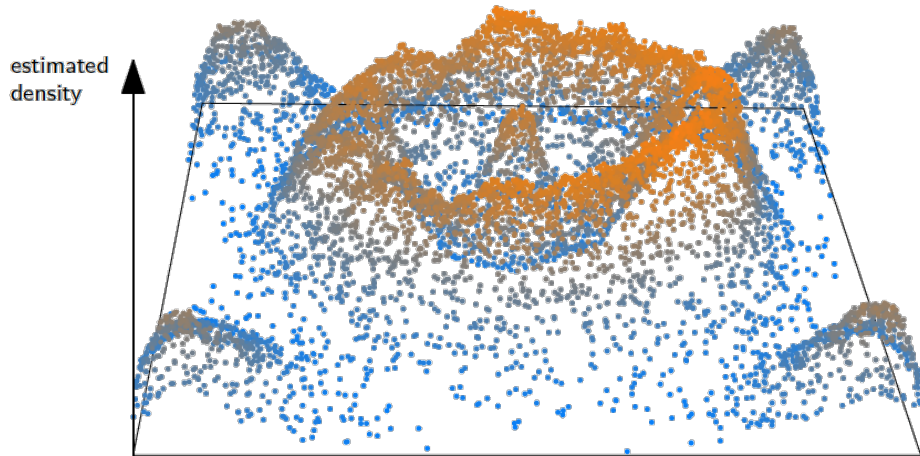
build neighborhood graph



approximate gradient  
by a graph edge  
at each data point



# Instability in density estimate can cause unstable output



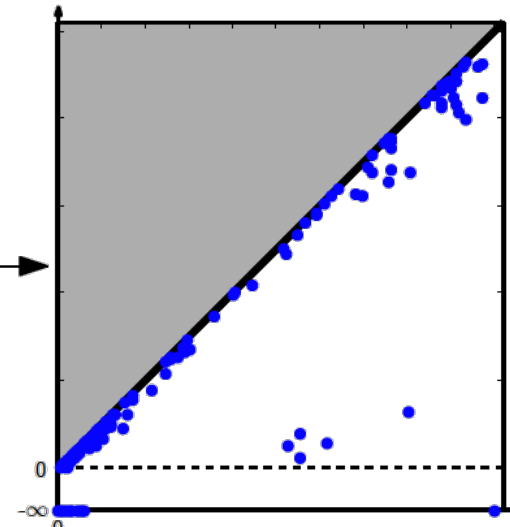
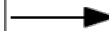
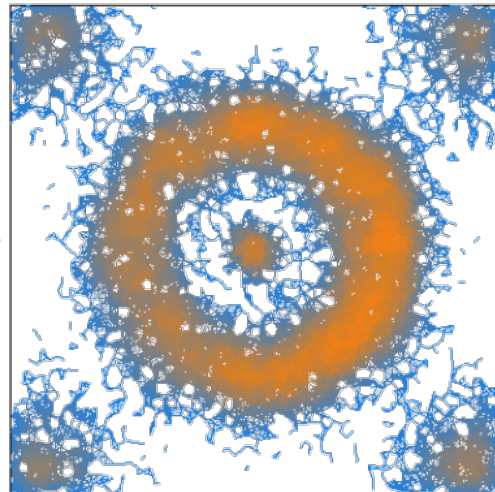
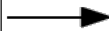
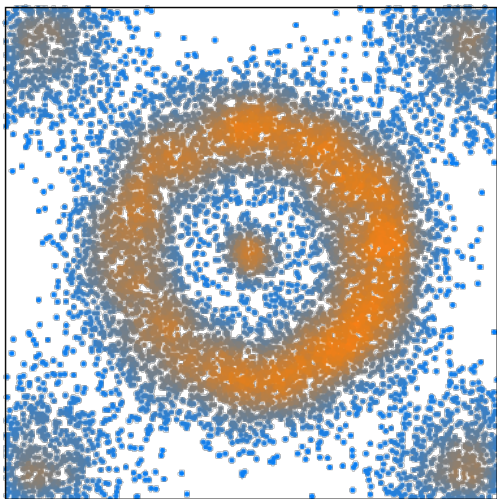
Sources of instability:

- Variations (noise) in density estimate
- Bad neighborhood graph

# Topological Mode Analysis Tool (ToMATo)

Chazal, Oudot, Skraba, Guibas *Persistence-Based Clustering in Riemannian Manifolds*

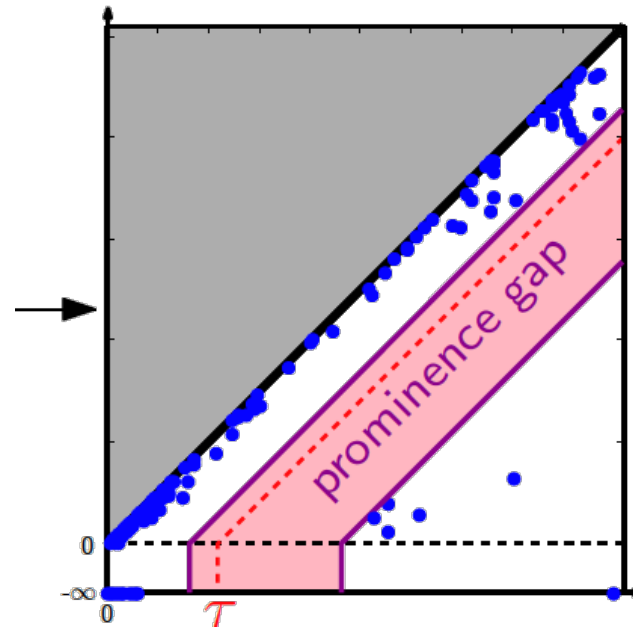
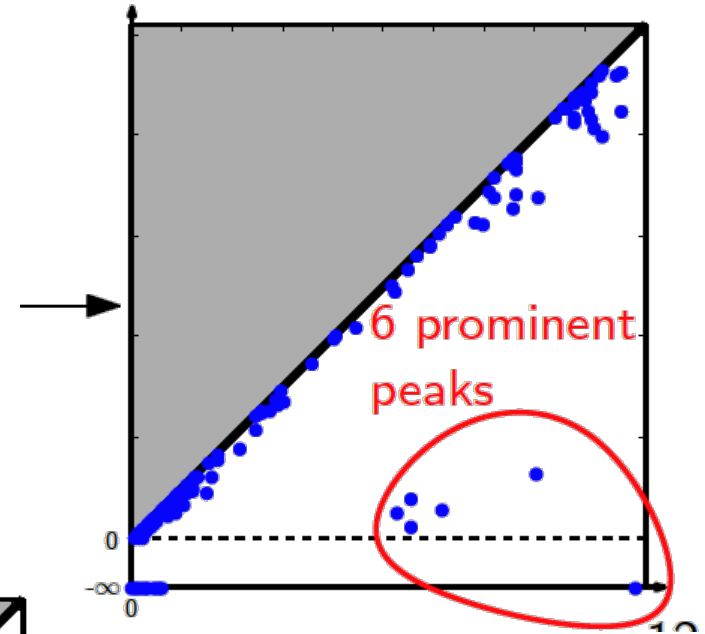
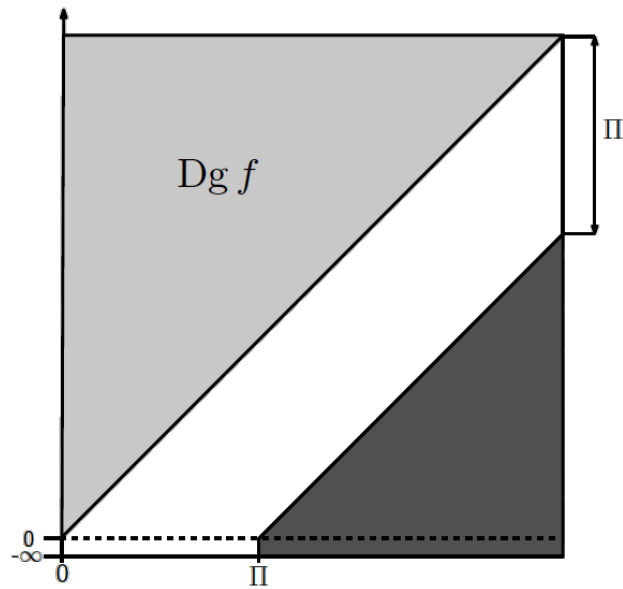
- Density estimator  $\hat{f}$  defines an order on the point cloud  
(sort data points by **decreasing** estimated density values)
- Extend order to the graph edges  $\rightarrow$  *upper-star filtration*  
( $\hat{f}([u, v]) = \min\{\hat{f}(u), \hat{f}(v)\}$ )
- Compute the 0-dimensional persistence diagram of this filtration  
(apply 0-dimensional persistence algorithm  $\rightarrow$  union-find data structure)



0-d persistence can be computed via Kruskal's minimum spanning tree algorithm + union-find data structure for  $O(\alpha(n) \cdot n^2)$  complexity, where  $\alpha(n)$  is an inverse Ackermann function

Q: Why the flipped diagram?

# Estimating the merge parameter

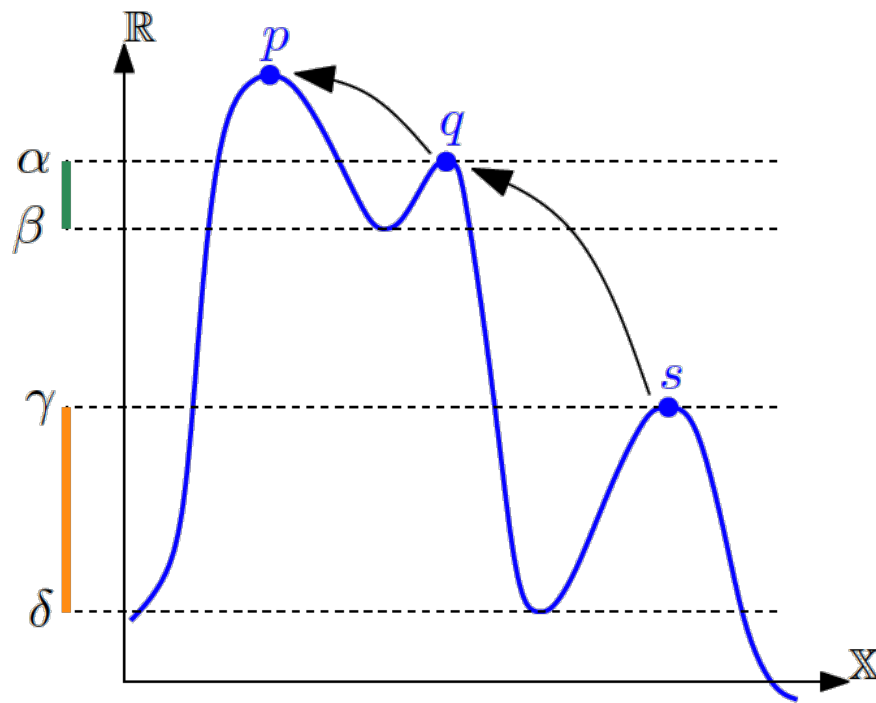


The gap parameter  $\tau$

# Merging clusters

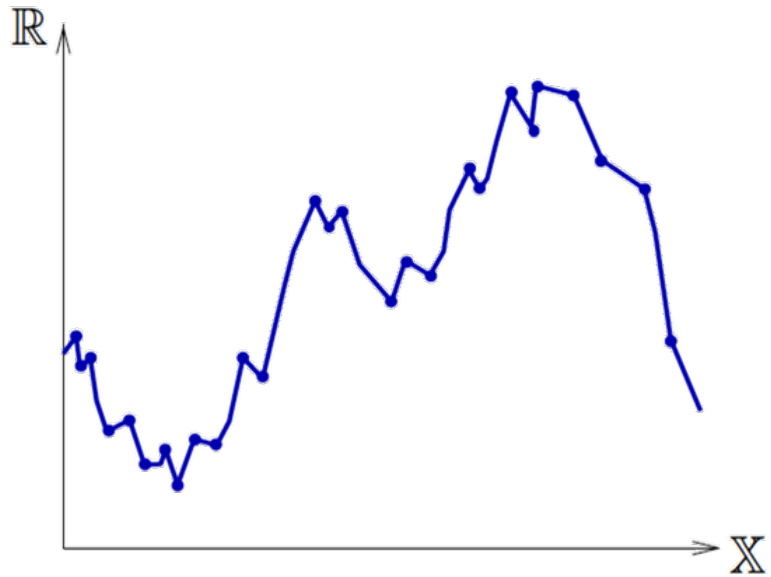
- 0-dimensional persistence builds a hierarchy of the peaks of  $\hat{f}$  (merge tree)
- merge clusters according to the hierarchy (merge each cluster into its parent)
- given a fixed threshold  $\tau \geq 0$ , only merge those clusters of prominence  $< \tau$

$$\gamma - \delta < \tau \leq +\infty$$



**Prominence** of a peak: Difference in height of peak and the level at which its basin of attraction meets that of a higher peak

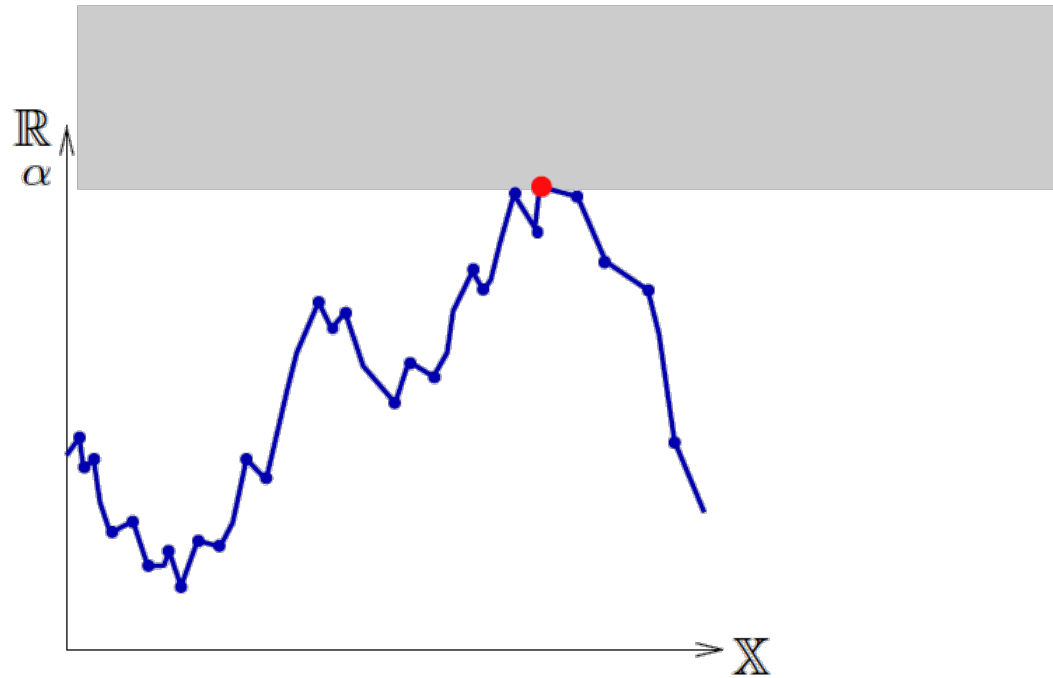
# Computing segments – another illustration



Merge clusters if prominence  $< \tau$

Keep separate otherwise

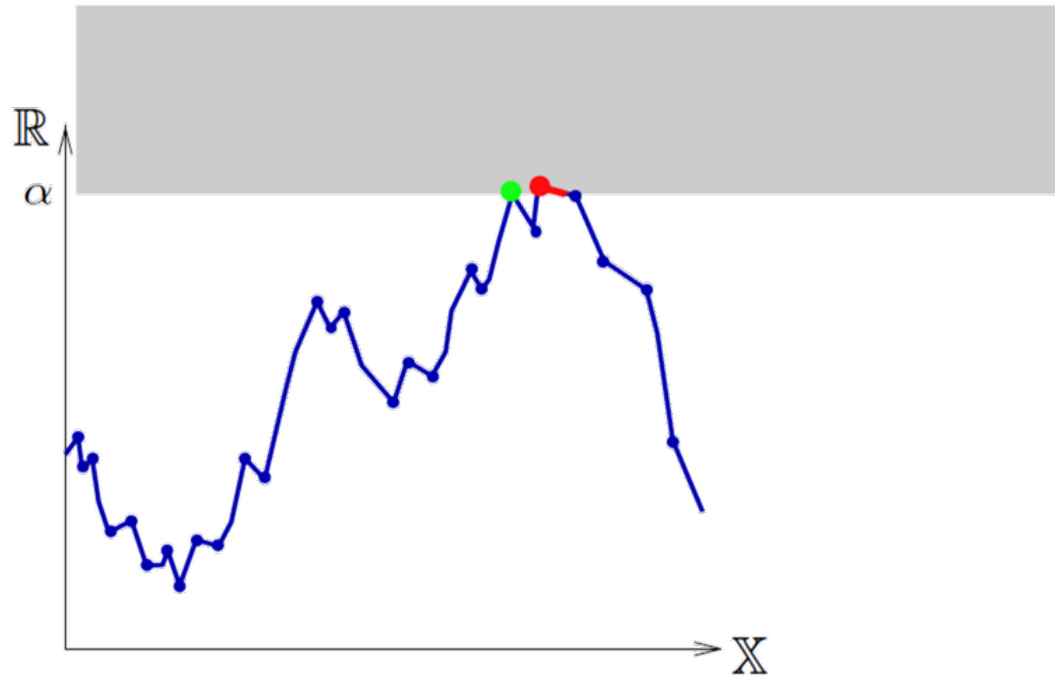
# Computing segments – another illustration



Merge clusters if prominence  $< \tau$

Keep separate otherwise

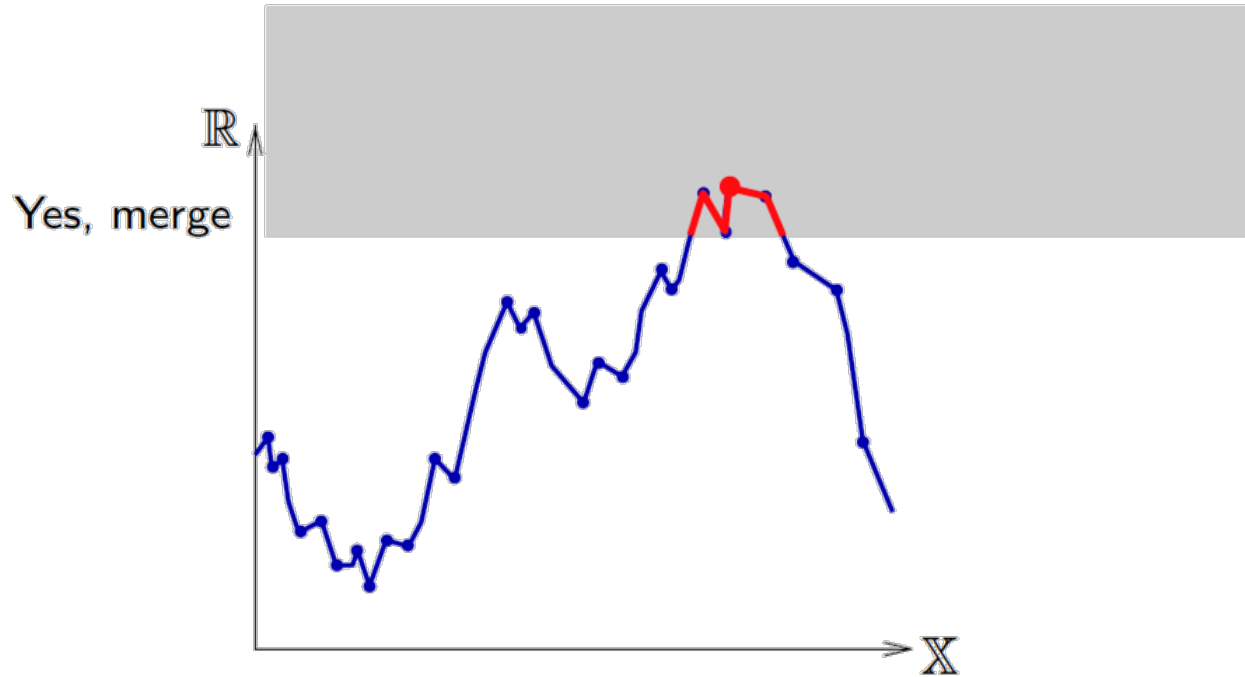
# Computing segments – another illustration



Merge clusters if prominence  $< \tau$

Keep separate otherwise

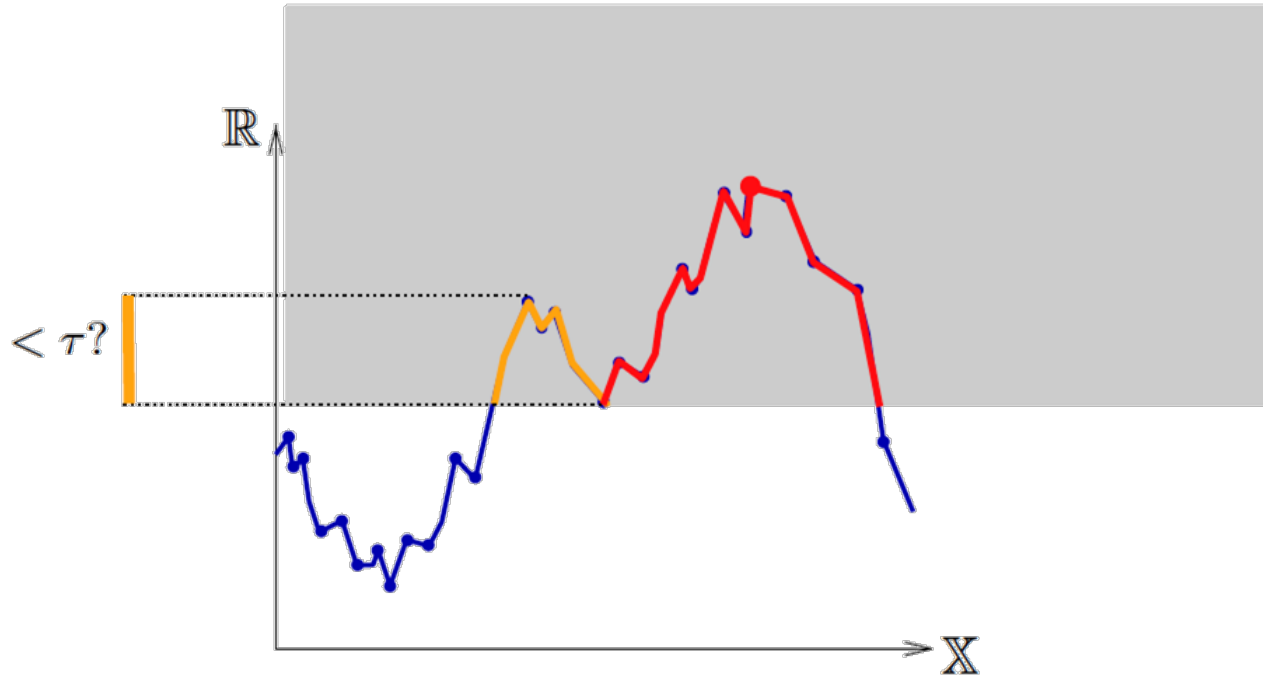
# Computing segments – another illustration



Merge clusters if prominence  $< \tau$

Keep separate otherwise

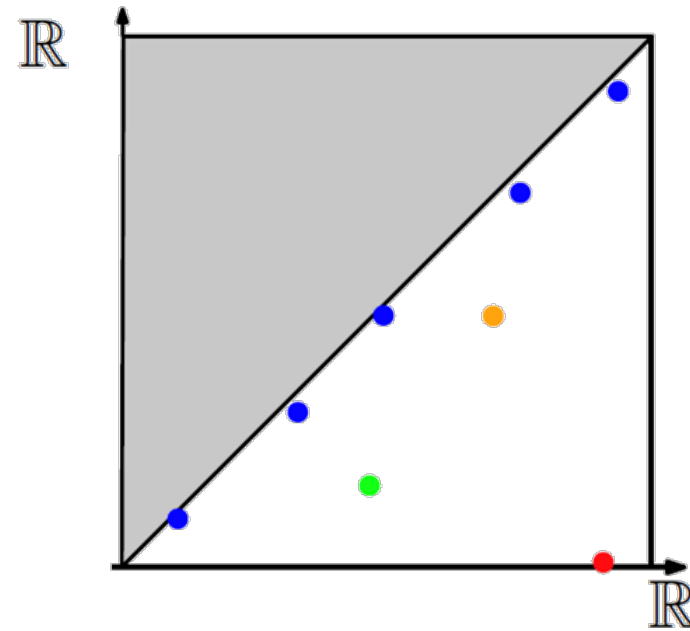
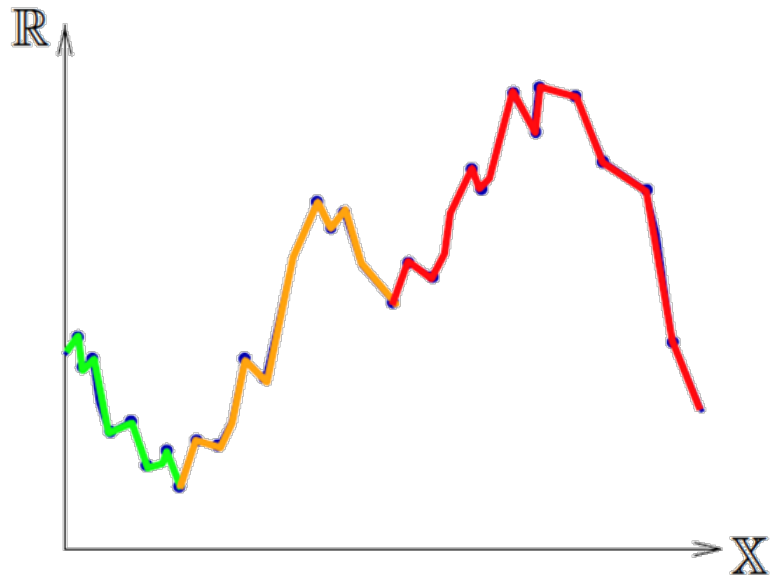
# Computing segments – another illustration



Merge clusters if prominence  $< \tau$

Keep separate otherwise

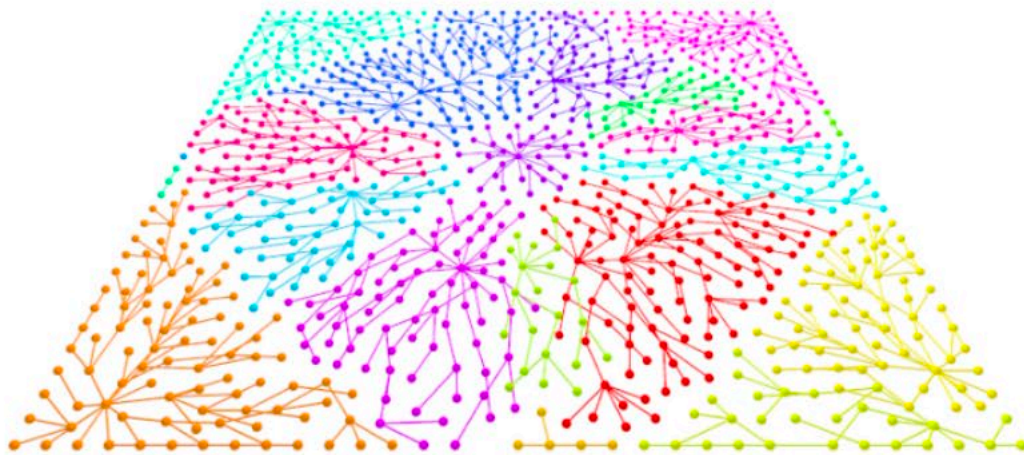
# Computing segments – another illustration



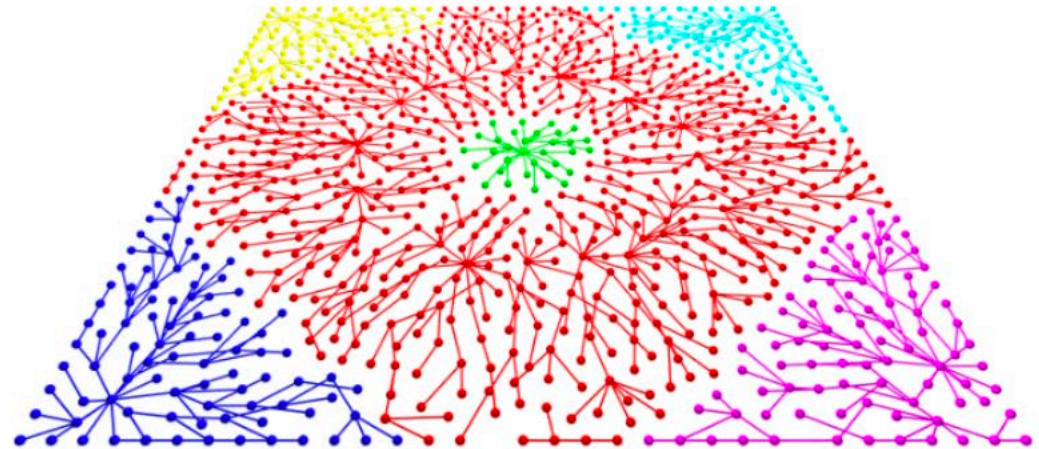
Merge clusters if prominence  $< \tau$

Keep separate otherwise

# Effect of persistence-guided cluster merging

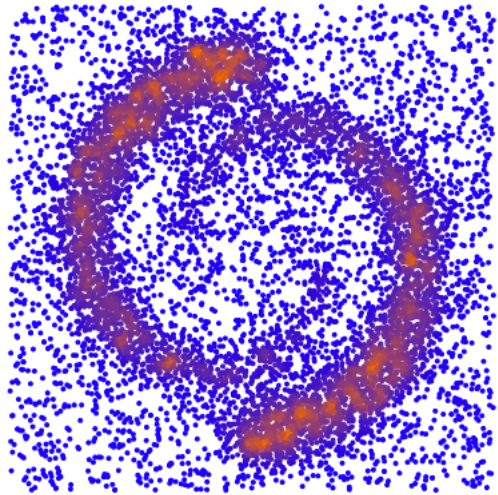


Output of hill climbing, before merge

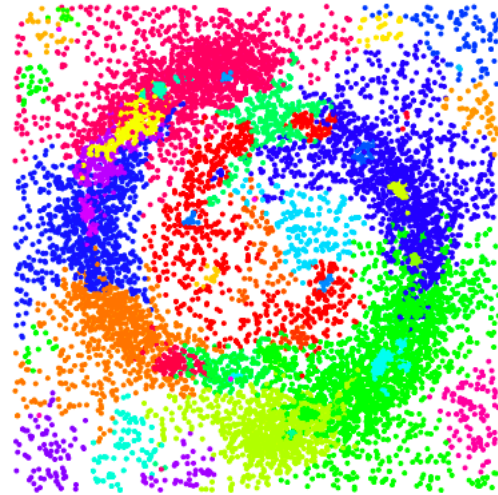


After merge

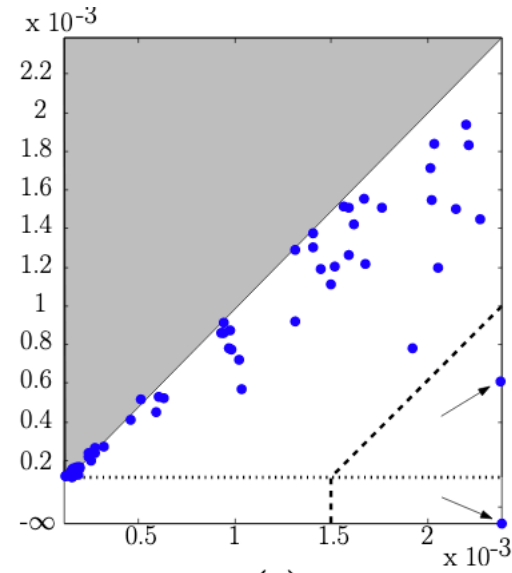
# Effect of persistence-guided cluster merging



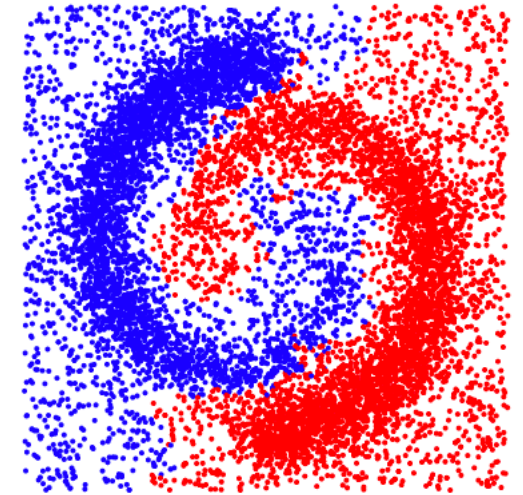
(a)



(b)



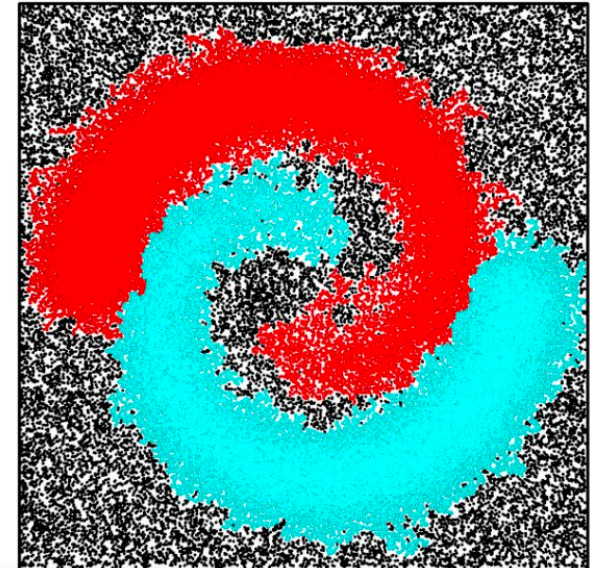
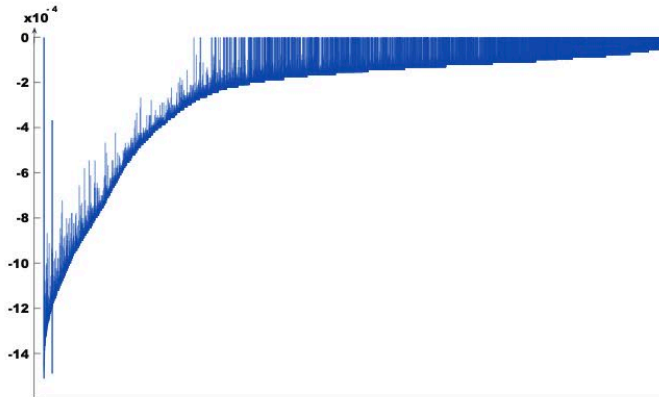
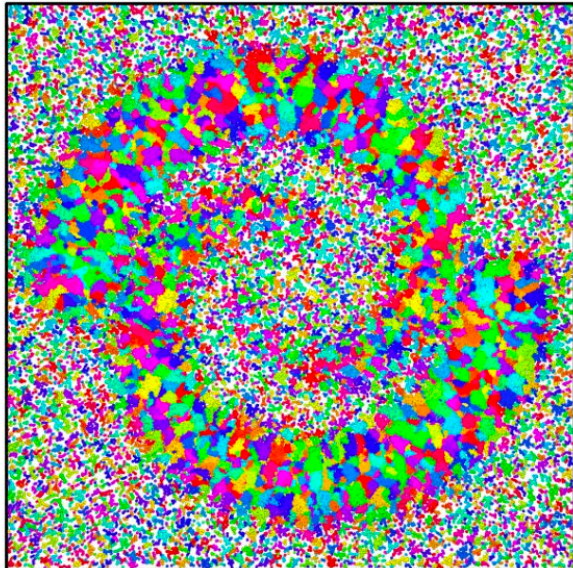
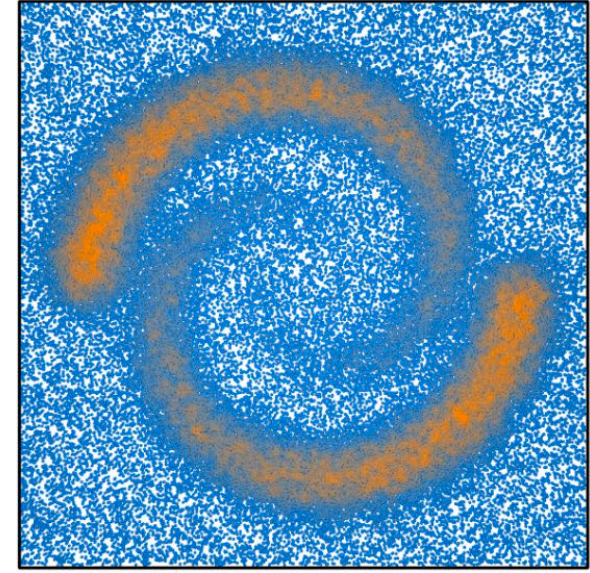
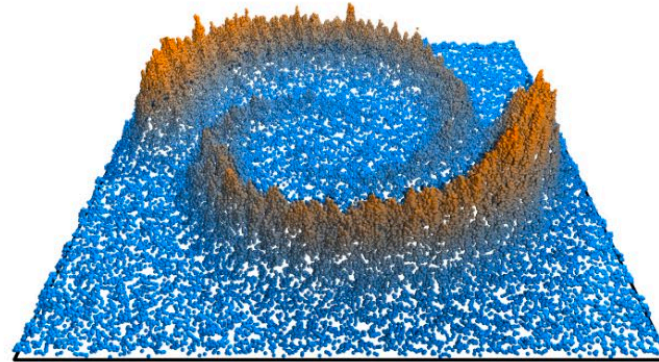
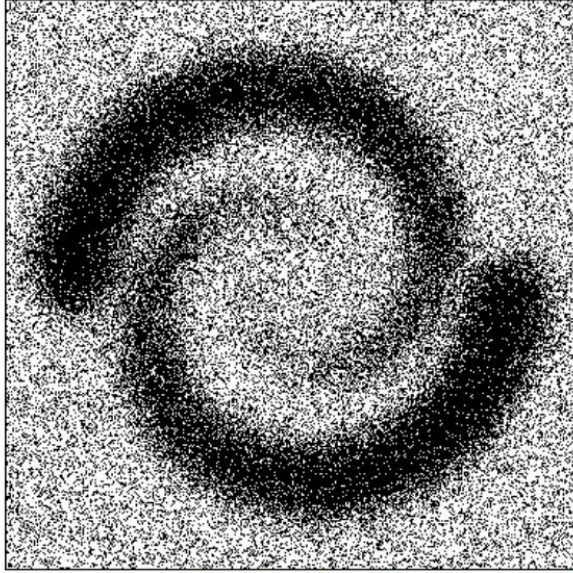
(c)



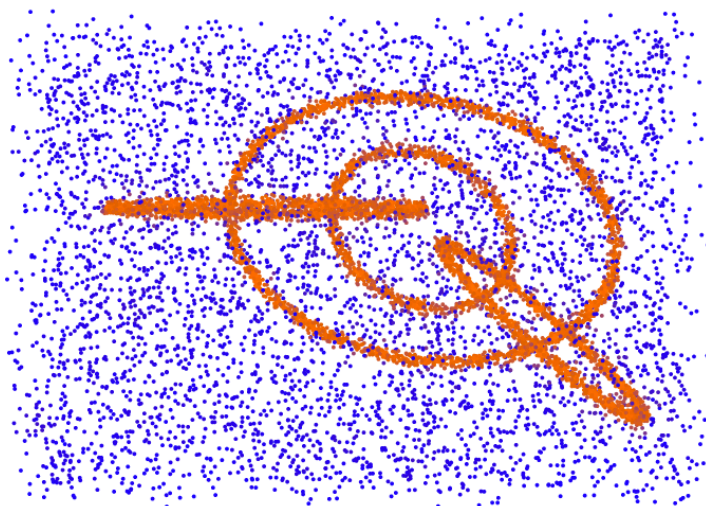
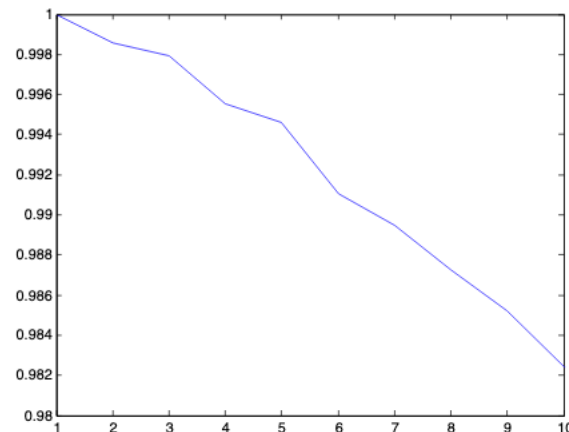
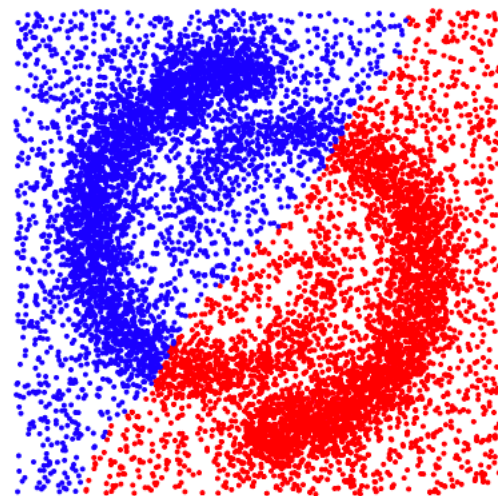
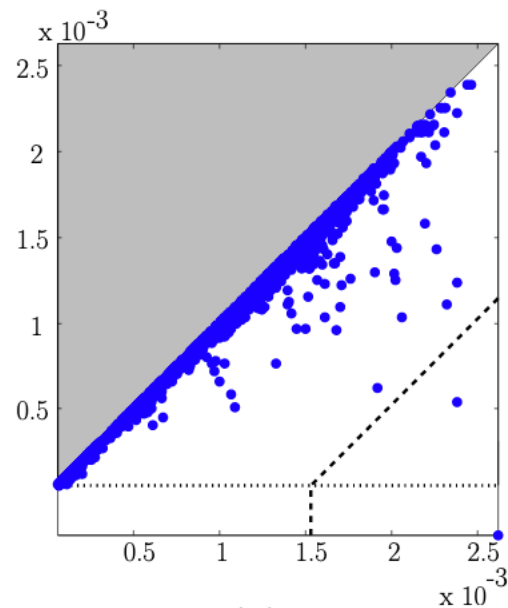
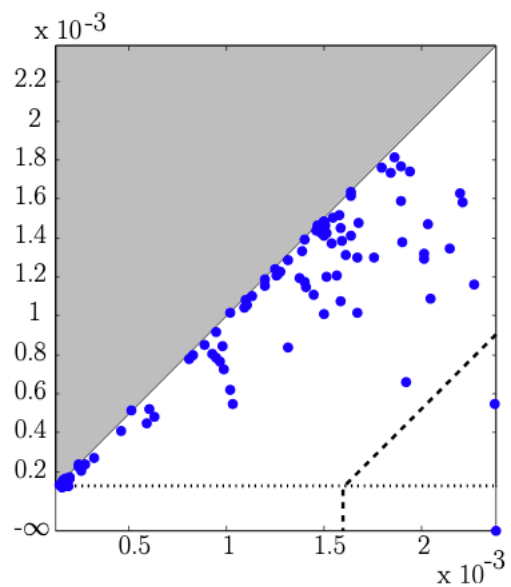
(d)

Theoretical guarantees available!

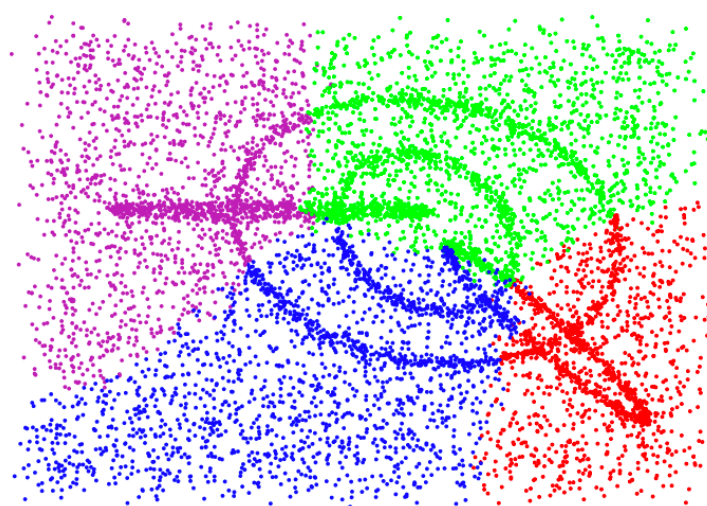
# Effect of persistence-guided cluster merging



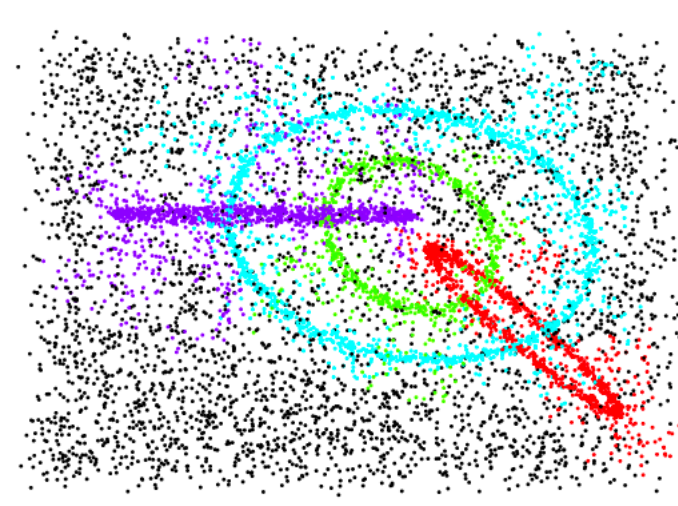
# Comparison to spectral clustering



Data



Spectral

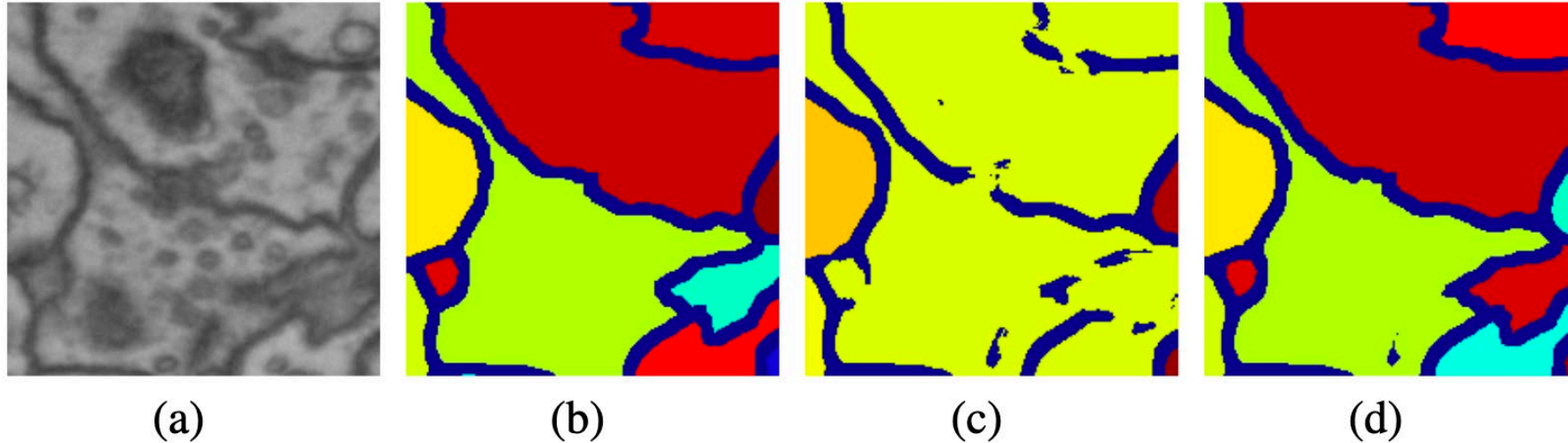


ToMATo

# Topological regularization for deep learning applications

# Topology for Image Segmentation

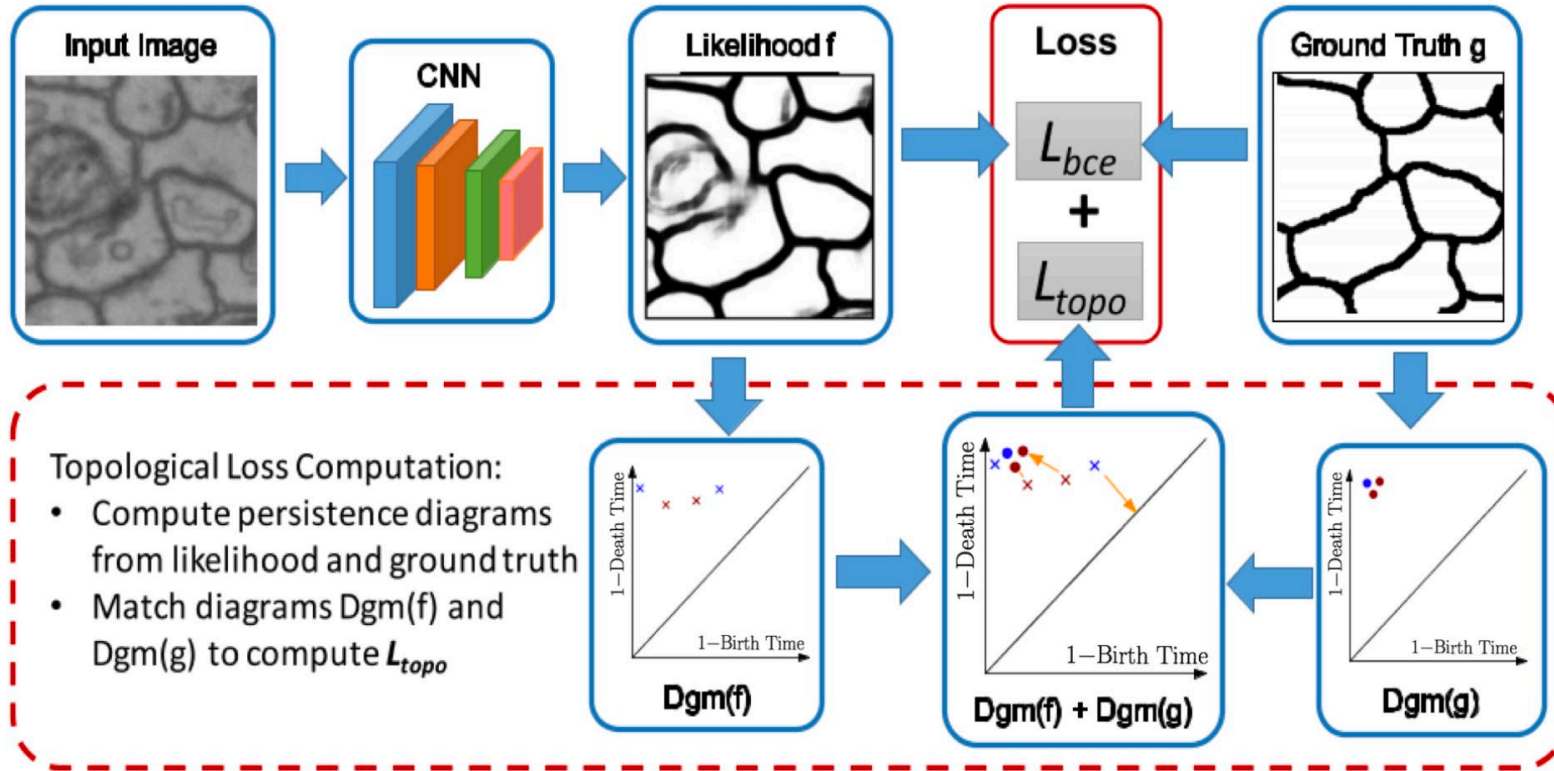
Hu, Fuxin, Samaras, Chen. *Topology-preserving deep image segmentation. NeuRIPS 2019*



- ◆ Segmentation errors in fine structures (e.g. membranes and vessels in biomedical imaging) introduce marginal per-pixel error, but major functional error
- ◆ Figure above: (a) input neuron image, (b) ground-truth segmentation, (c) baseline method without topological guarantees, (d) TopoLoss reconstruction
- ◆ Why *persistent* homology was needed: Betti numbers are discrete, but need a continuous, differentiable function for backprop---provided by persistent homology

# Pipeline

Hu, Fuxin, Samaras, Chen. *Topology-preserving deep image segmentation. NeuRIPS 2019*

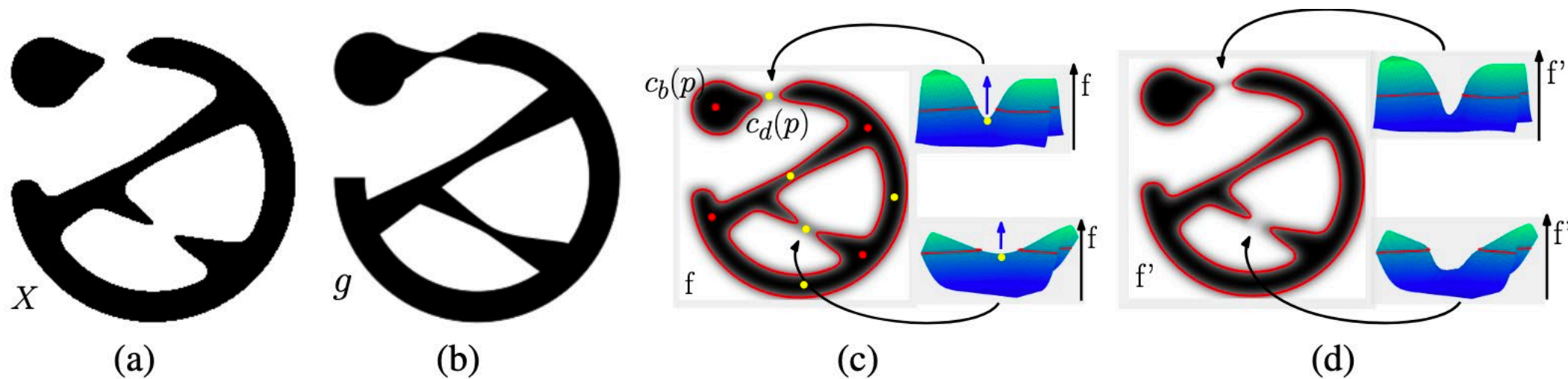


$f$  the likelihood map predicted by the network,  $g$  the ground truth,  $L_{ce}$  the cross-entropy loss,  $L_{topo}$  the topological loss,  $\lambda$  a regularization parameter. Loss function:

$$L(f, g) = L_{ce}(f, g) + \lambda L_{topo}(f, g)$$

# Superlevel set filtration on likelihood

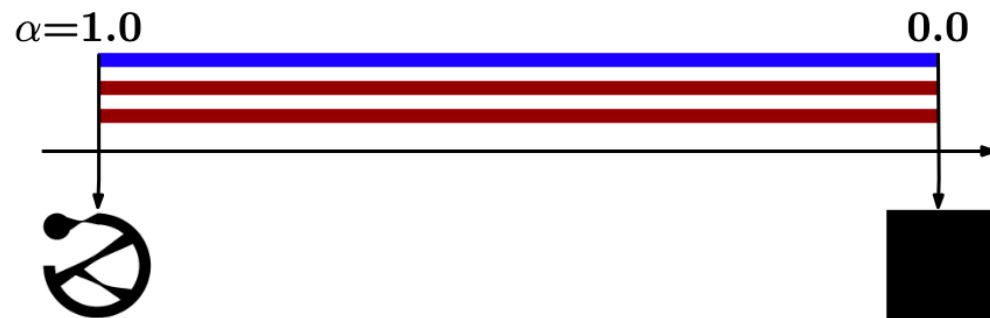
Hu, Fuxin, Samaras, Chen. *Topology-preserving deep image segmentation. NeuRIPS 2019*



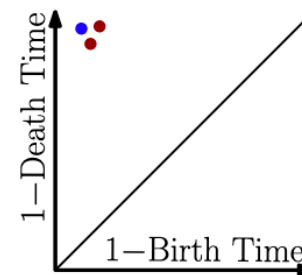
Note: likelihood maps are valued in  $[0,1]$

- (a) example segmentation  $X$  with one loop and two connected components
- (b) ground truth segmentation with two loops and one connected component---view  $g$  as binary  $\{0,1\}$ -valued map
- (c,d) likelihood maps  $f, f'$ , both produce segmentation  $X$  if we threshold at  $\alpha = 0.5$ . But  $f$  is closer to being correct, due to shallower gaps
- Conclusion: single threshold  $\alpha = 0.5$  not enough, but **persistent homology**  $\rightarrow$  all possible threshold values

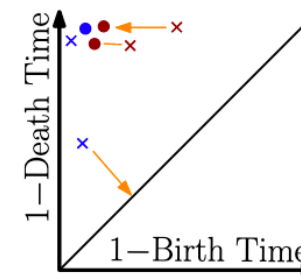
# Topological loss



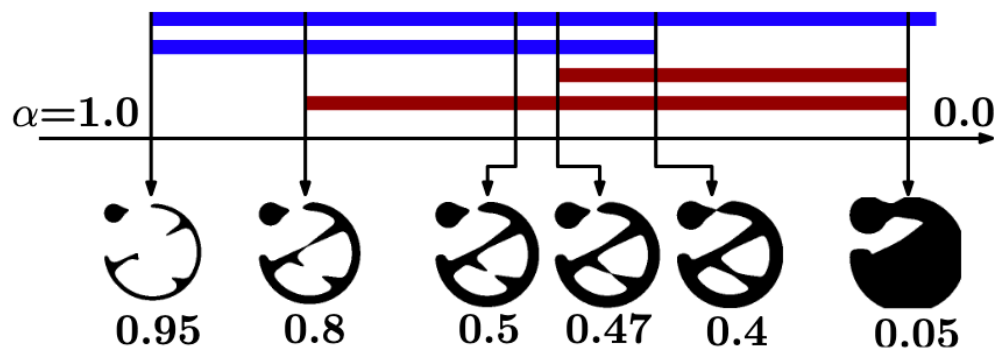
(a) Filtration induced by the ground truth function,  $g$ .



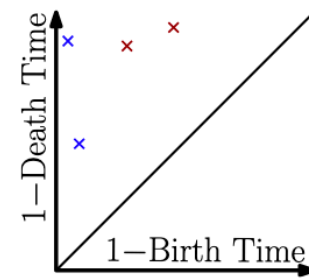
(b)  $Dgm(g)$



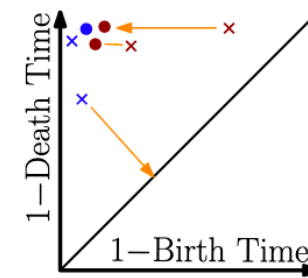
(c)  $Dgm(g)+Dgm(f)$



(d) Filtration induced by the likelihood function,  $f$ .



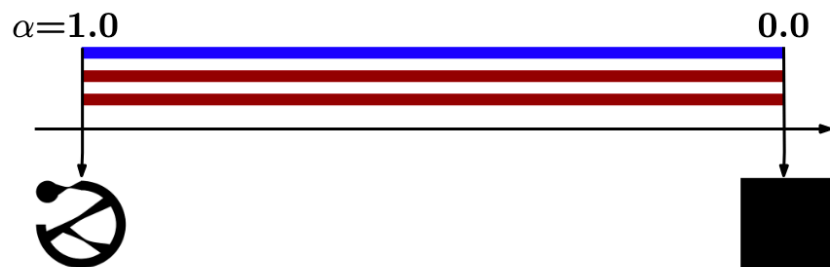
(e)  $Dgm(f)$



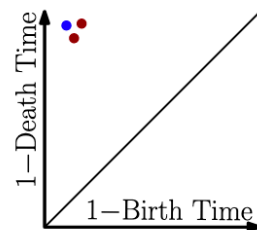
(f)  $Dgm(g)+Dgm(f')$

# Topological loss

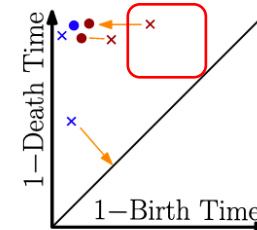
Hu, Fuxin, Samaras, Chen. *Topology-preserving deep image segmentation. NeuRIPS 2019*



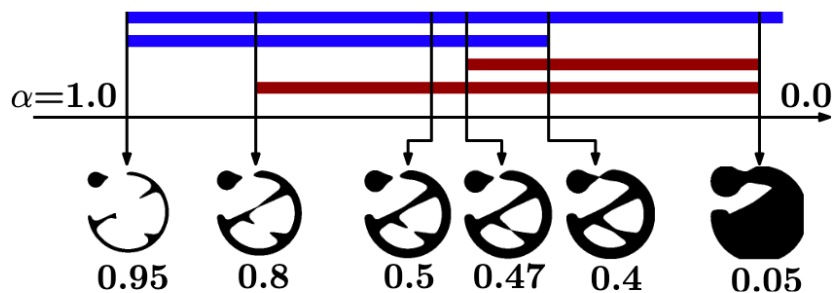
(a) Filtration induced by the ground truth function,  $g$ .



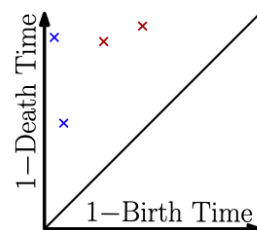
(b)  $Dgm(g)$



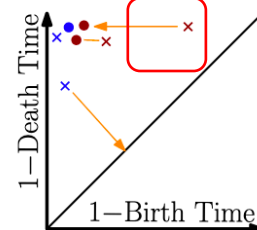
(c)  $Dgm(g)+Dgm(f)$



(d) Filtration induced by the likelihood function,  $f$ .



(e)  $Dgm(f)$



(f)  $Dgm(g)+Dgm(f')$

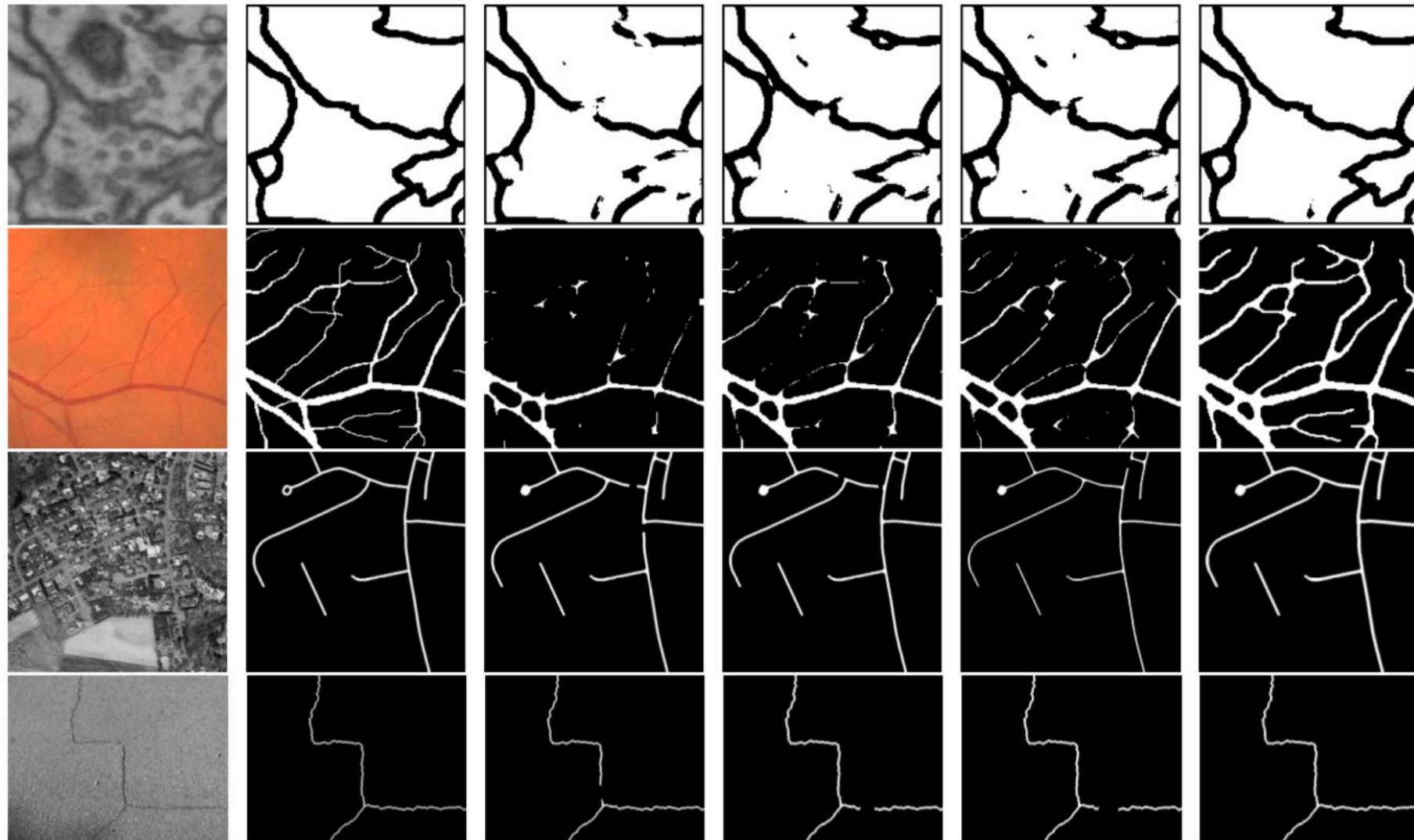
A slightly modified bottleneck distance:  $\gamma^*$  an optimal matching  $Dgm_k(f) \rightarrow Dgm_k(g)$ ,  $k \geq 0$ ,

$$L_{top}(f, g) = \sum_k \sum_{p \in Dgm_k(f)} \|p - \gamma^*(p)\|_2^2 = \sum_k \sum_{p \in Dgm_k(f)} [\text{birth}(p) - \text{birth}(\gamma^*(p))]^2 + [\text{death}(p) - \text{death}(\gamma^*(p))]^2$$

Intuition:  $L_{top}(f, g)$  measures the cost of changing  $f$  to look like  $g$ .

# Results

Hu, Fuxin, Samaras, Chen. *Topology-preserving deep image segmentation. NeuRIPS 2019*



Sample images

ground truth

DIVE '16

U-Net '15

Mosin '18

**TopoLoss'19**

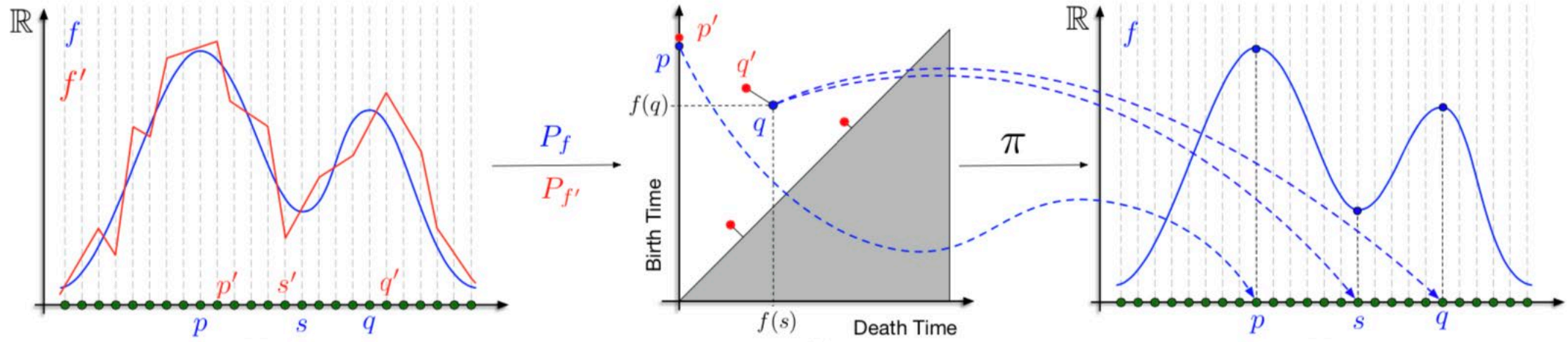
# A closer look at the topological loss

Poulenard, Skraba, Ovsjanikov. *Topological Function Optimization for Continuous Shape Matching*. SGP '18

- ◆ Neural network parameters  $\alpha$  produced a likelihood function  $f$
- ◆ Superlevel set filtration of  $f$  created a persistence diagram  $\text{Dgm}(f)$
- ◆ Consider functional  $\mathcal{L} := L_{top}(-, g)$ , where  $g$  is the ground truth function and  $L_{top}$  measures the cost of matching  $\text{Dgm}(-)$  to  $\text{Dgm}(g)$
- ◆ Want to optimize  $f$  to minimize  $L_{top}(f, g)$ , i.e. need gradient  $\nabla_{\alpha} \mathcal{L}$
- ◆ First step: for a point  $(b, d)$  in a persistence diagram, compute:  
$$\frac{\partial b}{\partial \alpha} \quad \text{and} \quad \frac{\partial d}{\partial \alpha}$$
- ◆ Strategy:  $(b, d)$  came from a pairing  $(\sigma, \tau)$ ---use this!

# Gradients for persistence diagrams

Poulenard, Skraba, Ovsjanikov. *Topological Function Optimization for Continuous Shape Matching*. SGP '18



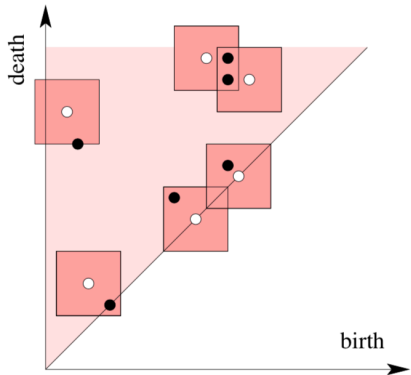
$$\zeta: (b, d) \rightarrow (\sigma, \tau), \quad \eta: \sigma \rightarrow v_\sigma \text{ where } v_\sigma \in \arg \min_{v \in \sigma} f(v)$$

$$\pi := (\eta, \eta) \circ \zeta \quad \text{“reverse” map from persistence diagram to pairs of vertices}$$

By stability,  $\pi$  remains unchanged for small perturbations of the diagram, and so:

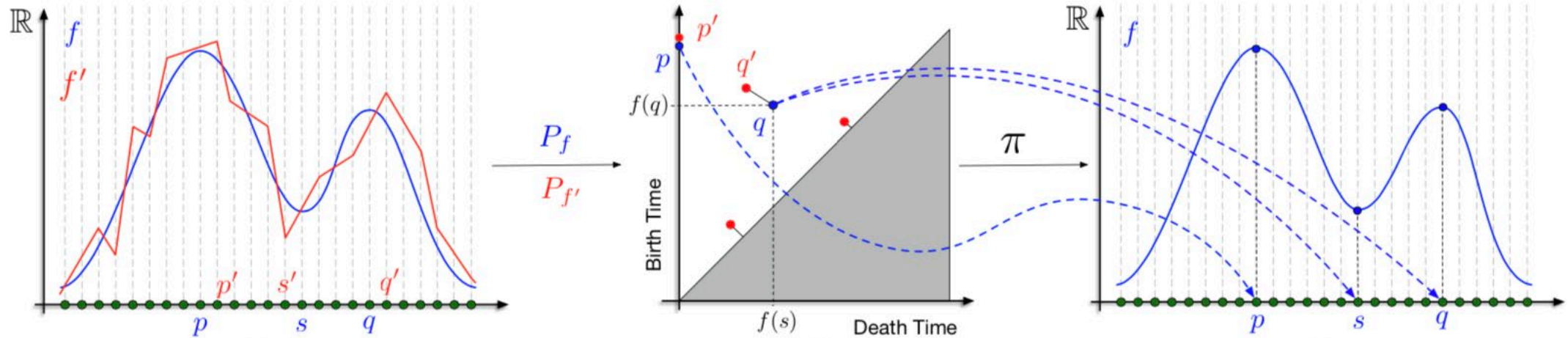
$$\frac{\partial b}{\partial \alpha} = \frac{\partial f(\pi(b))}{\partial \alpha} = \frac{\partial f(v_\sigma)}{\partial \alpha}, \text{ and similarly } \frac{\partial d}{\partial \alpha} = \frac{\partial f}{\partial \alpha}(v_\tau)$$

**Conclusion:** “the derivative (of the diagram) is equivalent to the derivative of the function evaluated at the image of the map  $\pi$ ”



# Gradients for persistence diagrams

Poulenard, Skraba, Ovsjanikov. *Topological Function Optimization for Continuous Shape Matching*. SGP '18

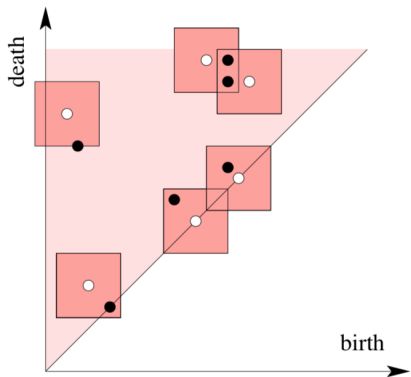


By chain rule, we have  $\frac{\partial \mathcal{L}}{\partial \alpha} = \sum_{(b_i, d_i) \in Dgm(f)} \frac{\partial \mathcal{L}}{\partial b_i} \frac{\partial b_i}{\partial \alpha} + \frac{\partial \mathcal{L}}{\partial d_i} \frac{\partial d_i}{\partial \alpha}$

Let  $\gamma^*(b_i), \gamma^*(d_i)$  denote the birth-death pair of the ground truth  $g$  that  $(b_i, d_i)$  is matched to. From before, we had:

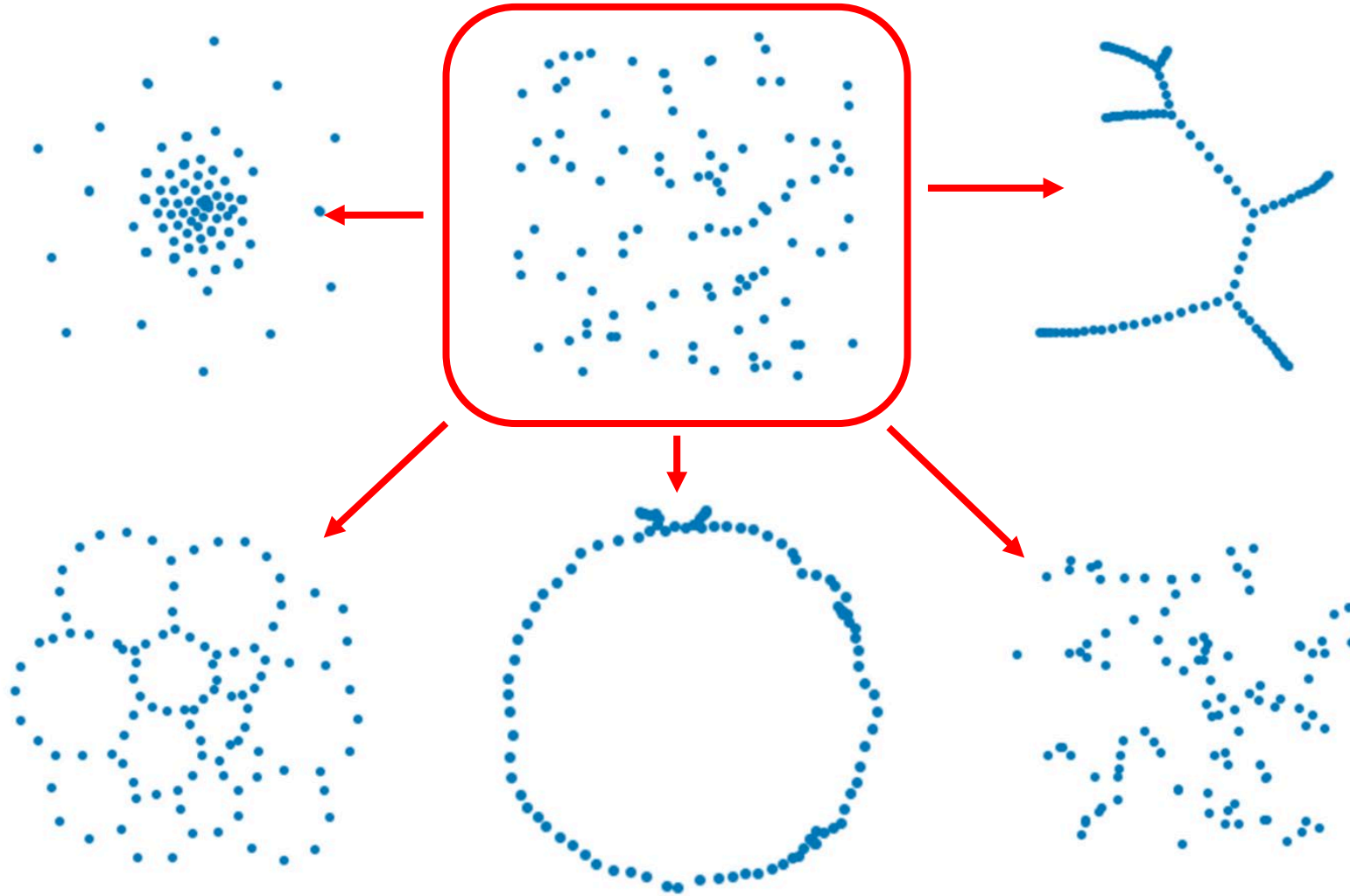
$\frac{\partial \mathcal{L}}{\partial b_i} = \frac{\partial}{\partial b_i} \sum_i [b_i - \gamma^*(b_i)]^2 = 2[b_i - \gamma^*(b_i)]$ , and likewise for  $\frac{\partial \mathcal{L}}{\partial d_i}$ . Summarizing,

$$\frac{\partial \mathcal{L}}{\partial \alpha} = 2 \sum_i (b_i - \gamma^*(b_i)) \frac{\partial f}{\partial \alpha}(v_\sigma) + 2 \sum_i (d_i - \gamma^*(d_i)) \frac{\partial f}{\partial \alpha}(v_\tau)$$



# Topological noise reduction

Bruel-Gabrielsson, Nelson, Dwaraknath, Skraba, Guibas, Carlsson, *A topology layer for machine learning*. AISTATS 2020



# Topological time series analysis for video data

# Sliding window embeddings

Chris Tralie and Jose Perea, *(Quasi)Periodicity Quantification in Video Data, Using Topology*

- Consider a video dataset as time-series data. I.e. fix integers  $W$  (width) and  $H$  (height), and consider the function (for grayscale videos):

$$X: \mathbb{N} \rightarrow \mathbb{R}^{W \times H}, \text{ or, via interpolation, } X: \mathbb{R}_+ \rightarrow \mathbb{R}^{W \times H}$$

- Fix  $\tau > 0$  (delay) and  $d \in \mathbb{Z}_{\geq 0}$  (dimension). The **sliding window embedding** of  $X$  at time  $t$  and with parameters  $d$  and  $\tau$  is:

$$SW_{d,\tau}X(t) = \begin{bmatrix} X(t) \\ X(t + \tau) \\ X(t + 2\tau) \\ \vdots \\ X(t + d\tau) \end{bmatrix} \in \mathbb{R}^{W \times H \times (d+1)}$$

- Sliding window embedding converts time series data into point cloud data

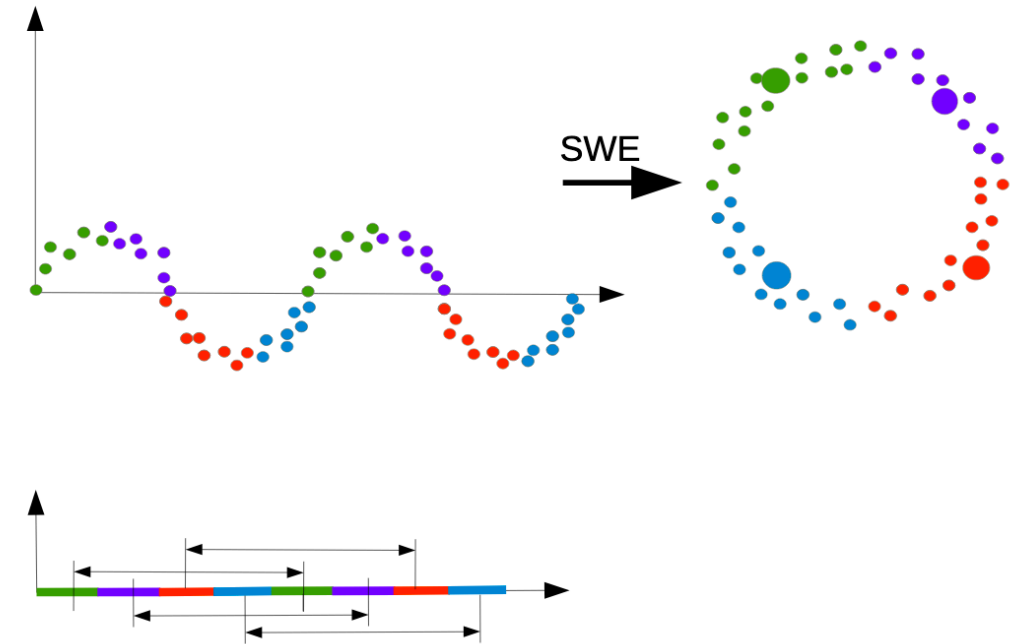


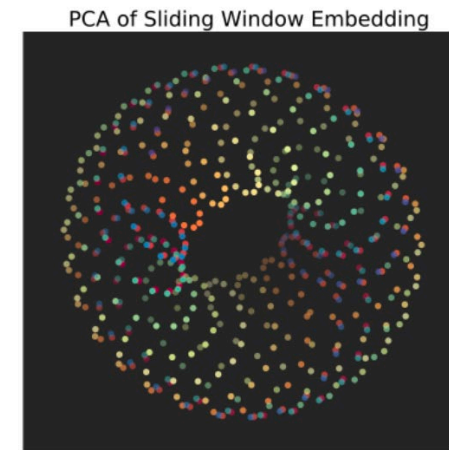
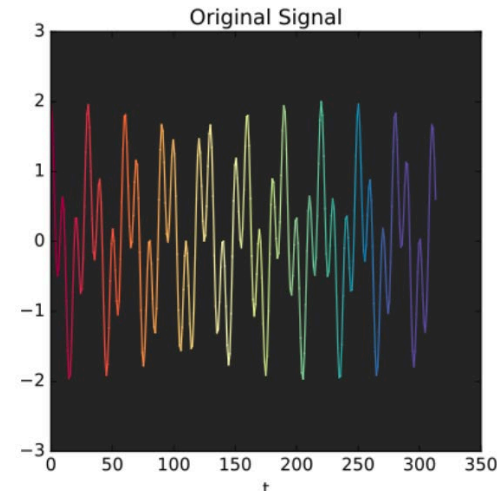
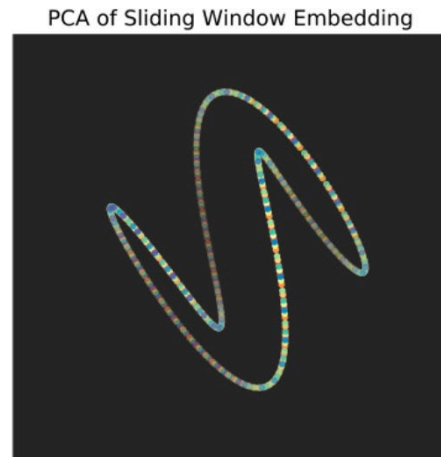
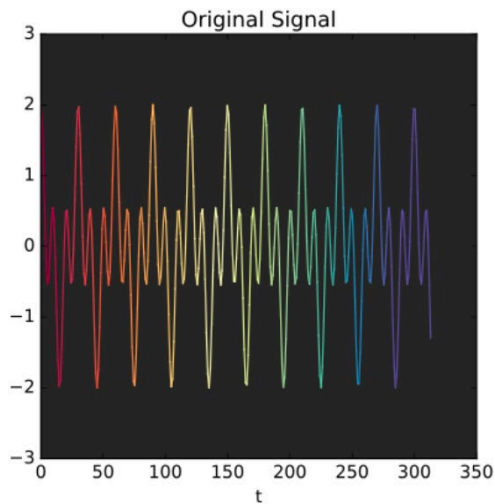
Figure from Dlotko, Qiu, Rudin, *Cyclicality, Periodicity, and the Topology of Time Series*

# Geometry missed by the power spectrum

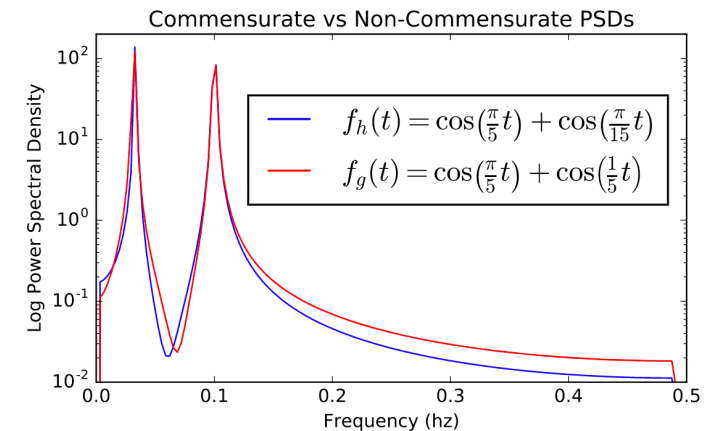
Chris Tralie and Jose Perea, *(Quasi)Periodicity Quantification in Video Data, Using Topology*

- ◆ SWEs reveal topology and geometry that are ignored by conventional methods. Consider two functions

$$f_h(t) = \cos\left(\frac{\pi}{5}t\right) + \cos\left(\frac{\pi}{15}t\right), \quad f_q(t) = \cos\left(\frac{\pi}{5}t\right) + \cos\left(\frac{1}{5}t\right)$$



- ◆ Clear differences in topology and geometry, but the power spectrum does not see this

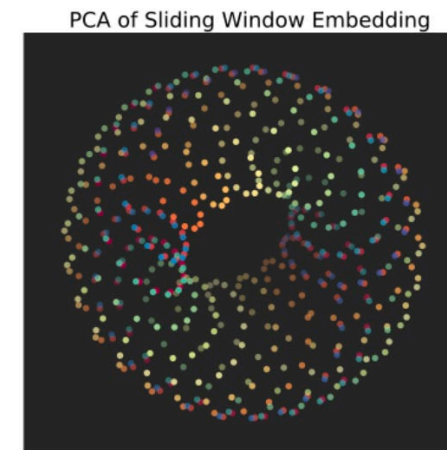
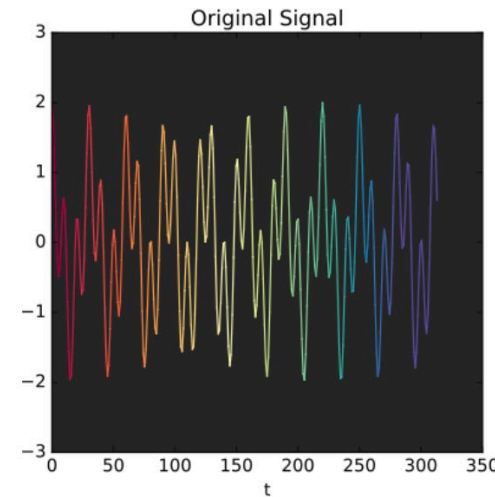
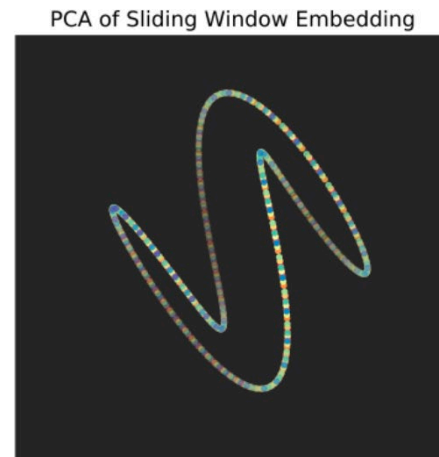
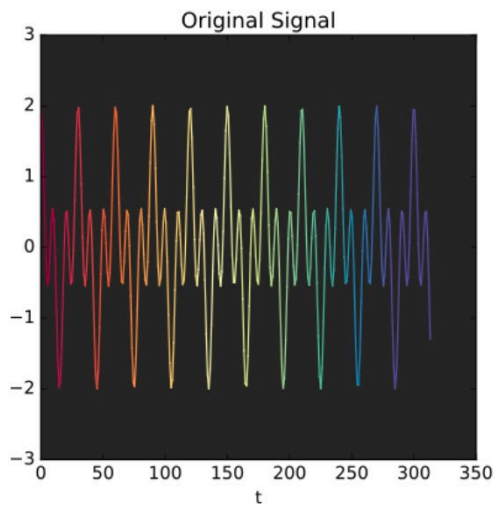


# Periodic and quasiperiodic functions have distinct topology

Chris Tralie and Jose Perea, *(Quasi)Periodicity Quantification in Video Data, Using Topology*

$$f_h(t) = \cos\left(\frac{\pi}{5}t\right) + \cos\left(\frac{\pi}{15}t\right), \quad f_q(t) = \cos\left(\frac{\pi}{5}t\right) + \cos\left(\frac{1}{5}t\right)$$

- ◆ To say  $f_h$  is periodic means the constituent frequencies  $\frac{1}{10}$  and  $\frac{1}{30}$  are linearly dependent (**commensurate**) over  $\mathbb{Q}$ , and to say  $f_q$  is quasiperiodic means the constituent frequencies  $\frac{1}{10}, \frac{1}{10\pi}$  are linearly independent (**incommensurate**) over  $\mathbb{Q}$

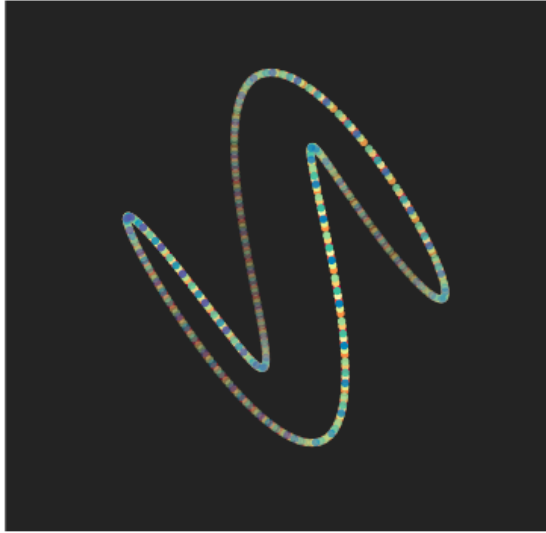


- ◆ **Theorem (Perea, Harer '15):** Given a periodic function  $f: [0, 2\pi] \rightarrow \mathbb{R}$  with  $N$  harmonics, the sliding window embedding  $SW_{d,\tau}f$  (for  $d, \tau$  in prescribed ranges) is a **topological circle** that wraps around an  $N$ -dimensional torus  $\mathbb{T}^N$ . On the other hand, given a quasiperiodic function with  $N$  incommensurate harmonics, the sliding window embedding is **dense in  $\mathbb{T}^N$** , i.e. it fills out the  $N$ -torus.

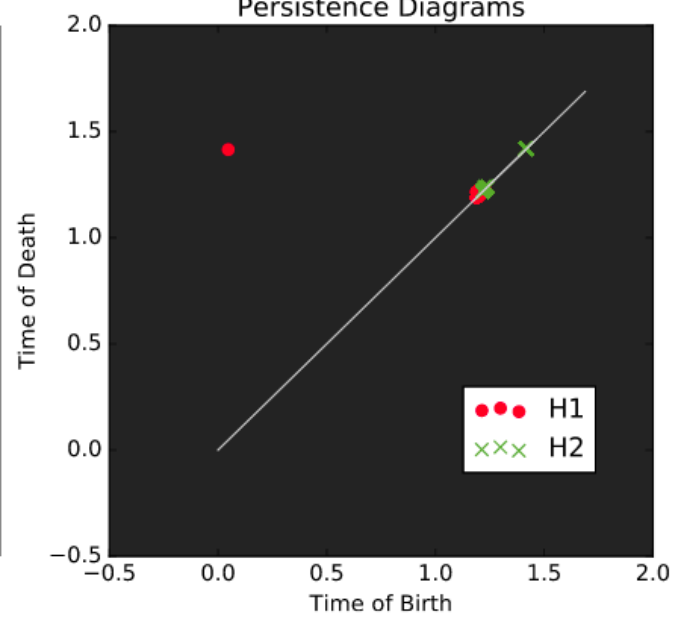
# An application of persistent $H_2$

Chris Tralie and Jose Perea, *(Quasi)Periodicity Quantification in Video Data, Using Topology*

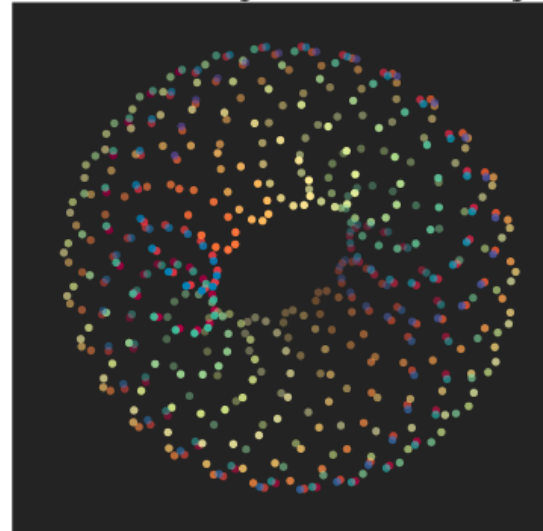
PCA of Sliding Window Embedding



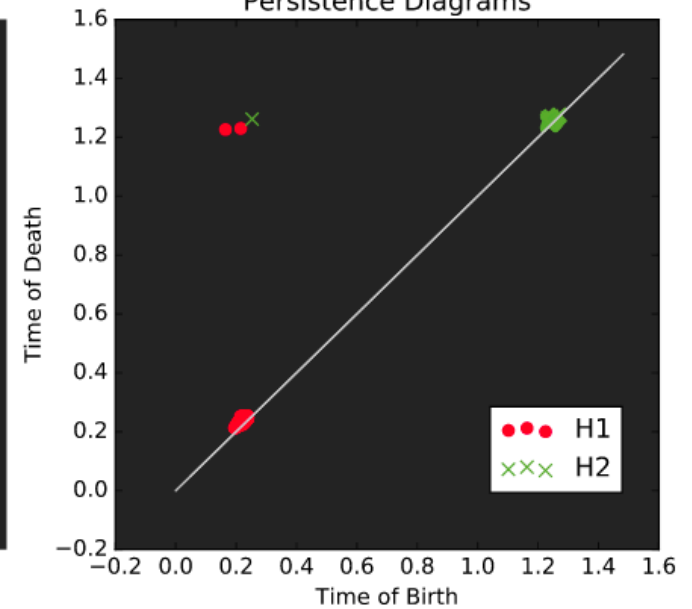
Persistence Diagrams



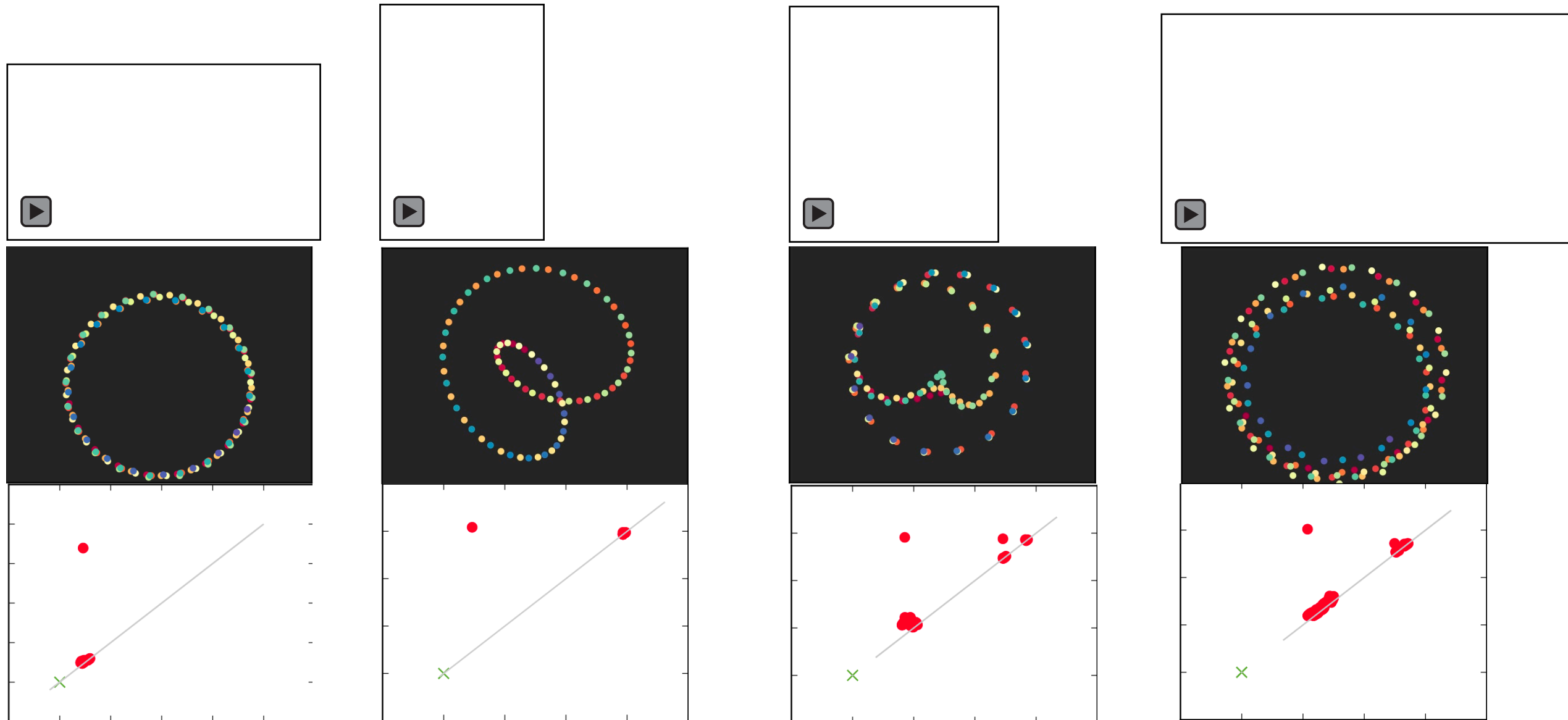
PCA of Sliding Window Embedding



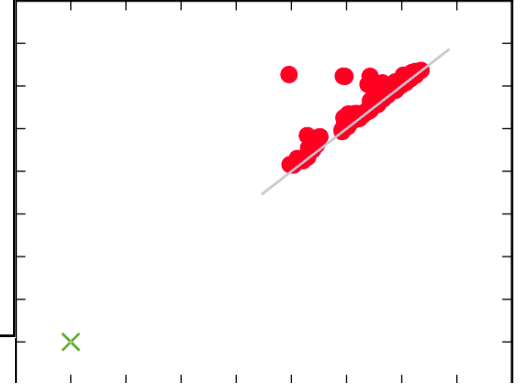
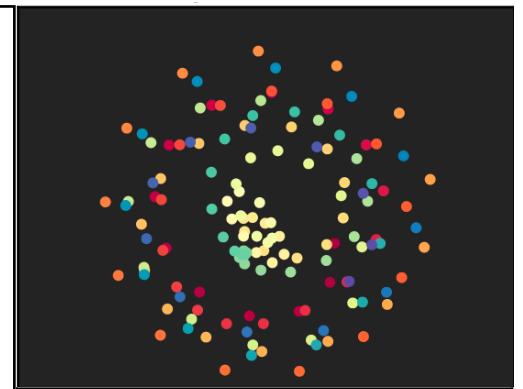
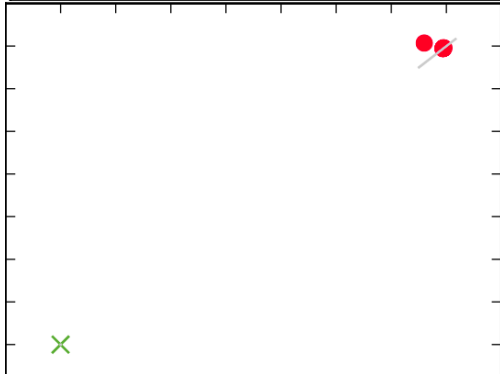
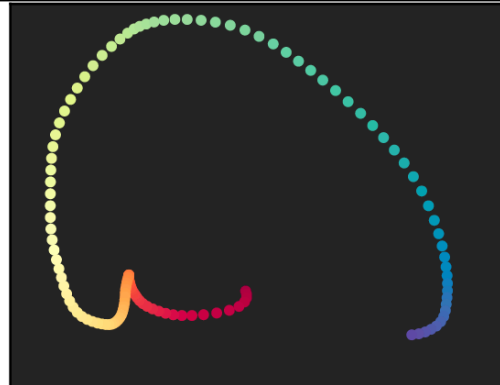
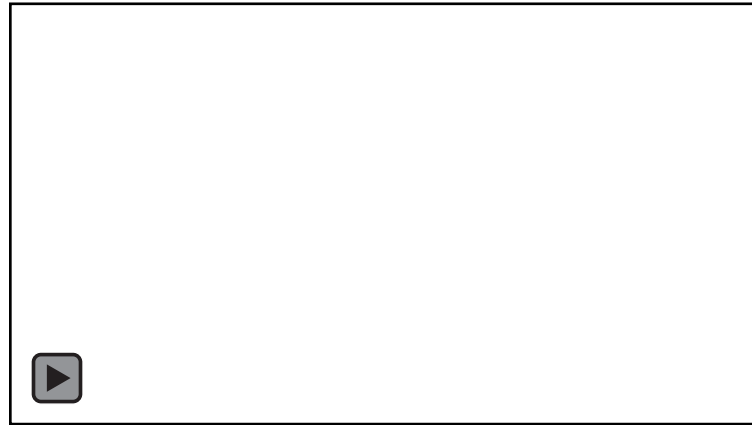
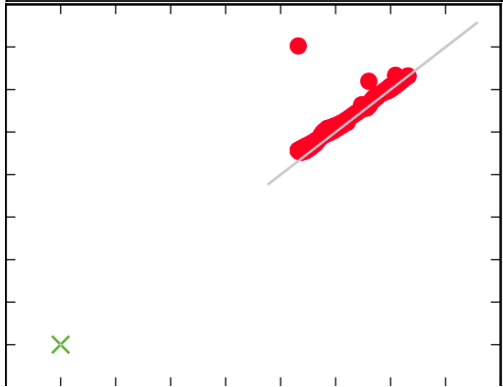
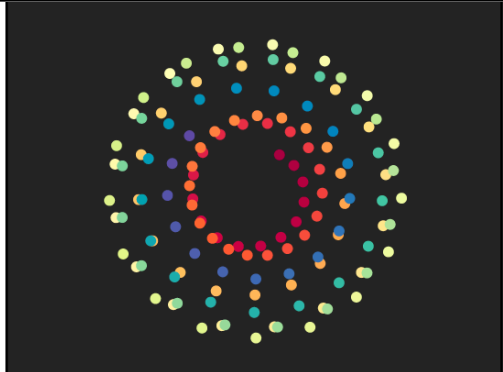
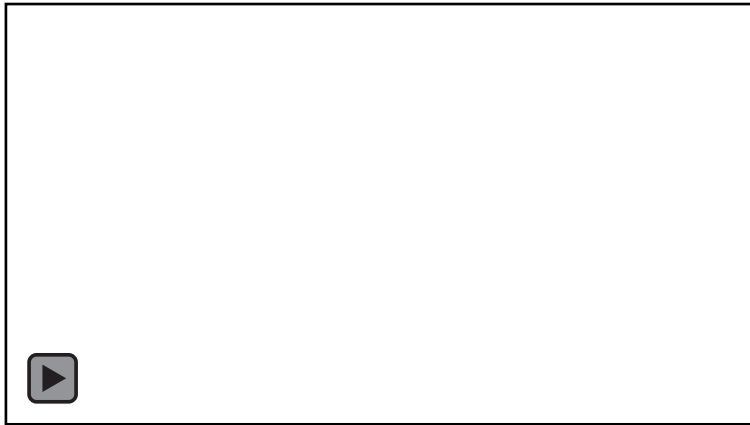
Persistence Diagrams



# Videos showing periodicity



# Non-periodicity and motion blur

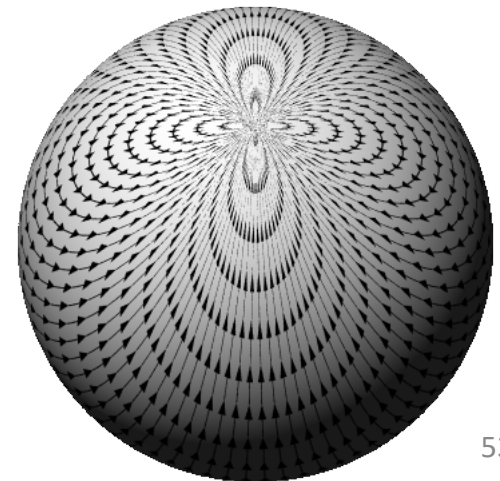


# Underlying theory: Takens' embedding theorem

- ◆ A remarkable result of Takens uses sliding windows to reconstruct a manifold  $M$  simply from a dynamical system defined on that manifold
- ◆ Let  $\Phi: \mathbb{R} \times M \rightarrow M$  be a continuous time dynamical system. Also fix an observation function  $F: M \rightarrow \mathbb{R}$  (e.g. temperature on the earth's surface) and, for any  $p \in M$ ,  $\phi_p: \mathbb{R} \rightarrow \mathbb{R}$  defined by  $t \mapsto F \circ \Phi(t, p)$ .
- ◆ For  $d \geq 2 \dim M$ ,  $\tau > 0$ , consider the map  $\phi: M \rightarrow \mathbb{R}^{d+1}$  given by  $p \mapsto (\phi_p(0), \phi_p(\tau), \dots, \phi_p(d\tau))$ .
- ◆ Takens' embedding theorem states that (under some extra hypotheses) the map  $\phi$  reconstructs a copy of the manifold  $M$  in  $\mathbb{R}^{d+1}$ .

## In practice:

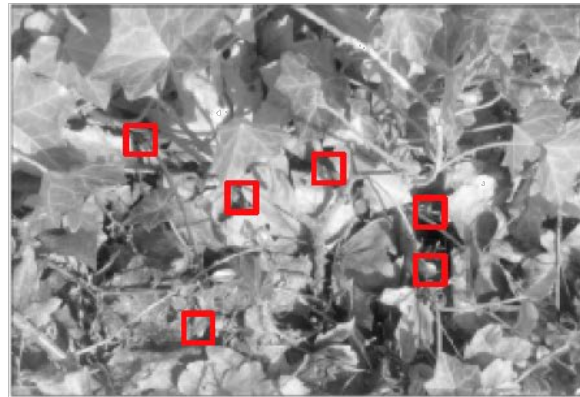
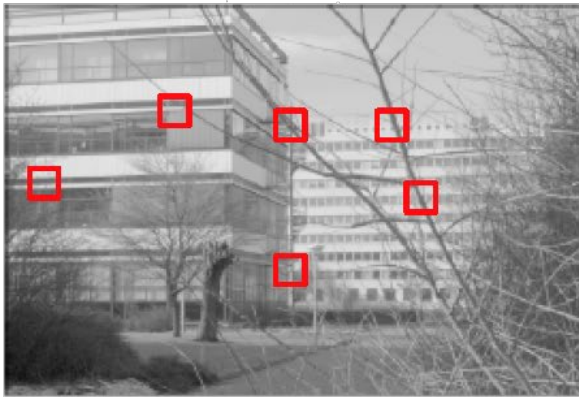
- ◆ Dynamical system  $(M, \Phi)$  unknown, only have time series  $f(t) = \phi_p(t)$
- ◆ Takens' theorem implies that  $SW_{d,\tau} f$  provides a topological copy of  $\{\Phi(t, p): t \in T\}$



# Topology of image patches

# Natural image statistics

**Input:** 4 million data points on  $\mathbb{S}^7$ , coming from high-contrast  $3 \times 3$  image patches



(source: [Lee, Pederson, Mumford 03])

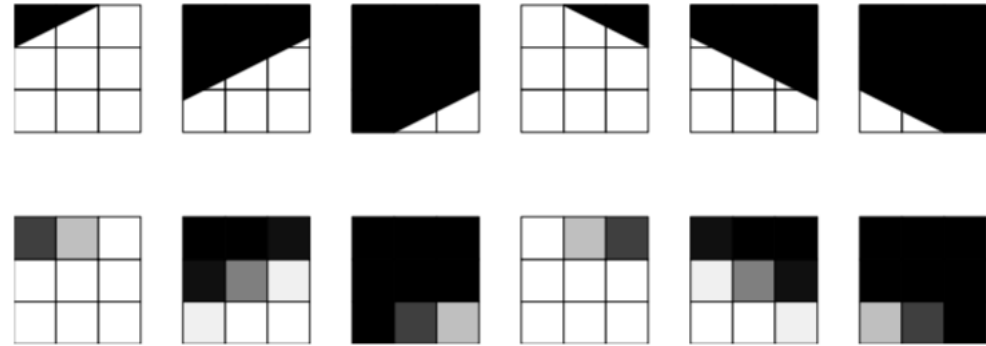
Preprocessing notes:

- Start with vector in  $\mathbb{R}^9$
- Subtract mean intensity, rescale to unit length
- Output: points in  $\mathbb{S}^7 \subseteq \mathbb{R}^8$

# Natural image statistics

Expect to see high concentration of edge features

- Parametrized by angle and distance from center, expected to live on an annulus



# Natural image statistics

Expect to see high concentration of edge features

- Parametrized by angle and distance from center, expected to live on an annulus
- 2D view below---why does the cross appear?

$K = 15, \text{cut} = 10\%$



$K = 15, \text{cut} = 20\%$



$K = 15, \text{cut} = 30\%$



$K = 100, \text{cut} = 10\%$



$K = 100, \text{cut} = 20\%$



$K = 100, \text{cut} = 30\%$



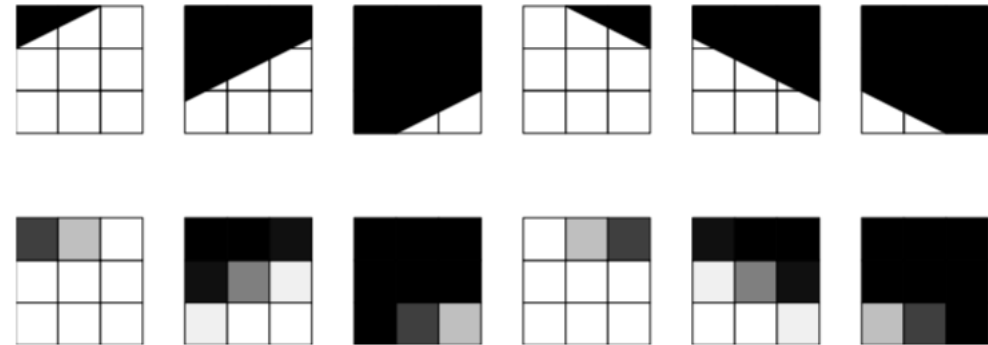
$K = 300, \text{cut} = 10\%$



$K = 300, \text{cut} = 20\%$



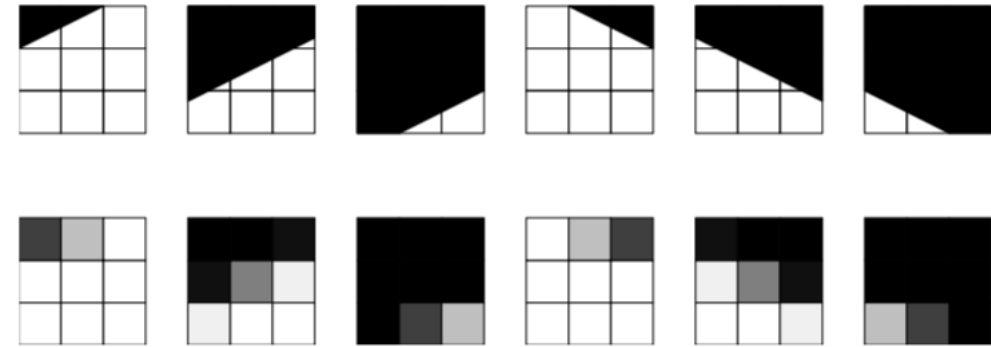
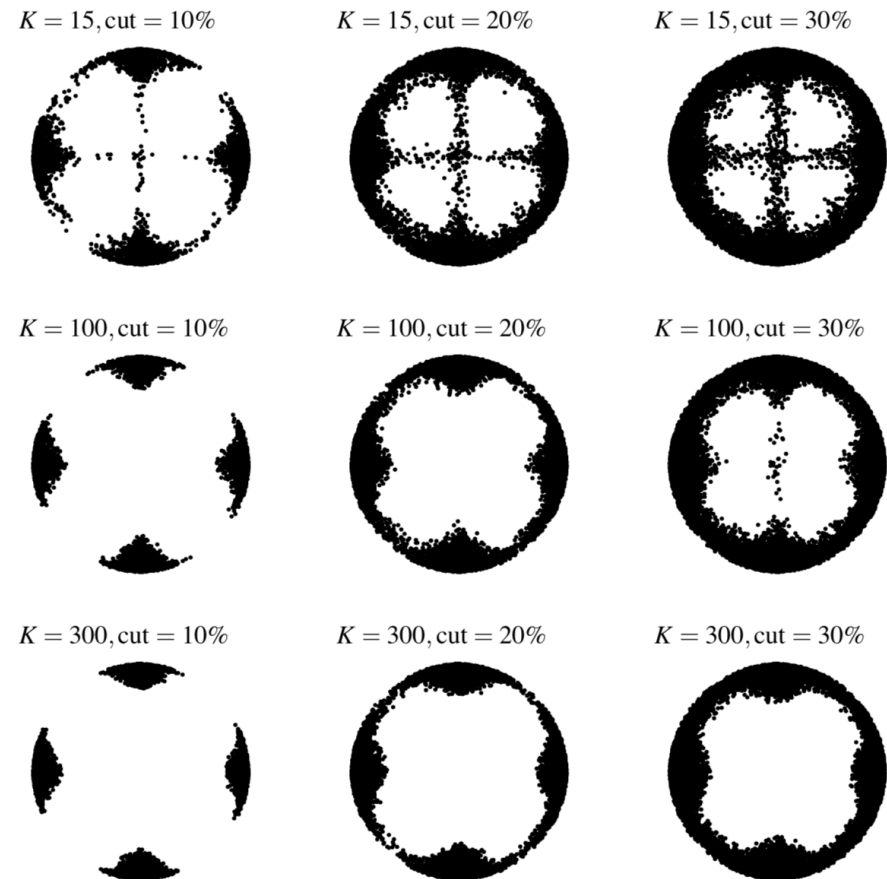
$K = 300, \text{cut} = 30\%$



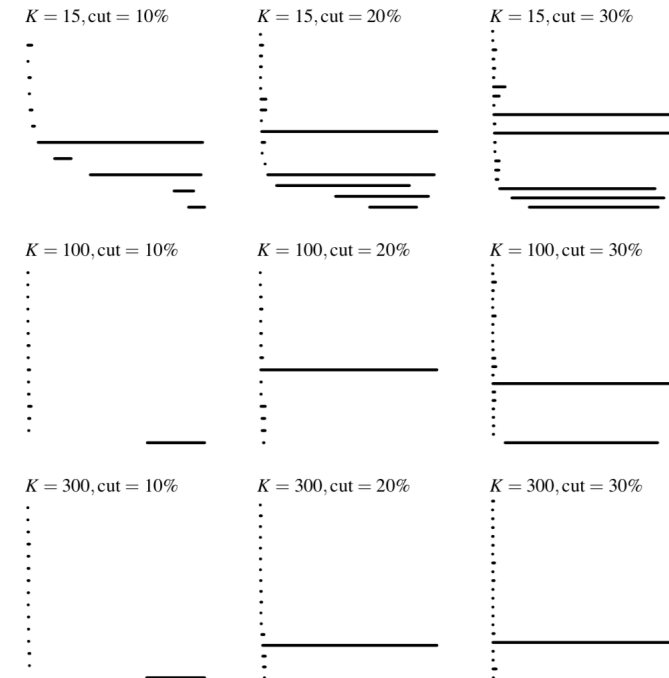
# Natural image statistics

Expect to see high concentration of edge features

- Parametrized by angle and distance from center, expected to live on an annulus
- 2D view below---why does the cross appear?

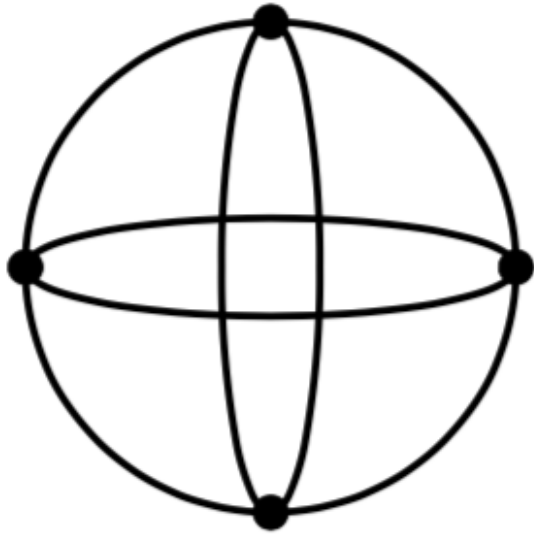


Betti numbers suggest  $\beta_1 = 5$ .  
Explanation?

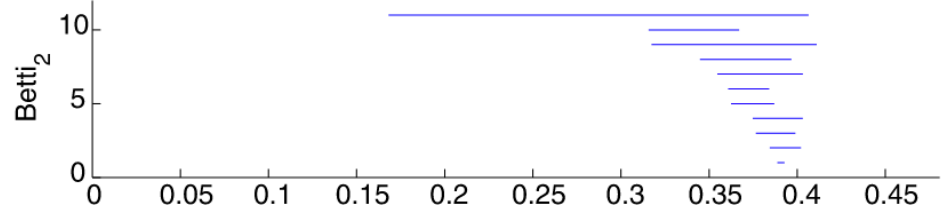
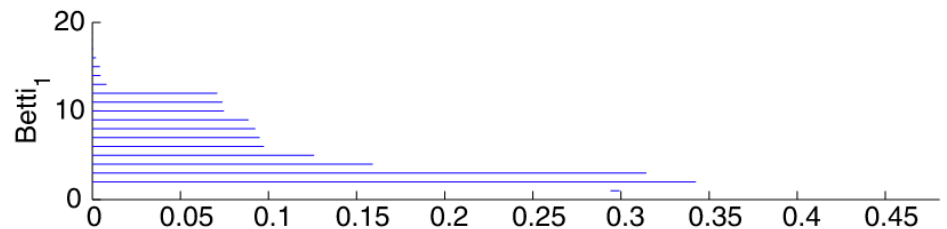
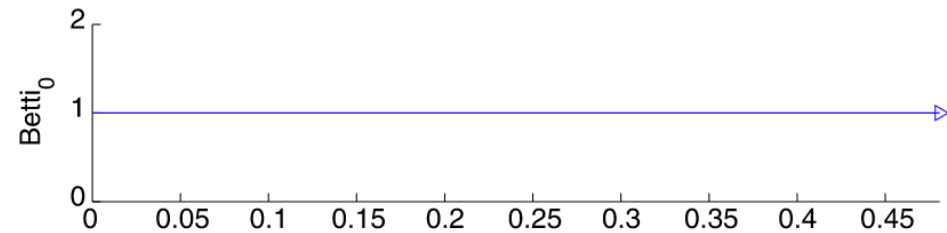
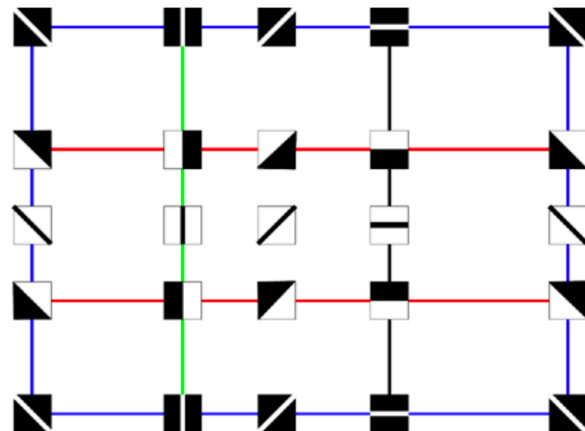
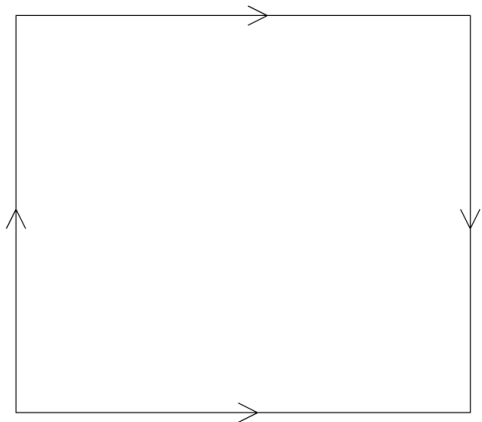


# Three circle model

Carlsson, Ishkanov, de Silva, Zomorodian, *On the local behavior of spaces of natural images*

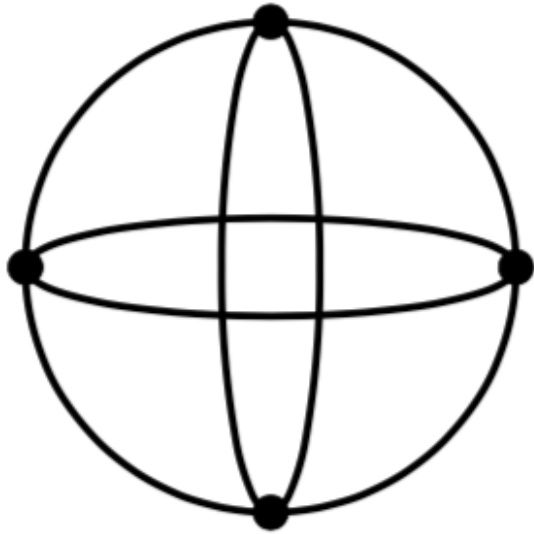


- Vertical and horizontal circles do not intersect
- Euler characteristic computation:
- $\beta_1 = \# \text{ arcs} - \# \text{ vertices} + \# \text{ connected components} = 8 - 4 + 1 = 5$
- PLEX results suggested 2-manifold. Torus or Klein bottle?

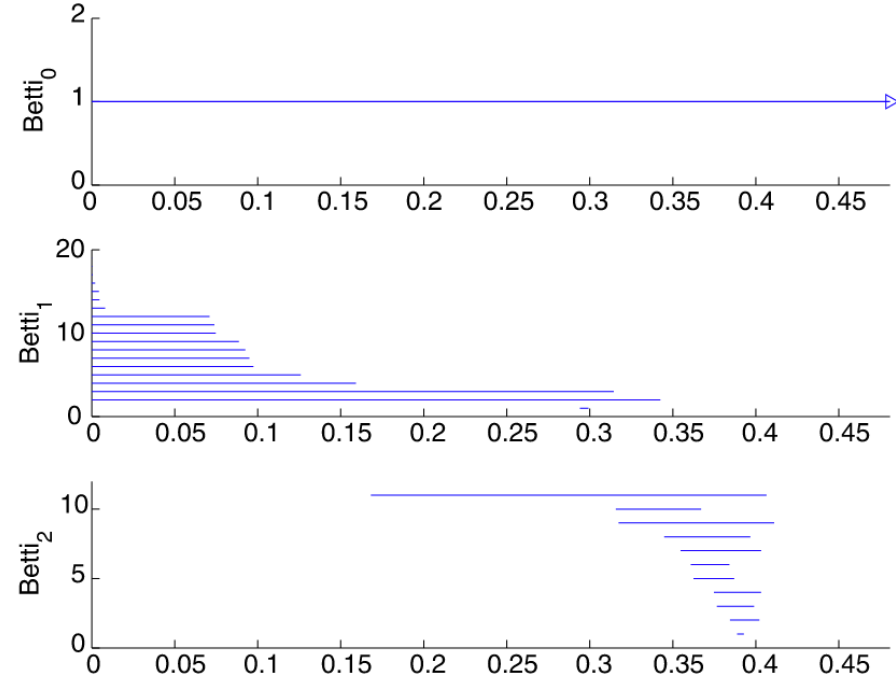
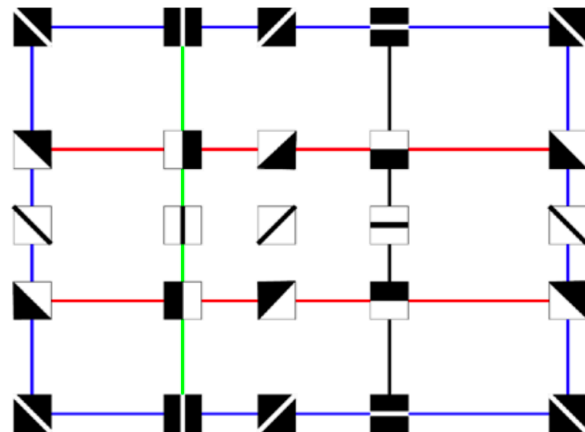
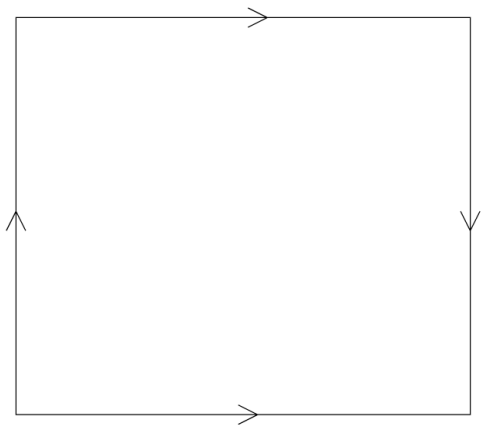


# Three circle model

Carlsson, Ishkanov, de Silva, Zomorodian, *On the local behavior of spaces of natural images*

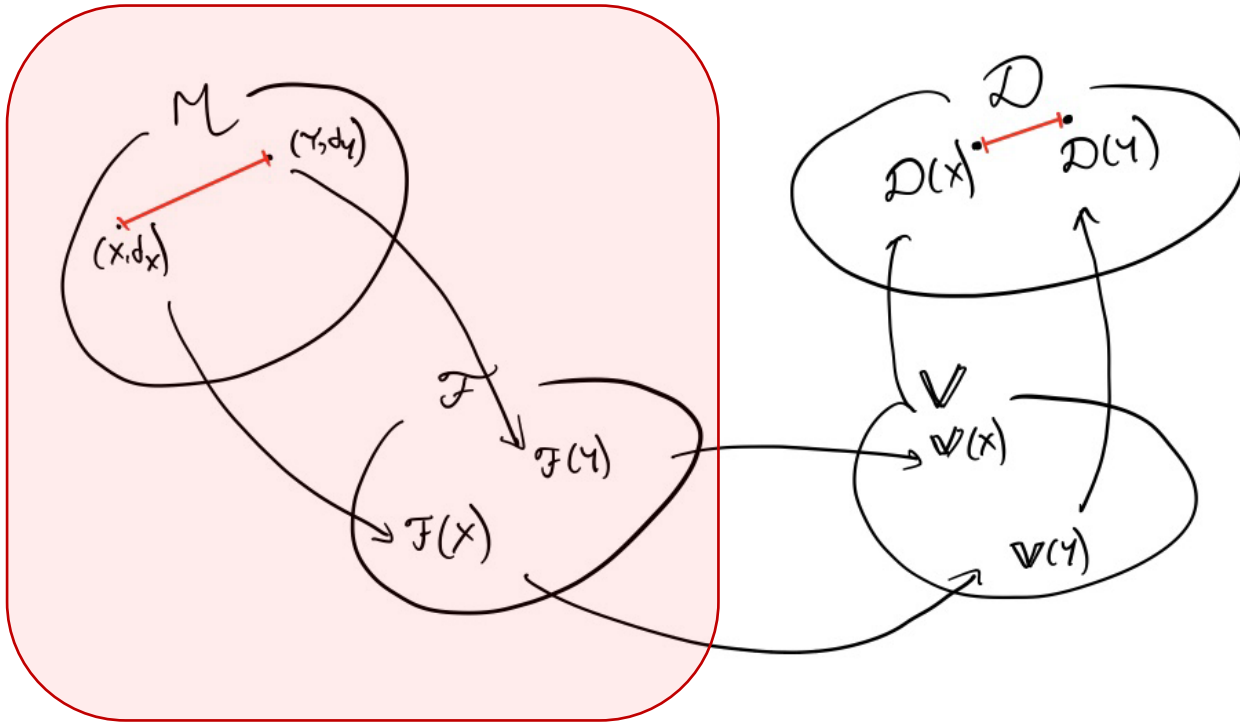


- Vertical and horizontal circles do not intersect
- Euler characteristic computation:
- $\beta_1 = \# \text{ arcs} - \# \text{ vertices} + \# \text{ connected components} = 8 - 4 + 1 = 5$
- PLEX results suggested 2-manifold.
- Computational trick: augment data with ideal Klein bottle, observe that barcode remains unchanged. So all homology comes from the Klein bottle.



# Adding geometry to topology

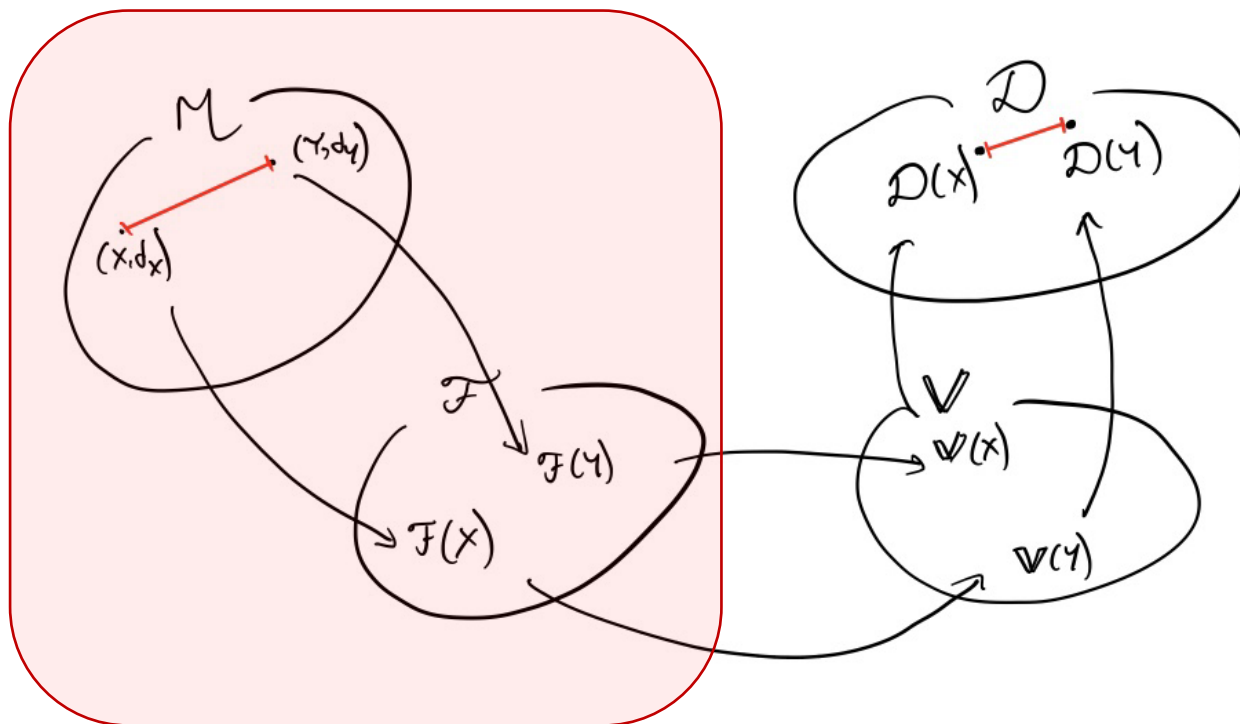
# Synthetic filtrations are possible, and informative



Why only build complexes capturing proximity?

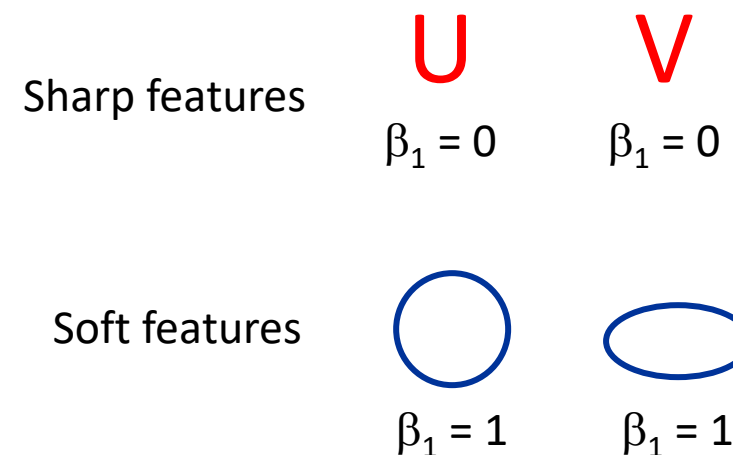
- Possible to create “derived complexes” that capture different information
- Natural to consider geometry-dependent filtrations

# Synthetic filtrations are possible, and informative



Why only build complexes capturing proximity?

- Possible to create “derived complexes” that capture different information
- Natural to consider geometry-dependent filtrations



Geometry  
discriminating

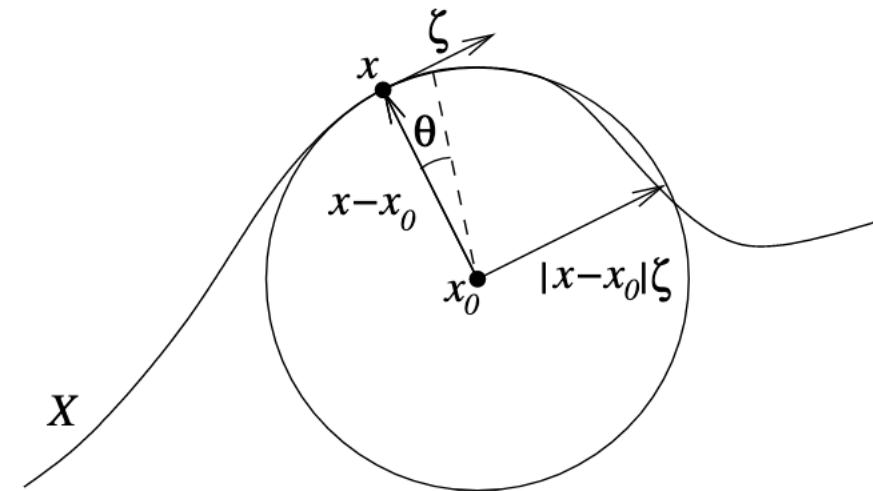
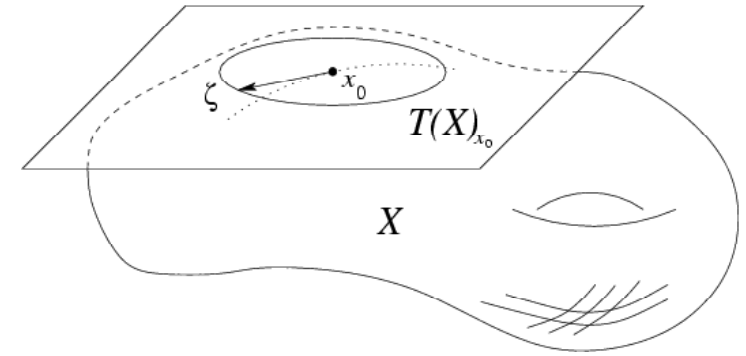
Topology  
classifying

# The (filtered) tangent complex

Collins, Zomorodian, Carlsson, Guibas, *A barcode shape descriptor for curve point cloud data*, CaG'04

Setup:  $X \subseteq \mathbb{R}^n$

- Tangent complex  $T(X) \subseteq X \times \mathbb{S}^{n-1}$ :
  - unit tangent vectors at all points of  $X$ , i.e. pairs  $(x, \zeta)$  where  $x \in X$  and  $\zeta$  is a tangent vector
- Filtered tangent complex: filter the points in the tangent complex by increasing curvature
  - Curvature at point  $(x, \zeta)$  is  $1/\rho$ , where  $\rho$  is radius of osculating circle
  - $T_\delta(X) =$  points with curvature  $< \delta$
  - Filtered tangent complex  $T^{filt}(X) := \{T_\delta(X)\}_{\delta > 0}$



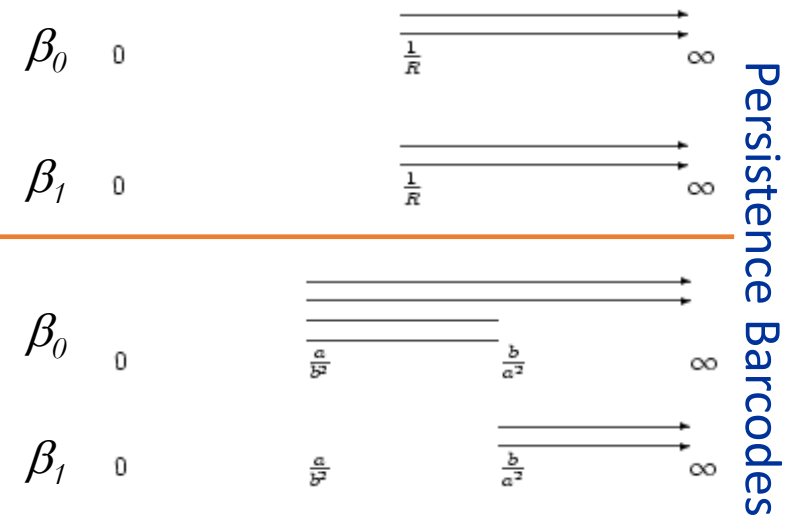
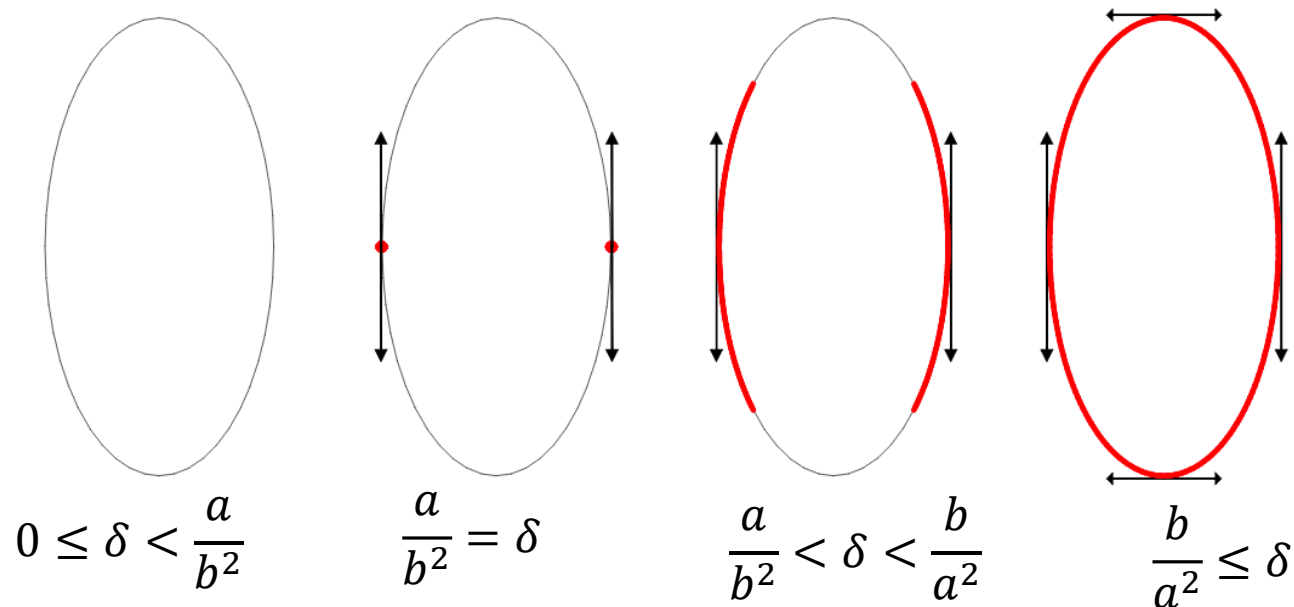
# Examples: circle vs ellipse

**Circle of radius R:** Tangent complex is  $S^1 \times S^0$ , as there are two tangent directions at each point.

- $T^{filt}$  is empty until  $1/R$ , then full complex enters at once

**Ellipse**  $\frac{x^2}{a^2} + \frac{y^2}{b^2} = 1$ :

- evolves through **four stages**: points at *lower* curvature appear earlier.



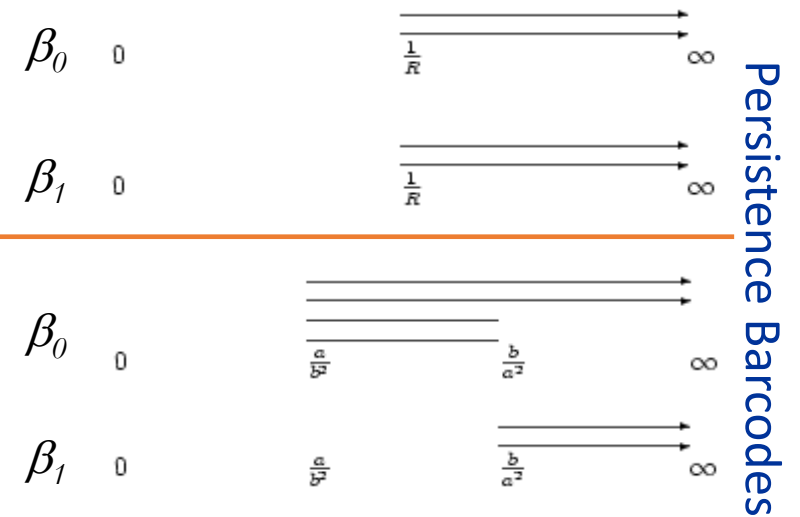
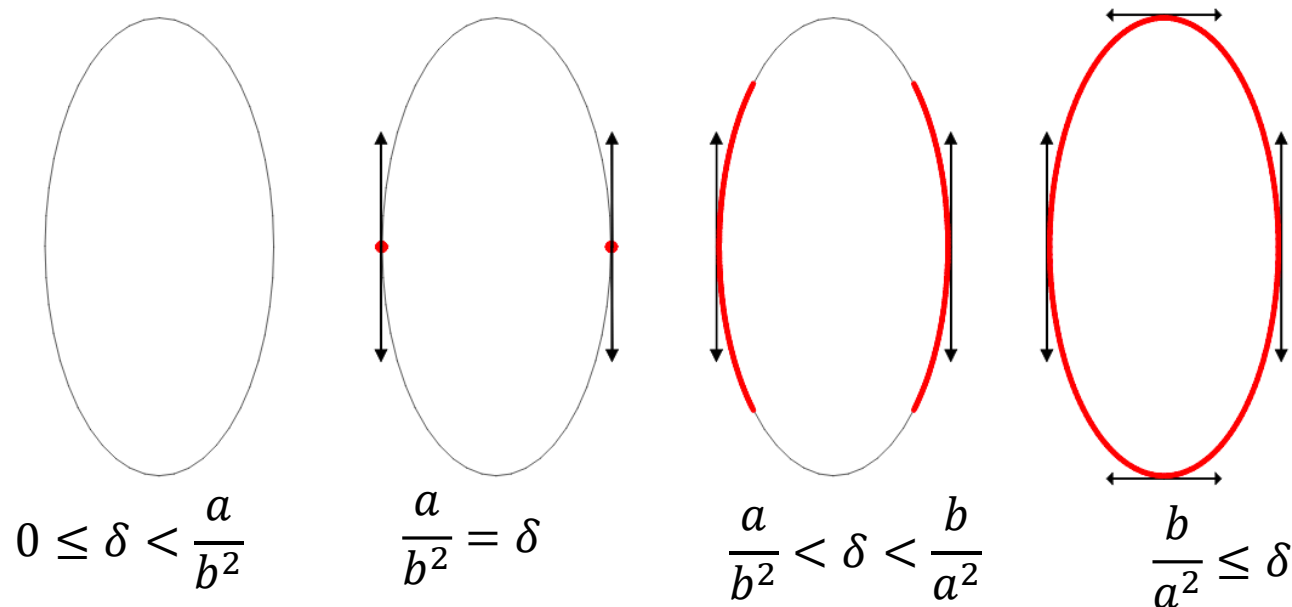
# Examples: circle vs ellipse

**Circle of radius R:** Tangent complex is  $S^1 \times S^0$ , as there are two tangent directions at each point.

- $T^{filt}$  is empty until  $1/R$ , then full complex enters at once

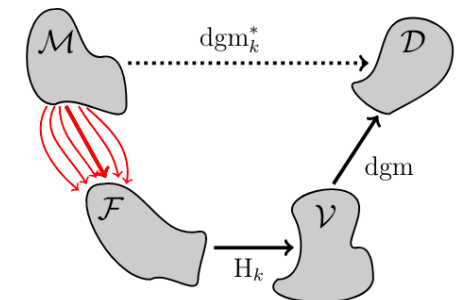
**Ellipse**  $\frac{x^2}{a^2} + \frac{y^2}{b^2} = 1$ :

- evolves through **four stages**: points at *lower* curvature appear earlier.



Proposed framework:

- Information is distributed across a variety of properties
- Use **multiple** barcodes to interrogate the data
- We will see more of this perspective later...



# The Mapper Algorithm

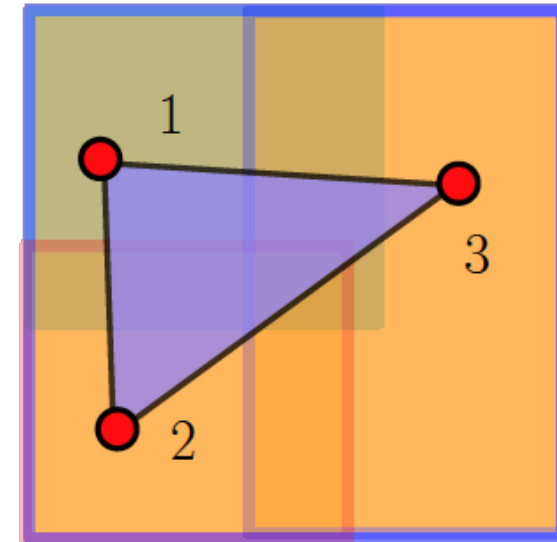
# Recall: covers and nerves

## Finite cover of a topological space $X$

- ▶  $\mathcal{U} = \{U_\alpha\}_{\alpha \in A}$  for a finite index set  $A$ .
- ▶ each  $U_\alpha \subseteq X$  is open and  $X = \bigcup_{\alpha \in A} U_\alpha$

## Nerve of a cover

- ▶ Simplicial complex:  $N(\mathcal{U})$  with vertex set  $A$ .
- ▶ simplices:  $A \supseteq \sigma \in N(\mathcal{U}) \Leftrightarrow \bigcap_{\alpha \in \sigma} U_\alpha \neq \emptyset$ .



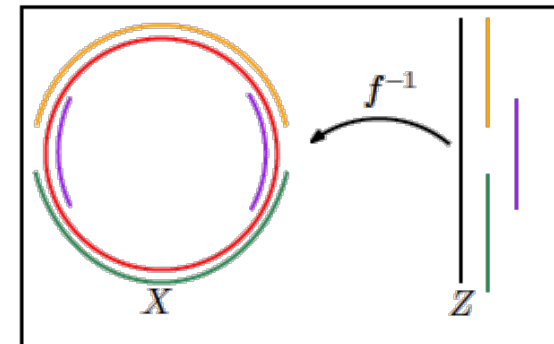
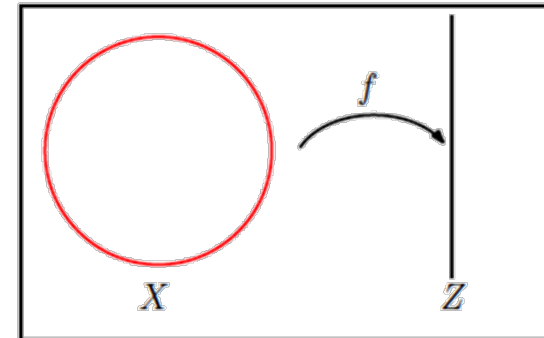
# Pullback covers and their nerves

- ▶ Assume you have  $f : X \rightarrow Z$  well behaved continuous function and  $\mathcal{U} = \{U_\alpha\}_{\alpha \in A}$  finite open cover of  $Z$ .
- ▶ For each  $\alpha \in A$  consider the **connected components** of  $f^{-1}(U_\alpha) = \{V_{i,\alpha}, 1 \leq i \leq j_\alpha\}$ .
- ▶ Let  $f^*(\mathcal{U})$  be the (finite) open cover of  $X$  thus induced:

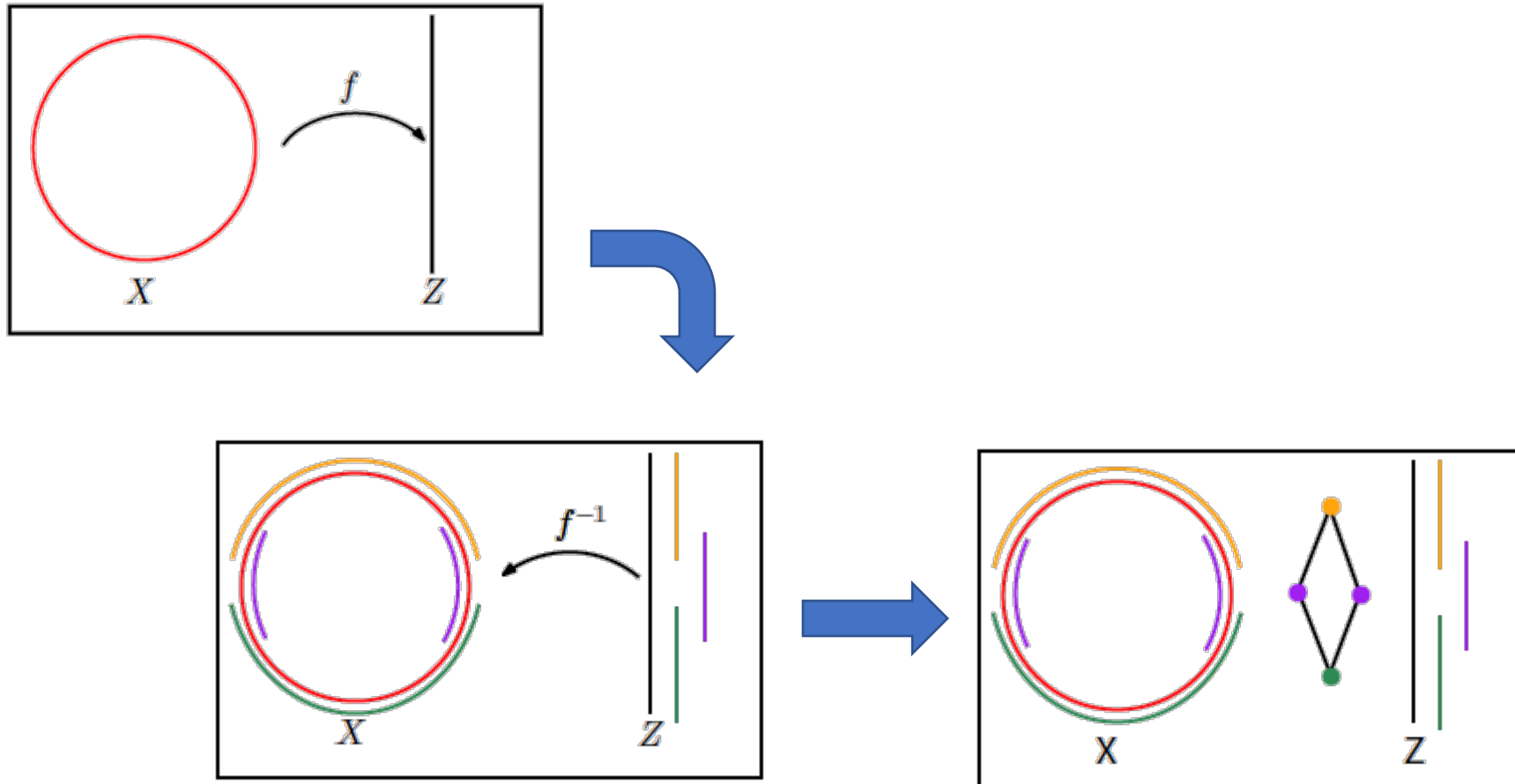
$$f^*(\mathcal{U}) := \{V_{i,\alpha}, 1 \leq i \leq j_\alpha, \alpha \in A\}.$$

This is the **pullback** of  $\mathcal{U}$  via  $f$ .

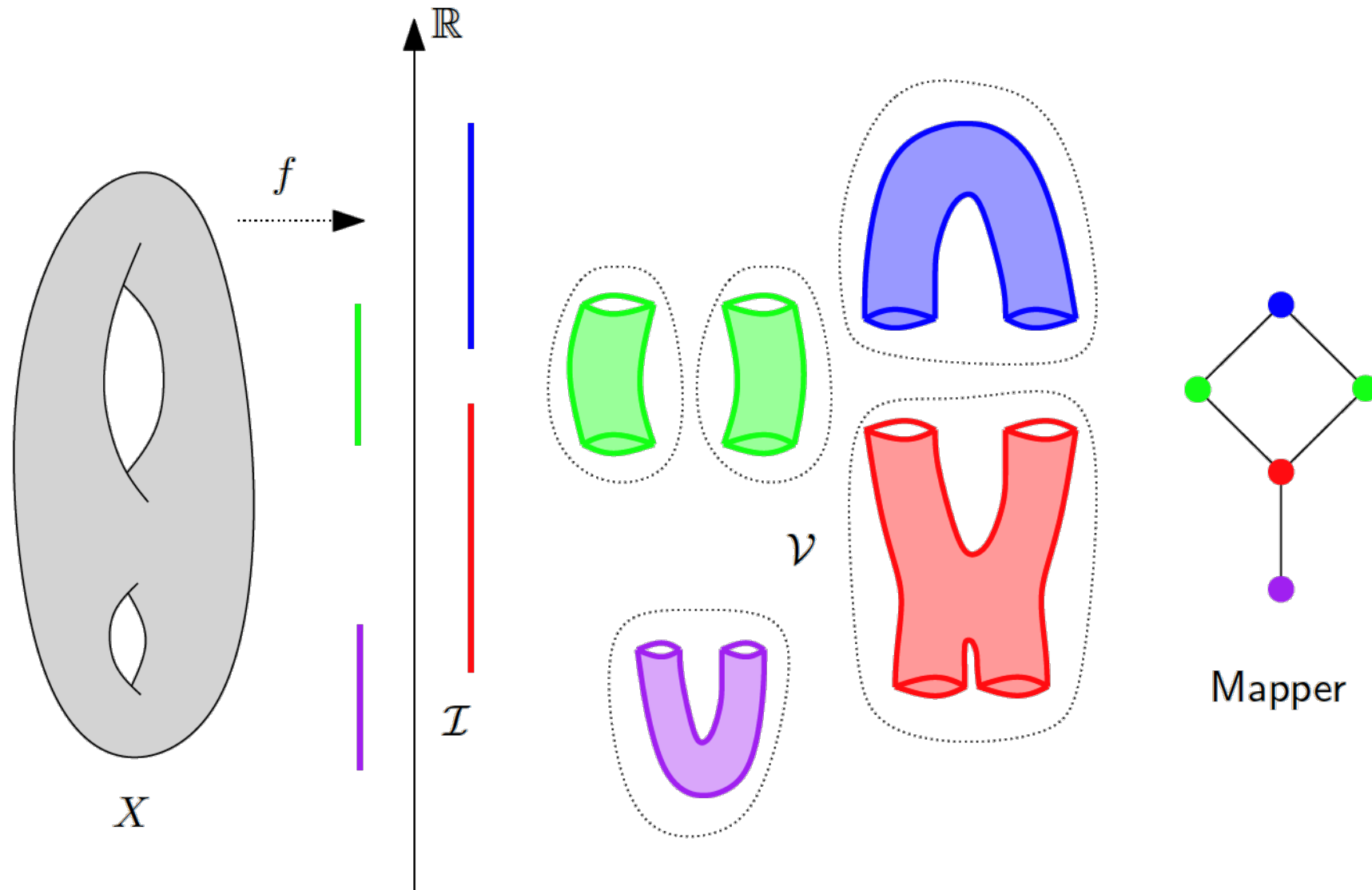
- ▶ Now consider the nerve of the pullback:  $N(f^*(\mathcal{U}))$ . This complex often retains structural information about underlying space  $X$ .



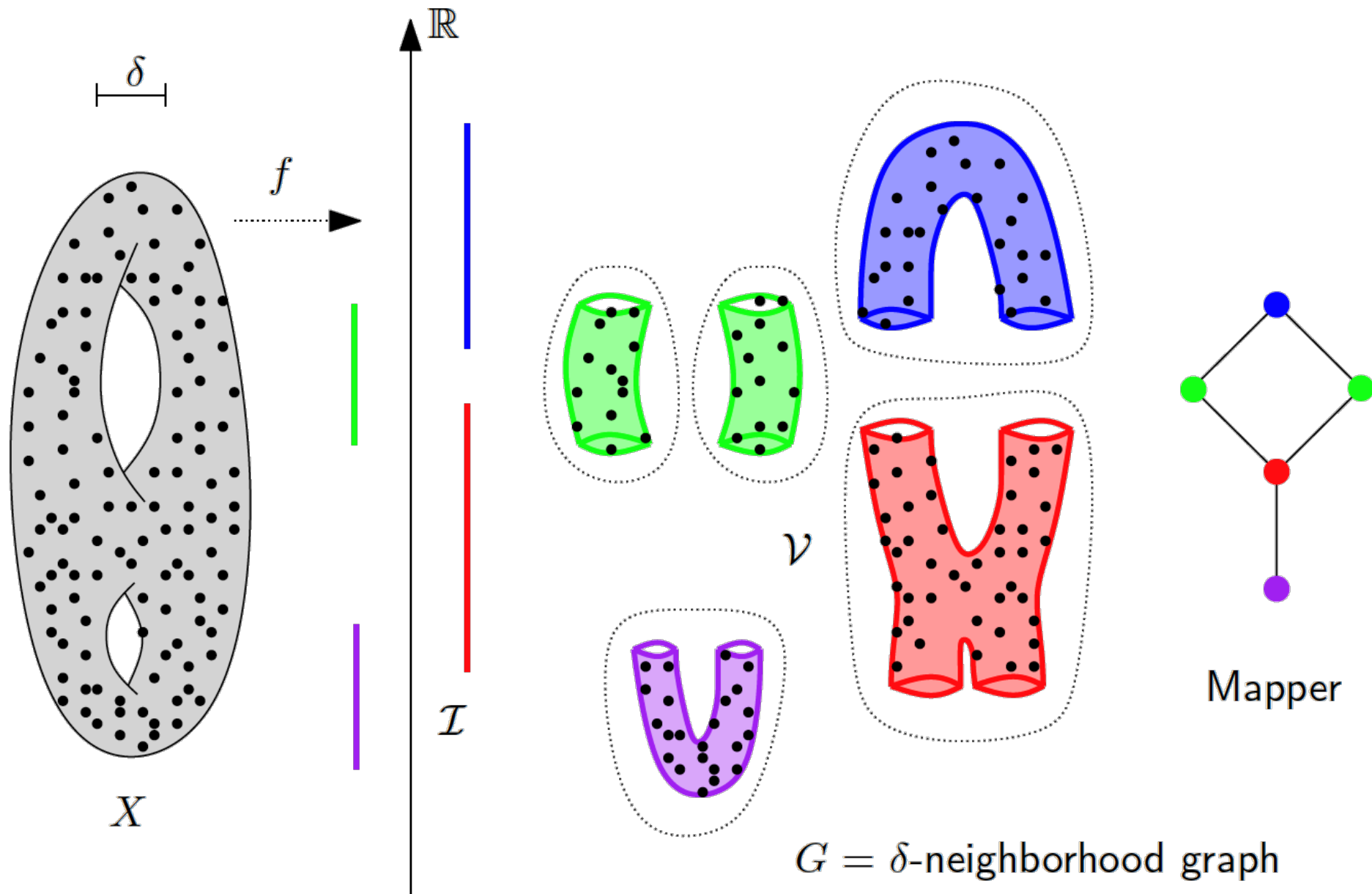
# Pullback covers and their nerves



# Choice of lens



# Choice of lens

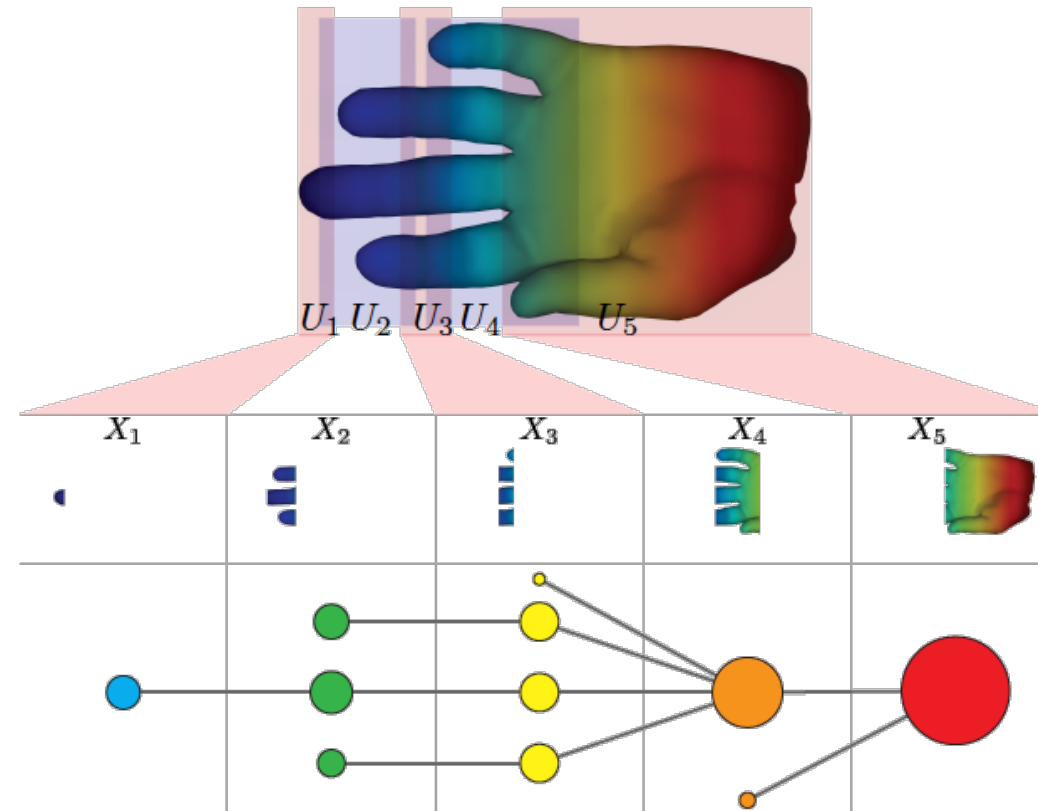


# The Mapper algorithm

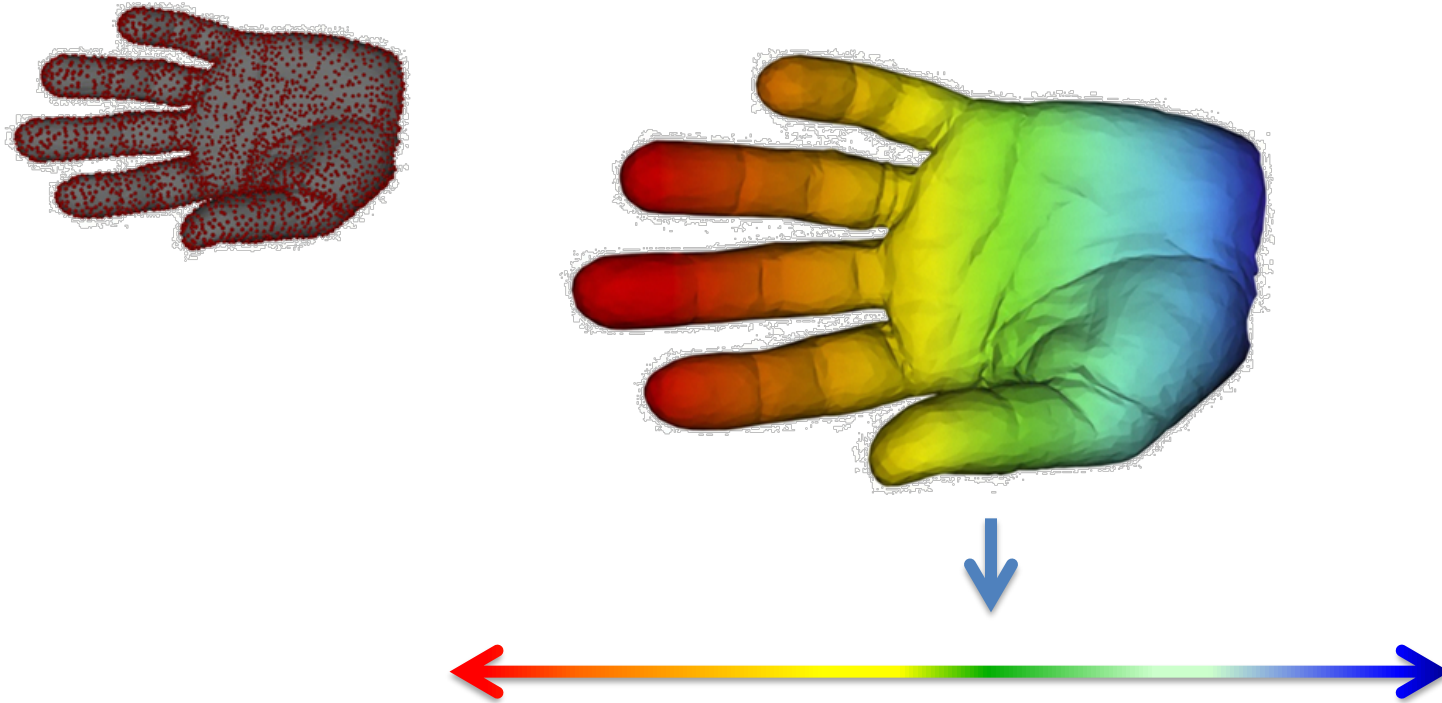
Singh, Mémoli, Carlsson - *Topological Methods for the Analysis of High Dimensional Data Sets and 3D Object Recognition*

Let  $f : X \rightarrow Z$  be well behaved and continuous and  $\mathcal{U}$  be finite open cover of  $Z$ , then the **Mapper** output corresponding to  $\mathcal{U}$  and  $f$  is

$$M(\mathcal{U}, f) := N(f^*(\mathcal{U})).$$



# Step 1: Choose a Lens / Filter Function



Function  $f$  : Data Set  $\rightarrow \mathbf{R}$

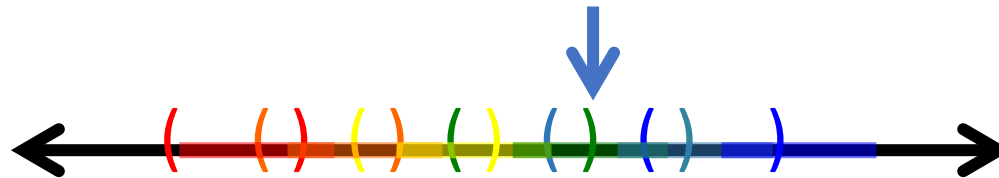
Ex 1:  $x$ -coordinate  $f : (x, y, z) \rightarrow x$

# Step 2: Partition into Overlapping Bins

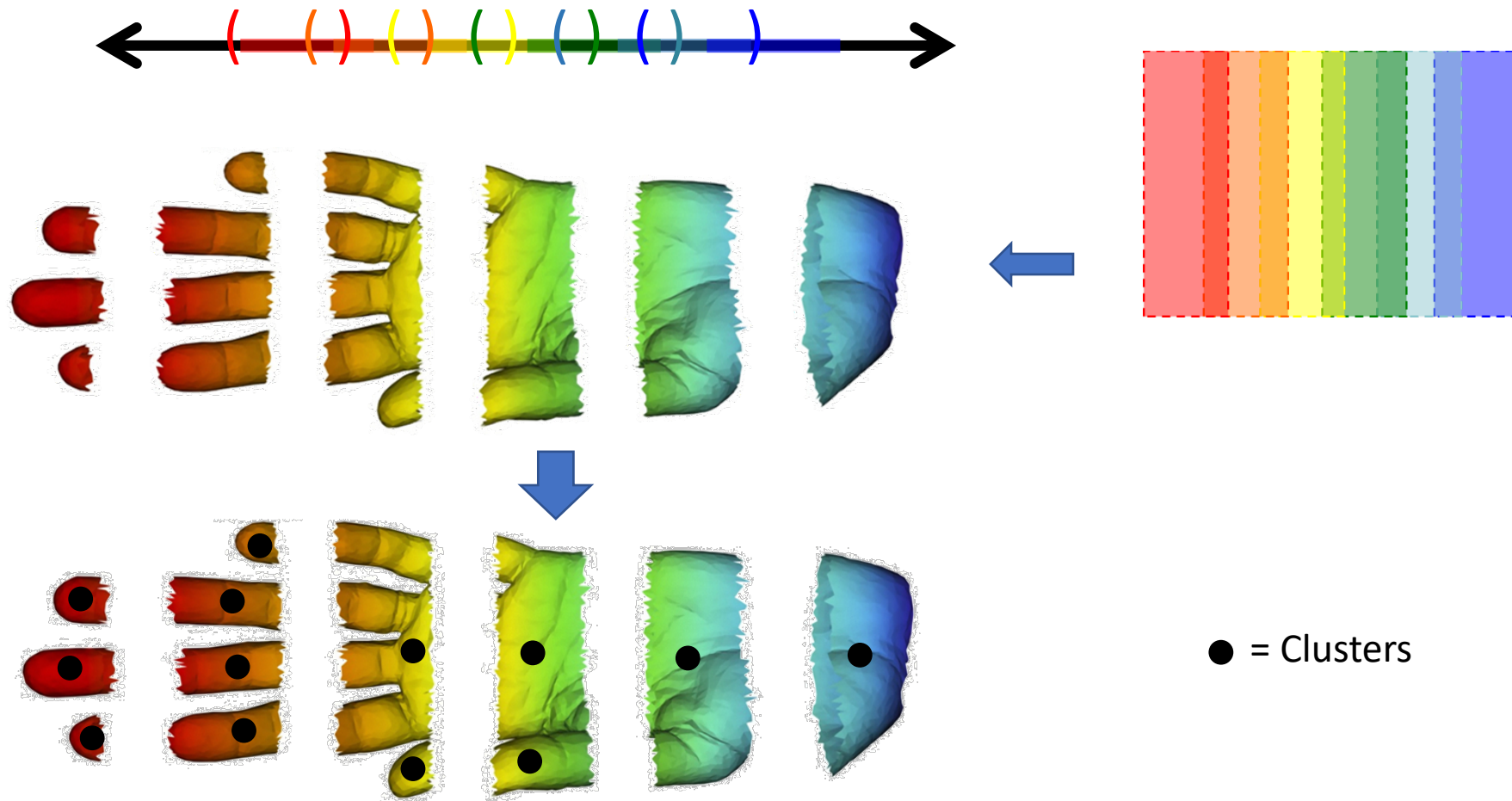


Cover data via overlapping bins.

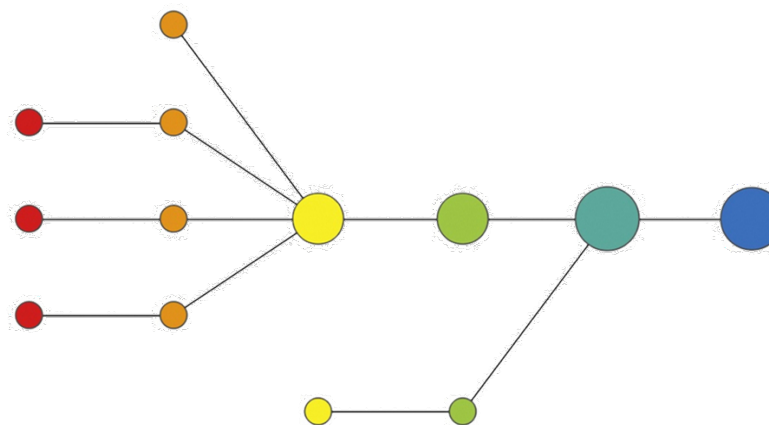
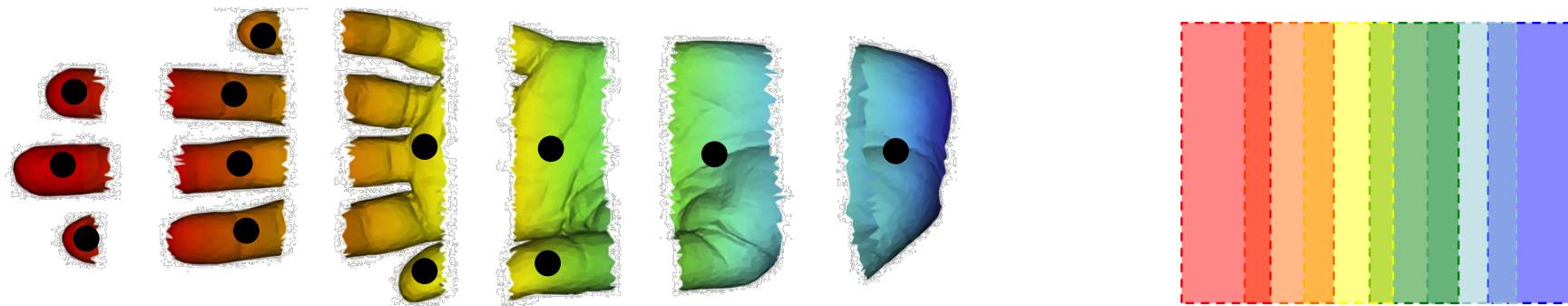
Example:  $f^{-1}(a_i, b_i)$



# Step 3: Form Connected Components in the Bins

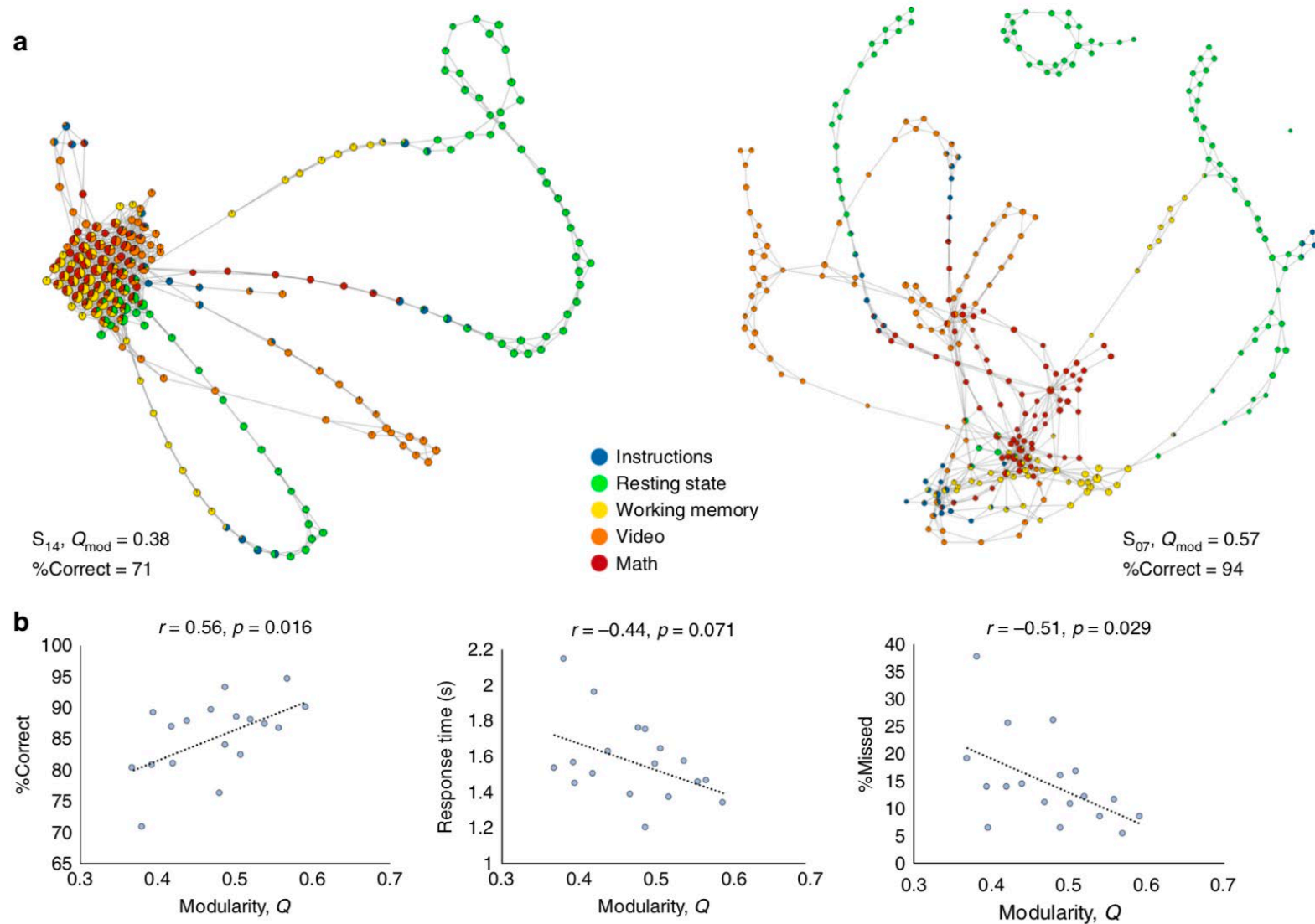


# Step 4: Form a Network of Intersecting Clusters



# Mapper in computational psychiatry

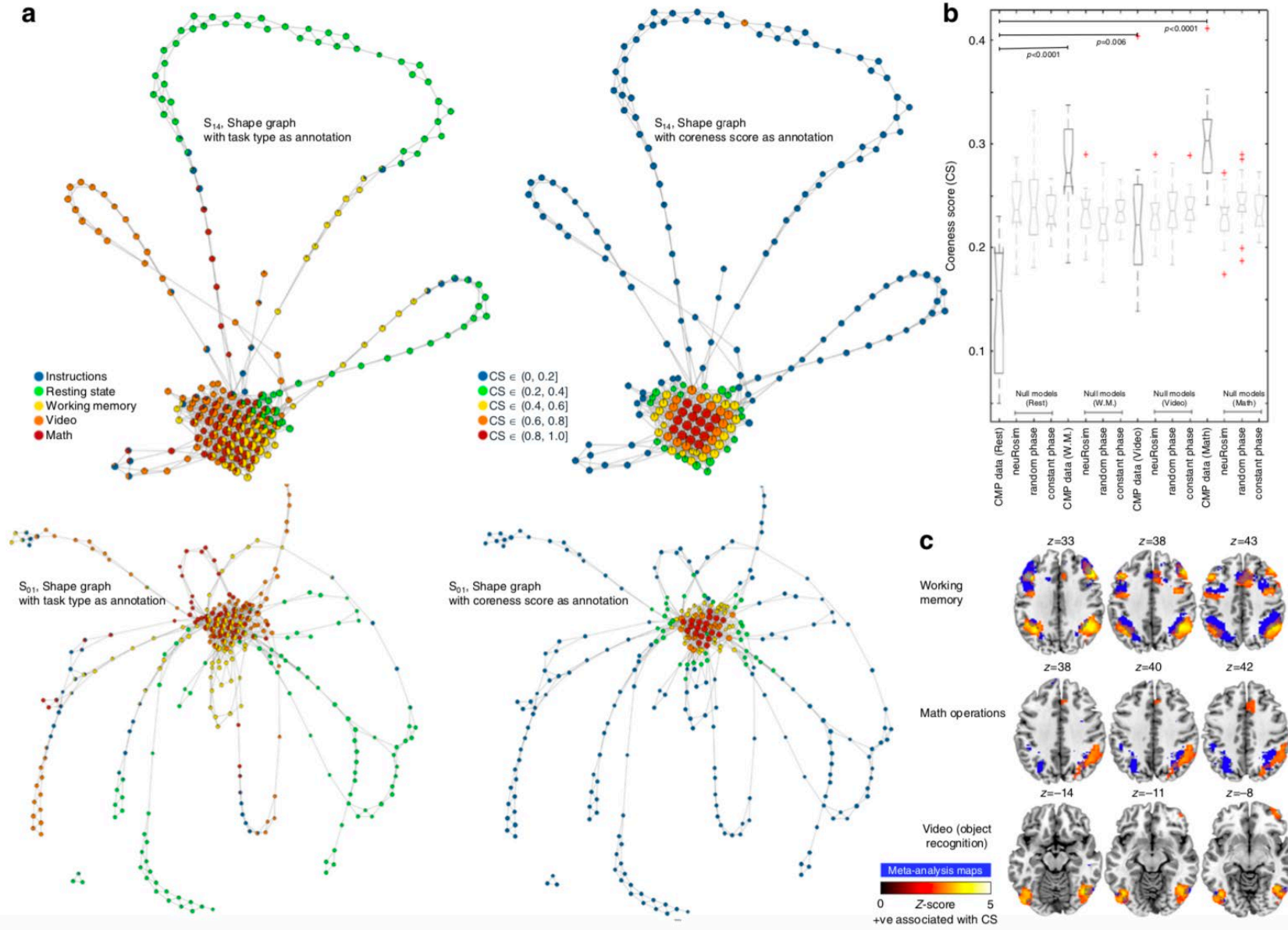
Saggar et al., *Towards a new approach to reveal dynamical organization of the brain*



- Community structure of the mapper graph shown to be positively correlated with performance on a task

# Mapper in computational psychiatry

Saggar et al., *Towards a new approach to reveal dynamical organization of the brain*



- Community structure of the mapper graph shown to be positively correlated with performance on a task
- Nodes related to high cognitive load buried deep in the core of the graph
- Nodes related to rest stay in the periphery



The End